


## RESEARCH ARTICLE

# Mathematical Modeling on the Transmission Dynamics of HIV and Hepatitis B (HBV) Co-Infection in the United States

Festus Abiodun Oguntolu<sup>1</sup> | Olumuyiwa James Peter<sup>2,3,4</sup>  | Dipo Aldila<sup>5</sup> | Ghaniyyat Bolanle Balogun<sup>6</sup> | Aminat Olabisi Ajiboye<sup>7</sup> | Benjamin Idoko Omede<sup>8</sup>

<sup>1</sup>Department of Mathematics, Federal University of Technology, Minna, Niger State, Nigeria | <sup>2</sup>Department of Mathematics, Saveetha School of Engineering, SIMATS, Saveetha University, Chennai, Tamil Nadu, India | <sup>3</sup>Department of Mathematical and Computer Sciences, University of Medical Sciences, Ondo, Ondo State, Nigeria | <sup>4</sup>Department of Epidemiology and Biostatistics, School of Public Health, University of Medical Sciences, Ondo, Ondo State, Nigeria | <sup>5</sup>Department of Mathematics, Faculty of Mathematics and Natural Sciences, Universitas Indonesia, Depok, Indonesia | <sup>6</sup>Department of Computer Science, Faculty of Communication and Information Sciences, University of Ilorin, Ilorin, Nigeria | <sup>7</sup>Department of Mathematics, Federal University Oye-Ekiti, Oye-Ekiti, Ekiti State, Nigeria | <sup>8</sup>Department of Mathematical Sciences, Prince Abubakar Audu (Formerly Kogi State) University, Anyigba, Nigeria

**Correspondence:** Olumuyiwa James Peter ([peterjames4real@gmail.com](mailto:peterjames4real@gmail.com))

**Received:** 6 February 2025 | **Revised:** 26 May 2025 | **Accepted:** 2 June 2025

**Funding:** The authors received no specific funding for this work.

**Keywords:** basic reproduction number | bifurcation | HIV and HBV co-infection | sensitivity analysis | stability

## ABSTRACT

Human immunodeficiency virus (HIV) and hepatitis B virus (HBV) are major public health concern worldwide, contributing to significant morbidity and mortality. Managing co-infection between HIV and HBV presents additional challenges in clinical treatment and patient outcomes. In this article, we developed a comprehensive co-infection model to explore the complex transmission dynamics between HIV and HBV in the United States. Our model incorporates crucial factors such as infection through birth or migration, HBV vaccination, and the possibility of reinfection following HBV recovery. Our mathematical analysis started with the analysis of the two non-co-infection submodels, that is, for HIV-only and HBV-only models. We derived the basic reproduction number for each submodel and applied the Routh-Hurwitz criterion to assess the local stability of their respective disease-free equilibrium points. Our investigation revealed that the HIV-only submodel is globally asymptotically stable when its basic reproduction number remains below one. Conversely, the HBV-only submodel exhibits a backward bifurcation, meaning that both disease-free and endemic equilibrium states can coexist even when the reproduction number falls below one. This phenomenon complicates HBV control strategies under such conditions. However, in the absence of reinfection, the HBV-only model reaches global stability at the disease-free equilibrium whenever its reproduction number is below one. Using center manifold theory, we further demonstrated that the full HIV-HBV co-infection model also undergoes backward bifurcation. A sensitivity analysis was conducted on the basic reproduction numbers of HIV and HBV to identify critical parameters influencing the transmission dynamics of both infections. Our results indicate a positive correlation between the spread of one infection and the prevalence of the other. Additionally, we validated the model by fitting it to annual cumulative data on new HIV cases and reported acute HBV infections in the United States. Numerical simulations suggest that increasing condom use adherence, enhancing treatment coverage for both infections, and boosting HBV vaccination rates can substantially reduce the prevalence of HIV, HBV, and their co-infection.

**MSC Classification:** 92B05, 92D30, 92-10, 34D20

[Correction added on 04 July 2025, after first online publication: First author name and Affiliation 1 have been updated in this version.]

## 1 | Introduction

For many years, infectious disease has become a major health program in many countries in the world, including the human immunodeficiency virus (HIV) and hepatitis B virus (HBV). HIV is a virus that attacks the immune systems of humans, specifically targeting the T cells. T cells are crucial for maintaining the human immune response to possible infection by infectious diseases [1]. With this infection, the virus will replicate and damage T cells. At the end, humans become easier to get infected with infectious diseases, and the symptoms become more severe if HIV progresses into acquired immunodeficiency syndrome (AIDS), and if it is left untreated, it can lead to life-threatening illness. First identified in the early 1980s, HIV has impacted millions globally, with sub-Saharan Africa being the most severely affected region [2]. According to the Joint United Nations Program on HIV/AIDS (UNAIDS), as of 2022, approximately 39 million people were living with HIV, with 1.3 million new infections and 630,000 AIDS-related deaths occurring globally each year [2]. There are several ways of HIV infections, such as through sexual intercourse, exposure to infected blood through blood transfusions, blood products, shared needles (mainly between drug-addicted individuals), and vertical transmission (from newborns or during breastfeeding). Although homosexual contact continues to be a major route of HIV transmission in the United States, heterosexual transmission has become the primary mode of HIV spread globally [3]. HIV symptoms can range from mild to severe, depending on the individual. In the initial infections, possible symptoms are flu, fever, headache, and so forth. When the symptoms start to weaken the immune systems, additional symptoms may arise and become more severe, such as weight loss, diarrhea, and any other health issues like tuberculosis, meningitis, and cancers [4]. Based on these big health issues caused by HIV, integrated interventions have been deployed by governments around the world, such as advocacy at the local and international levels, resource mobilization, and other possible interventions. The government prioritizes providing widespread access to antiretroviral therapy (ART) for infected individuals.

Almost similar to HIV, HBV is also caused by a virus from the family Hepadnaviridae. HBV infects liver hepatocytes through the interaction between the HBV surface antigen (HBsAg) and the sodium taurocholate cotransporting polypeptide (NTCP) receptor [5, 6]. Similar to HIV, HBV is also a serious and life-threatening disease if left untreated. Almost one million deaths per year are reported due to HBV [7]. According to the report by [8], HBV is very common in many parts of the Asia-Pacific and sub-Saharan Africa. It is estimated that around 45% of the world's population resides in high-risk regions for HBV. However, unlike HIV, a vaccine exists to prevent HBV infection. Furthermore, treatment is also available for individuals infected with HBV. HBV may spread among humans through percutaneous or mucosal contact with infected blood and body fluids [9]. There is a difference in the predominant transmission routes of HBV between low- and high-risk areas. In low-risk areas, HBV spreads during adolescence and early adulthood, often linked to high-risk behaviors such as unprotected sex and injection drug use [9]. In contrast, HBV is mostly transmitted vertically and horizontally in high-risk areas [10]. However, HBV is not transmitted through breastfeeding, kissing, sneezing, or sharing food or

[11]. Another important aspect of HBV is that it can remain infectious on moist surfaces for weeks [12, 13]. Since it was first time implemented massively in 1982, HBV vaccine already give a protection to vaccinated individuals and significantly reduce global HBV infections [11, 14]. This HBV vaccine available for any ages. In the United States, three single-antigen vaccines – ENGERIX-B, RECOMBIVAX HB, and HEPLISAV – are licensed, along with two combination vaccines, PEDIARIX and TWINRIX [11]. Although HBV vaccine succeeded to reduce the global spread of HBV, it is still a major concern worldwide because if HBV becomes more severe, it may lead to high morbidity and mortality rates. A significant number of people with HBV remain asymptomatic and may be oblivious to their illness.

Since it was first introduced by Kermack and McKendrick in 1927, modifications of the compartmental epidemic model have been widely used to model the spread of diseases in populations, including HIV, HBV, and co-infections between HIV and HBV [15–19]. A mathematical model for HIV/AIDS transmission in a population was introduced by Ayele et al. in [20], authors discussed the impact of screening and treatment strategies while also considering the effect of media campaigns on population awareness. They concluded that implementing both preventive measures and screening together is the most cost-effective strategy to reduce HBV transmission. Sharomi and Gumel [21] formulated and rigorously analyzed a deterministic mathematical model for HIV treatment, accounting for both wild (drug-sensitive) and drug-resistant strains. Their work provided insights into the dynamics of these strains and identified effective control measures for HIV spread. From this research, they concluded that the extensive implementation of therapy for the wild strain can lead to its eradication from the community, provided that the reduction in the infectiousness of treated individuals does not surpass a defined threshold. Omondi et al. [22] developed and qualitatively analyzed a model to examine the transmission dynamics of HIV among commercial sex workers and injection drug users. Their findings indicated that an increased uptake of pre-exposure prophylaxis (PrEP) correlates with a decrease in the number of HIV patients receiving ART. Ullah et al. [23] developed and analyzed a mathematical model to explore the dynamics of HBV, incorporating optimal control analysis with a focus on the hospitalized population. They introduced three time-varying control strategies: isolation of infected individuals, intensive public education and awareness campaigns, and treatment of hospitalized patients, along with early vaccination against HBV. Their findings indicated that simultaneously implementing all three strategies could significantly reduce the number of infected individuals. Khan et al. [24] presented a mathematical model for the transmission dynamics of acute and chronic hepatitis B epidemics in a community. Their study revealed that treatment, isolation, and vaccination control are effective in eradicating HBV from the community. Furthermore, same author in [25] proposed and qualitatively analyzed a mathematical model for HBV with a convex incidence rate.

Omede et al. [26] developed a deterministic mathematical model to investigate the transmission dynamics of HIV and

Zika virus co-infection, integrating both vertical and horizontal transmission routes. Their research shown that both diseases can endure when their fundamental reproduction numbers surpass one. Moreover, they observed that higher HIV treatment rates substantially lower the prevalence of Zika virus co-infection. Nwankwo and Okuonghae [27] formulated a mathematical model to describe the transmission dynamics of HIV and syphilis co-infection in a population where syphilis treatment is readily available. Although numerous models exist for various co-infections, relatively few have focused on HIV and HBV co-infection. Endashaw and Mekonnen [28] constructed and rigorously examined a deterministic model to assess the impact of hepatitis B vaccination and treatment interventions on disease dynamics. Their findings underscored that extensive immunization against HBV, together with effective treatment for both HBV and HIV/AIDS, is essential for reducing the transmission of both illnesses, which pose considerable public health challenges. Ullah et al. [29] introduced a fractional-order mathematical model to examine the co-infection dynamics of HBV and HIV in Taiwan. Their study suggested that expanding HBV vaccination programs has a favorable effect in reducing the burden of co-infection. Endashaw et al. [30] developed a mathematical framework to evaluate the role of mother-to-child transmission (MTCT) in shaping HBV and HIV co-infection trends. Their study revealed that elevated MTCT rates for both viruses exacerbated the co-infection burden, while a reduction in MTCT rates facilitated decreased transmission, potentially resulting in a decline in HBV and HIV/AIDS co-infection cases over time. James et al. [31] proposed a stochastic differential equation (SDE) model featuring continuous state and parameter spaces to examine the dynamics of HIV and HBV co-infection.

Recent research has established mathematical models to assess the dynamics and control tactics of HBV and HIV/AIDS co-infections, stressing the efficiency of combination therapies [32, 33]. Advanced modeling techniques have been used to study HIV transmission patterns, and optimal control strategies have been developed to prevent the spread of HBV and COVID-19 coepidemics [34–37].

This study enhances prior models by refining the compartmental framework for HBV infection. We specifically categorized the HBV-infected population into acute and chronic stages, thereby rectifying the limitations of prior models that treated HBV infection as a singular compartment. Moreover, in contrast to other models that concentrated mostly on mother-to-child HBV transmission, our model integrates the simultaneous transmission dynamics of both HBV and HIV. Another crucial element of our research is the categorization of the HIV-infected population into two distinct subgroups: individuals exhibiting clinical symptoms of AIDS and those who are asymptomatic—an important differentiation that has been largely overlooked in previous studies. This study is, to our knowledge, the first to comprehensively incorporate dual HBV-HIV transmission and the differentiation of HIV. A rigorous analysis of the proposed model has yielded novel insights into the dynamics of co-infection. The paper is structured as follows: We dedicated the model formulation in details along with all the model assumptions in Section 2; model analysis on submodel and co-infection model were analyzed in Section 3; numerical experiments conducted in Section 4; and Section 5 provides concluding observations.

## 2 | Model Formulation

We begin our model construction by dividing the total of human population ( $N(t)$ ) into 14 compartments based on their health status respect to HIV and/or HBV as follows:

1.  $S(t)$ : Susceptible compartment;
2.  $I_H(t)$ : Asymptomatic HIV-infected compartment;
3.  $A_H(t)$ : Symptomatic HIV-infected compartment;
4.  $T_H(t)$ : HIV-treated compartment;
5.  $V_B(t)$ : Vaccinated compartment against HBV;
6.  $I_{AB}(t)$ : HBV-infected acute compartment;
7.  $I_{CB}(t)$ : HBV-infected chronic compartment;
8.  $T_B(t)$ : HBV-treated compartment;
9.  $R(t)$ : Recovered compartment;
10.  $I_{HAB}(t)$ : Asymptomatic HIV with acute HBV infection compartment;
11.  $I_{HCB}(t)$ : Asymptomatic HIV with chronic HBV infection compartment;
12.  $I_{AAB}(t)$ : Symptomatic HIV with acute HBV infection compartment;
13.  $I_{ACB}(t)$ : Symptomatic HIV with chronic HBV infection compartment;
14.  $T_{HB}(t)$ : HIV-HBV-treated compartment.

Based on above description, we have

$$N(t) = S(t) + I_H(t) + A_H(t) + T_H(t) + V_B(t) + I_{AB}(t) + I_{CB}(t) + T_B(t) + R(t) + I_{HAB}(t) + I_{HCB}(t) + I_{AAB}(t) + I_{ACB}(t) + T_{HB}(t).$$

We start our model construction as follows. The population of susceptible compartment. The population of  $S$  increases due to recruitment from newborn or migration with a constant rate of  $\pi$ . Fraction  $\varepsilon_1$  of the newborn or migrated individuals assumed to be born with HIV,  $\varepsilon_2$  with HBV, and  $\varepsilon_3$  with both HIV and HBV. Furthermore, the HIV infection caused by effective contact with infected individuals of HIV is given by  $\lambda_H$ , which is

$$\lambda_H = \frac{(1-rz)\beta_H(I_H + c_1(A_H + I_{AAB} + I_{ACB}) + c_2(T_H + T_{HB}) + I_{HAB} + I_{HCB})}{N},$$

where  $r$  is the compliance rate to the usage of condom,  $z$  is the efficacy rate to the usage of condom,  $\beta_H$  is the HIV successful transmission probability, and  $c_1$  is a modification factor that reflects the heightened infectiousness associated with elevated viral loads in persons manifesting clinical signs of AIDS, as contrast to asymptomatic HIV-infected individuals. Likewise,  $c_2$  represents modification parameters that indicate the diminished transmission risk from patients getting treatment just for HIV ( $T_H(t)$ ) and those receiving treatment for both HIV and HBV co-infection ( $T_{HB}(t)$ ). This decrease arises from treated persons' awareness of their HIV status and their enhanced knowledge of preventative strategies to curtail the virus's transmission.

Similarly, vulnerable individuals may acquire HBV through direct contact with HBV-infected persons with a transmission rate of  $\lambda_B$ , defined as follows:

$$\lambda_B = \frac{(1 - rz)\beta_B(I_{AB} + I_{CB} + I_{HAB} + I_{HCB} + I_{AAB} + I_{ACB})}{N},$$

where  $\beta_B$  is the HBV successful transmission probability. Individuals at risk who encounter those infected with HIV contract the virus at a rate of  $\lambda_H$  and subsequently advance to exhibit clinical signs of AIDS at a rate of  $\eta$ . The parameters  $\sigma_1$  and  $\sigma_2$  denote the treatment rates for HIV-infected patients who are asymptomatic and symptomatic with AIDS, respectively. Individuals with HIV displaying clinical indications of AIDS may perish from the illness at a rate of  $\delta_H$ . Individuals who get infected with HIV, who do not exhibit clinical signs of AIDS, may acquire HBV by effective contact with HBV-infected persons at a rate of  $e_1\lambda_B$ , where  $e_1$  is a modification parameter indicating heightened sensitivity to HBV as a result of HIV infection. Individuals exhibiting clinical signs of AIDS contract HBV at a rate of  $e_2\lambda_B$ , where  $e_2$  represents the increased vulnerability linked to HIV infection. Furthermore, individuals undergoing treatment for HIV alone contract HBV through effective contact with HBV-infected individuals at a rate of  $e_3\lambda_B$ , where  $e_3$  denotes a modification factor that accounts for the diminished risk of HBV infection attributable to heightened awareness and education regarding sexually transmitted diseases during treatment.  $\phi_1\delta_H$  signifies the disease-induced mortality rate among persons with HIV who are receiving therapy, where  $\phi_1$  represents the decrease in HIV-related fatalities attributable to the medication.

Susceptible individuals exposed to HBV-infected individuals becomes acute HBV at a rate of  $\lambda_B$  and progress to the chronic stage at a rate of  $\psi$ . HBV vaccination occurs at a rate of  $\alpha$ , while the vaccine wanes over time at a rate of  $\gamma$ . The parameters  $\tau_1$  and  $\tau_2$  represent the treatment rates for individuals with acute and chronic HBV infections, respectively. Individuals receiving treatment for HBV infection recover at a rate of  $q$ , whereas those infected with HBV alone face disease-induced mortality at a rate of  $\delta_B$ . The mortality associated with HBV for treated individuals is represented by  $\phi_2\delta_B$ , where  $\phi_2$  reflects the decrease in HBV-related mortality attributable to therapy. Individuals who have recovered from HBV may experience reinfection at a rate of  $e_9\lambda_B$ , where  $e_9$  functions as a modification parameter reflecting the probability of reinfection. Vaccinated individuals may acquire HIV at a rate of  $e_7\lambda_H$ , where  $e_7$  represents the influence of the HBV vaccine on partial immunity. Those with acute HBV alone can contract HIV at a rate of  $e_4\lambda_H$ , with  $e_4$  reflecting a reduction in sexual activity due to illness. Likewise, individuals with chronic HBV get HIV at a rate of  $e_5\lambda_H$ , where  $e_5$  accounts for reduced sexual activity resulting from health issues. Individuals infected with HBV who are undergoing treatment may contract HIV at a rate of  $e_6\lambda_H$ , where  $e_6$  denotes the decreased risk of HIV infection attributable to enhanced knowledge and education on sexually transmitted infections during treatment. Furthermore, those who have recovered from HBV remain susceptible to contracting HIV at a rate of  $e_8\lambda_H$ , where  $e_8$  reflects the vulnerability of those previously infected with HBV to HIV.

The population of individuals co-infected with HIV (without clinical symptoms of AIDS) and acute HBV arises from various

transmission pathways. These include HIV-infected individuals without AIDS symptoms who contract HBV at a rate of  $e_1\lambda_B$ , as well as treated HIV-infected individuals who acquire HBV at a rate of  $(1 - d)e_3\lambda_B$ , where  $(1 - d)$  represents the proportion of treated HIV individuals who do not exhibit AIDS symptoms. Additionally, acute HBV-infected individuals who acquire HIV at a rate of  $e_4\lambda_H$  contribute to this population, along with treated HBV-infected individuals who contract HIV at a rate of  $(1 - p)e_6\lambda_H$ , where  $(1 - p)$  is the proportion of HBV-treated individuals still in the acute infection stage. Furthermore, a fraction of individuals with both infections from birth or migration enter this category at a rate of  $\epsilon_3\pi$ . The treatment rate for individuals co-infected with HIV (without clinical symptoms of AIDS) and acute HBV is given by  $\omega_1$ , while their disease-induced mortality occurs at a rate of  $\delta_{HAB}$ . The progression rate  $\nu$  determines the transition from this class to those infected with both HIV (with clinical symptoms of AIDS) and acute HBV, as well as those progressing to chronic HBV infection while still in the HIV-infected (without AIDS symptoms) stage.

The population of individuals infected with both HIV (asymptomatic) and chronic HBV infection comprises those with chronic HBV infection who contracted HIV at the rate  $e_5\lambda_H$ , treated individuals with HBV infection who acquired HIV at the rate  $pe_6\lambda_H$  (where  $p$  represents the fraction of treated individuals with chronic HBV), and the fraction of individuals with both HIV (asymptomatic) and acute HBV infection who transitioned to the class of individuals with both HIV (asymptomatic) and chronic HBV infection at the rate  $(1 - \kappa)\nu$ . Note that  $(1 - \kappa)$  denotes the fraction of individuals with both HIV (asymptomatic) and acute HBV infection that progressed to being infected with both HIV (asymptomatic) and chronic HBV infection. Furthermore, the rates  $\omega_2$  and  $\delta_{HCB}$  represent the treatment rate and the disease-induced mortality rate of infected persons with both HIV (asymptomatic for AIDS) and chronic HBV infection, respectively. There is a rate  $\xi_1$  that shows how fast people move from having HIV (without symptoms) and chronic HBV infection to having HIV (with symptoms of AIDS) and chronic HBV infection. The cohort of individuals infected with both HIV (exhibiting clinical symptoms of AIDS) and acute HBV infection arises from HIV-only infected individuals with clinical symptoms of AIDS who contracted HBV at a rate of  $e_2\lambda_B$ , treated HIV-only individuals who acquired HBV at a rate of  $de_3\lambda_B$  (where  $d$  represents the fraction of treated HIV individuals displaying clinical symptoms of AIDS), and the remaining fraction of individuals infected with both HIV (not exhibiting clinical symptoms of AIDS) and acute HBV infection who transitioned to the class of individuals infected with both HIV (showing clinical symptoms of AIDS) and acute HBV infection at a rate of  $\kappa\nu$ . The numbers  $\omega_3$  and  $\delta_{AAB}$  describe the treatment rate and the disease-related death rate of people who are infected with HIV (showing symptoms of AIDS) and acute HBV, respectively. The rate  $\xi_2$  denotes the transition rate from the infected class exhibiting both HIV (with clinical manifestations of AIDS) and acute HBV infection to the infected class exhibiting both HIV (with clinical manifestations of AIDS) and chronic HBV infection. The rates  $\omega_4$  and  $\delta_{ACB}$  represent the treatment rate and the disease-induced mortality rate of infected persons with both HIV (exhibiting clinical signs of AIDS) and chronic HBV infection, respectively. The rates  $\delta_{THB}$  and  $\mu$  represent the disease-induced mortality rate and the recovery rate of treated persons with both HIV/AIDS and HBV infections, who

**TABLE 1** | Description of the model variables and parameters.

Variable	Description
$S$	Susceptible individuals.
$I_H$	HIV-only-infected individuals with no clinical symptoms of AIDS.
$A_H$	HIV-only-infected individuals with clinical symptoms of AIDS.
$T_H$	Treated individuals with HIV only.
$V_B$	Vaccinated individuals against HBV.
$I_{AB}$	HBV-only-infected individuals with acute infection.
$I_{CB}$	HBV-only-infected individuals with chronic infection.
$T_B$	Treated individuals with HBV only.
$R$	Recovered individuals.
$I_{HAB}$	Infected individuals with both HIV (not showing clinical symptoms of AIDS) and acute HBV infection.
$I_{HCB}$	Infected individuals with both HIV (not showing clinical symptoms of AIDS) and chronic HBV infection.
$I_{AAB}$	Infected individuals with both HIV (showing clinical symptoms of AIDS) and acute HBV infection.
$I_{ACB}$	Infected individuals with both HIV (showing clinical symptoms of AIDS) and chronic HBV infection.
$T_{HB}$	Treated individuals dually infected with both HIV (showing and not showing clinical symptoms of AIDS) and HBV (acute and chronic) infection.
<b>Parameter</b>	<b>Description</b>
$\pi$	Recruitment rate.
$\theta$	Natural death rate.
$\varepsilon_1, \varepsilon_2, \varepsilon_3$	Fraction of individuals that are infected with HIV, HBV, and both HIV and HBV from birth or migration.
$\alpha$	HBV vaccination rate.
$\beta_B(\beta_H)$	Transmission rate for HBV (HIV).
$\gamma$	waning rate of HBV vaccination.
$r$	Compliance rate to the usage of condom.
$z$	Efficacy of condom usage.
$\sigma_1$	Treatment rate of HIV-only-infected individuals with no clinical symptoms of AIDS.
$\sigma_2$	Treatment rate of HIV-only-infected individuals showing clinical symptoms of AIDS.
$\eta$	Progression rate from $I_H$ to $A_H$ class.
$c_1$	Modification parameter that accounts for increase in infectiousness for individual showing clinical symptoms of AIDS.
$c_2$	Modification parameter that accounts for decrease in HIV infectiousness for individuals receiving HIV treatment.
$\delta_H$	HIV-only disease-included death rate.
$\psi$	Progression rate of individuals from $I_{AB}$ to $I_{CB}$ class.
$\tau_1$	Treatment rate for $I_{AB}$ class.
$\tau_2$	Treatment rate for $I_{CB}$ class.
$\delta_B$	HBV-only disease-induced death rate.
$\phi_1, \phi_2$	Modification parameters for reduction in disease-induced death while receiving treatment.
$q$	Recovery rate of treated individuals with HBV only.
$\mu$	The rate at which treated individuals with both HIV and HBV recovers from HBV only and continue receiving treatment for HIV only.
$\omega_1, \omega_2, \omega_3, \omega_4$	Treatment rate of individuals in $I_{HAB}$ class, $I_{HCB}$ class, $I_{AAB}$ class, and $I_{ACB}$ class, respectively.
$e_1, e_2, e_3$	Modification parameters that accounts for increase in susceptibility to HBV infection due to HIV infection.

(Continues)

**TABLE 1** | (Continued)

Variable	Description
$e_4, e_5, e_6$	Modification parameters that accounts for decrease in sexual activities due to ill health.
$e_7, e_8, e_9$	Modification parameters.
$\nu$	Progression rate from $I_{HAB}$ class to either $I_{HCB}$ class or $I_{AAB}$ class.
$\kappa$	Fraction of individuals in $I_{HAB}$ class that progressed to $I_{AAB}$ class.
$\xi_1$	Progression rate from $I_{HCB}$ class to $I_{ACB}$ class.
$\xi_2$	Progression rate from $I_{AAB}$ class to $I_{ACB}$ class.
$\delta_{HAB}$	Disease-induced death rate for individuals in $I_{HAB}$ class.
$\delta_{HCB}$	Disease-induced death rate for individuals in $I_{HCB}$ class.
$\delta_{AAB}$	Disease-induced death rate for individuals in $I_{AAB}$ class.
$\delta_{ACB}$	Disease-induced death rate for individuals in $I_{ACB}$ class.
$\delta_{THB}$	Disease-induced death rate for individuals in $T_{HB}$ class.
$d$	Fraction of HIV-treated individuals that are showing clinical symptoms of AIDS that contracted HBV infection.
$p$	Fraction of HBV-treated individuals with chronic infection that contracted HIV infection.

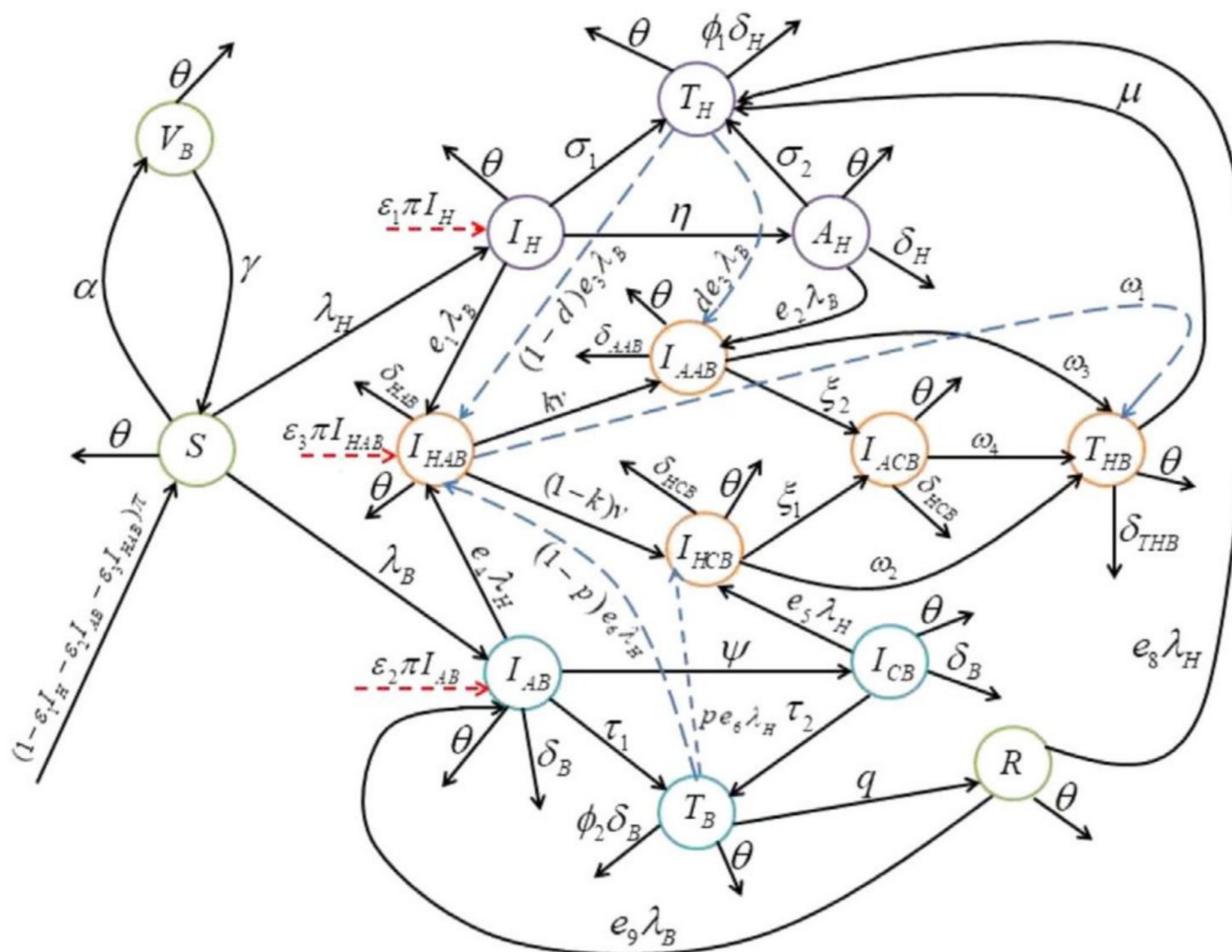


**FIGURE 1** | Flowchart of the HIV-HBV co-infection model. [Colour figure can be viewed at [wileyonlinelibrary.com](https://onlinelibrary.wiley.com)]

recover only from HBV while continuing treatment exclusively for HIV (Table 1).

Based on the above formulation and assumptions, the HIV and HBV co-infection model is given by the following set of nonlinear differential equations (Figure 1):

$$\begin{aligned} \frac{dS}{dt} &= (1 - \varepsilon_1 I_H - \varepsilon_2 I_{AB} - \varepsilon_3 I_{HAB})\pi \\ &\quad - (\lambda_H + \lambda_B)S - (\alpha + \theta)S + \gamma V_B, \\ \frac{dI_H}{dt} &= \lambda_H S + \varepsilon_1 \pi I_H + e_7 \lambda_H V_B + e_8 \lambda_H R \\ &\quad - e_1 \lambda_B I_H - (\eta + \sigma_1 + \theta) I_H, \end{aligned}$$

$$\begin{aligned} \frac{dA_H}{dt} &= \eta I_H - e_2 \lambda_B A_H - (\sigma_2 + \delta_H + \theta) A_H, \\ \frac{dT_H}{dt} &= \sigma_1 I_H + \sigma_2 A + \mu T_{HB} - e_3 \lambda_B T_H - (\phi_1 \delta_H + \theta) T_H, \\ \frac{dV_B}{dt} &= \alpha S - e_7 \lambda_H V_B - (\gamma + \theta) V_B, \\ \frac{dI_{AB}}{dt} &= \lambda_B S + \varepsilon_2 \pi I_{AB} - e_4 \lambda_H I_{AB} + e_9 \lambda_B R \\ &\quad - (\psi + \tau_1 + \delta_B + \theta) I_{AB}, \end{aligned}$$

$$\begin{aligned}
 \frac{dI_{CB}}{dt} &= \psi I_{AB} - e_5 \lambda_H I_{CB} - (\tau_2 + \delta_B + \theta) I_{CB}, \\
 \frac{dT_B}{dt} &= \tau_1 I_{AB} + \tau_2 I_{CB} - e_6 \lambda_H T_B - (q + \phi_2 \delta_B + \theta) T_B, \\
 \frac{dR}{dt} &= q T_B - (e_8 \lambda_H + e_9 \lambda_B + \theta) R, \\
 \frac{dI_{HAB}}{dt} &= e_1 \lambda_B I_H + (1-d)e_3 \lambda_B T_H + e_4 \lambda_H I_{AB} \\
 &\quad + (1-p)e_6 \lambda_H T_B + \varepsilon_3 \pi I_{HAB} \\
 &\quad - (v + \omega_1 + \delta_{HAB} + \theta) I_{HAB}, \\
 \frac{dI_{HCB}}{dt} &= e_5 \lambda_H I_{CB} + p e_6 \lambda_H T_B + (1-\kappa)v I_{HAB} \\
 &\quad - (\xi_1 + \omega_2 + \delta_{HCB} + \theta) I_{HCB}, \\
 \frac{dI_{AAB}}{dt} &= e_2 \lambda_B A_H + d e_3 \lambda_B T_H + \kappa v I_{HAB} \\
 &\quad - (\xi_2 + \omega_3 + \delta_{AAB} + \theta) I_{AAB}, \\
 \frac{dI_{ACB}}{dt} &= \xi_1 I_{HCB} + \xi_2 I_{AAB} - (\omega_4 + \delta_{ACB} + \theta) I_{ACB}, \\
 \frac{dT_{HB}}{dt} &= \omega_1 I_{HAB} + \omega_2 I_{HCB} + \omega_3 I_{AAB} \\
 &\quad + \omega_4 I_{ACB} - (\delta_{THB} + \mu + \theta) T_{HB}, \tag{1}
 \end{aligned}$$

where

$$\begin{aligned}
 \lambda_H &= \frac{(1-rz)\beta_H(I_H + c_1(A_H + I_{AAB} + I_{ACB}) + c_2(T_H + T_{HB}) + I_{HAB} + I_{HCB})}{N}, \quad \text{and} \\
 \lambda_B &= \frac{(1-rz)\beta_B(I_{AB} + I_{CB} + I_{HAB} + I_{HCB} + I_{AAB} + I_{ACB})}{N}.
 \end{aligned}$$

It is pertinent to highlight some of the main assumptions in the model formulation:

1. Both HIV and HBV can be transmitted from mother to child during pregnancy or child birth [3, 10].
2. Disease-induced death rate occurs to only HIV-infected individuals showing clinical symptoms of AIDS.
3. There is no recovery from HIV.
4. Natural death rate is the same in all compartments.
5. Infection can still take place in the treatment classes.

## 2.1 | Basic Properties of the Model

### 2.1.1 | Positivity of Solution

The biological validity of the HIV and HBV co-infection model (1) relies on ensuring that the solution of the system remains positive for all values of time  $t$ . Thus, it is essential to demonstrate that all state variables in the HIV and HBV co-infection model (1) remain nonnegative for all  $t > 0$ .

**Theorem 1.** Let the initial data for the HIV and HBV co-infection model (1) be  $S(0) > 0, I_H(0) \geq 0, A_H(0) \geq 0, T_H(0) \geq 0, V_B(0) \geq 0, I_{AB}(0) \geq 0, I_{CB} \geq 0, T_B(0) \geq 0, R(0) \geq 0, I_{HAB}(0) \geq 0, I_{HCB}(0) \geq 0, I_{AAB}(0) \geq 0, I_{ACB}(0) \geq 0, T_{HB}(0) \geq 0$ . Then, the solutions  $(S, I_H, A_H, T_H, V_B, I_{AB}, I_{CB}, T_B, R, I_{HAB}, I_{HCB}, I_{AAB}, I_{ACB}, T_{HB})$  of the HIV and HBV co-infection model are nonnegative for all time  $t > 0$ .

*Proof.* Let  $t_f = \sup \{t > 0 : (S > 0, I_H > 0, A_H > 0, T_H > 0, V_B > 0, I_{AB} > 0, I_{CB} > 0, T_B > 0, R > 0, E_{HZ} > 0, H_1 > 0, H_2 > 0, H_3 > 0, I_{HZ} > 0, I_{AZ} > 0, T_{HZ} > 0, S_m > 0, E_m > 0, I_m > 0) \in [0, t]\}$ .

From the first equation of the HIV and HBV co-infection model system (1), we have

$$\begin{aligned}
 \frac{dS}{dt} &= (1 - \varepsilon_1 I_H - \varepsilon_2 I_{AB} - \varepsilon_3 I_{HAB}) \pi \\
 &\quad - (\lambda_H + \lambda_B) S - (\alpha + \theta) S + \gamma V_B. \tag{2}
 \end{aligned}$$

Solving the above equation, we obtained

$$\begin{aligned}
 \frac{d}{dt} \left\{ S(t) \left[ \exp \left( \int_0^t (\lambda_H(v) + \lambda_B(v)) dv + (\alpha + \theta)t \right) \right] \right\} \\
 = ((1 - \varepsilon_1 I_H - \varepsilon_2 I_{AB} - \varepsilon_3 I_{HAB}) \pi + \gamma V_B) \times \\
 \exp \left( \int_0^t (\lambda_H(v) + \lambda_B(v)) dv + (\alpha + \theta)t \right). \tag{3}
 \end{aligned}$$

Integrating the above equation at the range  $[0, t_f]$ , we obtained

$$\begin{aligned}
 \left\{ S(t) \exp \left[ \int_0^{t_f} (\lambda_H(v) + \lambda_B(v)) dv + (\alpha + \theta)t_f \right] \right\} - S(0) \\
 = ((1 - \varepsilon_1 I_H - \varepsilon_2 I_{AB} - \varepsilon_3 I_{HAB}) \pi + \gamma V_B) \times \\
 \int_0^{t_f} \exp \left[ \int_0^x (\lambda_H(v) + \lambda_B(v)) dv + (\alpha + \theta)x \right] dx.
 \end{aligned}$$

So that

$$\begin{aligned}
 S(t) &= S(0) \exp \left[ - \left( \int_0^{t_f} (\lambda_H(v) + \lambda_B(v)) dv + (\alpha + \theta)t_f \right) \right] \\
 &\quad + \exp \left[ - \left( \int_0^{t_f} (\lambda_H(v) + \lambda_B(v)) dv + (\alpha + \theta)t_f \right) \right] \\
 &\quad \times ((1 - \varepsilon_1 I_H - \varepsilon_2 I_{AB} - \varepsilon_3 I_{HAB}) \pi + \gamma V_B) \int_0^{t_f} \\
 &\quad \exp \left[ \int_0^x (\lambda_H(v) + \lambda_B(v)) dv + (\alpha + \theta)x \right] dx > 0.
 \end{aligned}$$

Similarly, it can be shown that  $I_H > 0, A_H > 0, T_H > 0, V_B > 0, I_{AB} > 0, I_{CB} > 0, T_B > 0, R > 0, I_{HAB} > 0, I_{HCB} > 0, I_{AAB} > 0, I_{ACB} > 0$ , and  $T_{HB} > 0$ .  $\square$

## 2.1.2 | Invariant Region

**Lemma 1.** *The region*

$$\Omega = \left\{ (S, I_H, A_H, T_H, V_B, I_{AB}, I_{CB}, T_B, R, I_{HAB}, I_{HCB}, I_{AAB}, I_{ACB}, T_{HB}) \in \mathbb{R}_+^{14} : N \leq \frac{\pi}{\theta} \right\}$$

is positively invariant and attracts all solution in  $\mathfrak{R}_+^{10}$  [38].

*Proof.* By adding the equations of the HIV and HBV co-infection model (1), the rate of change of the total population is given by

$$\begin{aligned} \frac{dN}{dt} = & \pi - \theta N - \delta_H(A_H + \phi_1 T_H) \\ & - \delta_B(I_{AB} + I_{CB} + \phi_2 T_B) - \delta_{HAB} I_{HAB} - \delta_{HCB} I_{HCB} \\ & - \delta_{AAB} I_{AA} - \delta_{ACB} I_{ACB} - \delta_{THB} T_{HB}. \end{aligned} \quad (4)$$

Thus,  $\frac{dN}{dt} < 0$  whenever  $N > \frac{\pi}{\theta}$ . Because it follows that the right-hand side of the inequality (4) is bounded by  $\pi - \theta N$ , it can be shown using a standard comparison theorem from [39] that

$$N(t) \leq N(0)e^{-\theta t} + \frac{\pi}{\theta}(1 - e^{-\theta t}) \quad (5)$$

Hence, it follows that  $N(t) \leq \frac{\pi}{\theta}$ , if  $N(0) \leq \frac{\pi}{\theta}$ . Thus, the closed region  $\Omega$  is positively invariant and attracts all the solution in  $\mathbb{R}_+^{14}$ . Consequently, the HIV and HBV co-infection model (1) is both mathematically and biologically well-posed within the region  $\Omega$ . Thus, it is adequate to analyze the dynamics of the HIV and HBV co-infection model (1) within this region, as established in prior studies [38, 40].  $\square$

## 3 | Model Analysis

In this section, we will conduct a thorough analysis of the HIV and HBV co-infection model (1). Our analysis will include the calculation of the basic reproduction number, an evaluation of the stability of both the disease-free and endemic equilibria, a sensitivity analysis of the basic reproduction number, and an exploration of how each disease influences the other. To facilitate our analysis, we will decompose the co-infection model into two submodels: one focusing solely on HIV and the other on HBV.

### 3.1 | HIV-Only Submodel

The HIV-only submodel is derived by setting the HBV and co-infection compartments to zero, specifically  $V_B = I_{AB} = I_{CB} = T_B = R = I_{HAB} = I_{HCB} = I_{AAB} = I_{ACB} = T_{HB} = 0$  in the HIV and HBV co-infection model (1). Consequently, the HIV-only submodel is represented as follows:

$$\begin{aligned} \frac{dS}{dt} &= (1 - \varepsilon_1 I_H)\pi - \lambda_H S - \theta S, \\ \frac{dI_H}{dt} &= \lambda_H S + \varepsilon_1 \pi I_H - (\eta + \sigma_1 + \theta)I_H, \\ \frac{dA_H}{dt} &= \eta I_H - (\sigma_2 + \delta_H + \theta)A_H, \\ \frac{dT_H}{dt} &= \sigma_1 I_H + \sigma_2 A_H - (\phi_1 \delta_H + \theta)T_H, \end{aligned} \quad (6)$$

where

$$\lambda_H = \frac{(1 - rz)\beta_H(I_H + c_1 A_H + c_2 T_H)}{N}.$$

It can be shown that the closed region

$$\Omega_1 = \left\{ (S, I_H, A_H, T_H) \in \mathbb{R}_+^4 : S + I_H + A_H + T_H \leq \frac{\pi}{\theta} \right\}$$

is positively invariant. Hence, it is adequate to consider the dynamics of the HIV-only submodel in  $\Omega_1$ .

#### 3.1.1 | The Disease-Free Equilibrium of the HIV-Only Submodel (DFEH)

The HIV disease-free equilibrium represents a steady state characterized by the absence of HIV infections within the population. This equilibrium is achieved by setting the right-hand side of the HIV-only submodel (6) to zero and ensuring that the infected variables (specifically  $I_H = A_H = T_H = 0$ ) are also set to zero. Therefore, the disease-free equilibrium for the HIV-only submodel is expressed as follows:

$$\chi_0^H = (S^*, I_H^*, A_H^*, T_H^*) = \left( \frac{\pi}{\theta}, 0, 0, 0 \right) \quad (7)$$

#### 3.1.2 | HIV Basic Reproduction Number

The HIV basic reproduction number, denoted as  $\mathcal{R}_0^H$ , is a critical parameter that influences the transmission dynamics of HIV within a population. It quantifies the expected number of secondary infections generated by a single HIV-infected individual introduced into a completely susceptible population. Understanding  $\mathcal{R}_0^H$  is essential for predicting the potential spread of the disease and for informing control measures aimed at preventing transmission. When  $\mathcal{R}_0^H$  exceeds 1, it indicates a potential outbreak, while a value below 1 suggests that the disease may not sustain transmission within the population. The HIV basic reproduction number can be calculated using the next generation operator method, as outlined in [41]. Following the methodology described in [41], the nonnegative matrix  $\mathcal{F}$  representing new infections and the nonsingular matrix  $\mathcal{V}$  for the remaining transition terms at the HIV-only disease-free equilibrium are defined as follows:

$$\mathcal{F} = \begin{bmatrix} (1 - rz)\beta_H + \varepsilon_1 \pi & (1 - rz)\beta_H c_1 & (1 - rz)\beta_H c_2 \\ 0 & 0 & 0 \\ 0 & 0 & 0 \end{bmatrix}, \text{ and}$$

$$\mathcal{V} = \begin{bmatrix} (\eta + \sigma_1 + \theta) & 0 & 0 \\ -\eta & (\sigma_2 + \delta_H + \theta) & 0 \\ -\sigma_1 & -\sigma_2 & (\phi_1 \delta_H + \theta) \end{bmatrix}.$$

Hence, it follows from [41] that  $\mathcal{R}_0^H = \rho(\mathcal{F}\mathcal{V}^{-1})$ , where  $\rho$  is the spectral radius or largest eigenvalue of the matrix  $\mathcal{F}\mathcal{V}^{-1}$ .

Thus,

$$\mathcal{R}_0^H = \frac{(1 - rz)\beta_H(K_2 K_3 + c_1 \eta K_3 + c_2(\sigma_1 K_2 + \eta \sigma_2))}{K_1 K_2 K_3} + \frac{\varepsilon_1 \pi}{K_1} \quad (8)$$

where  $K_1 = \eta + \sigma_1 + \theta$ ,  $K_2 = \sigma_2 + \delta_H + \theta$ , and  $K_3 = \phi_1 \delta_H + \theta$ .

### 3.1.3 | Local Stability of the HIV-Only Disease-Free Equilibrium

**Theorem 2.** *The disease-free equilibrium  $(\chi_0^H)$  of the HIV-only submodel (6) is locally asymptotically stable if  $\mathcal{R}_0^H < 1$  and unstable if  $\mathcal{R}_0^H > 1$ .*

*Proof.* We analyzed the local stability of the disease-free equilibrium of the HIV-only submodel by obtaining the Jacobian matrix of the HIV-only submodel (6) and evaluating at the HIV disease-free equilibrium, given by

$$J(\chi_0^H) = \begin{bmatrix} -\theta & -((1-rz)\beta_H + \varepsilon_1\pi) & -(1-rz)\beta_H c_1 & -(1-rz)\beta_H c_2 \\ 0 & ((1-rz)\beta_H + \varepsilon_1\pi) - K_1 & (1-rz)\beta_H c_1 & (1-rz)\beta_H c_2 \\ 0 & \eta & -K_2 & 0 \\ 0 & \sigma_1 & \sigma_2 & -K_3 \end{bmatrix},$$

where  $K_1 = \eta + \sigma_1 + \theta$ ,  $K_2 = \sigma_2 + \delta_H + \theta$ , and  $K_3 = \phi_1 \delta_H + \theta$ . The roots of the Jacobian matrix  $J(\chi_0^H)$  are  $\lambda_1 = -\theta$  and the roots of the characteristic equation below:

$$\mathcal{A}(\lambda) = \lambda^3 + \mathcal{P}_1 \lambda^2 + \mathcal{P}_2 \lambda + \mathcal{P}_3 \quad (9)$$

where

$$\begin{aligned} \mathcal{P}_1 &= K_1 + K_2 + K_3 - ((1-rz)\beta_H + \varepsilon_1\pi), \\ \mathcal{P}_2 &= K_1 K_2 + K_1 K_3 + K_2 K_3 \\ &\quad - ((1-rz)\beta_H (K_2 + K_3 + \eta c_1 + \sigma_1 c_2) + \varepsilon_1 \pi (K_2 + K_3)), \\ \mathcal{P}_3 &= K_1 K_2 K_3 (1 - \mathcal{R}_0^H). \end{aligned}$$

Applying the Routh-Hurwitz criterion [42] to the polynomial in Equation (9), which states that all roots of the characteristic polynomial  $\mathcal{A}(\lambda)$  have negative real parts if  $\mathcal{P}_1 > 0$ ,  $\mathcal{P}_2 > 0$ ,  $\mathcal{P}_3 > 0$ , and  $\mathcal{P}_1 \mathcal{P}_2 > \mathcal{P}_3$ . For all this condition to be satisfied,  $\mathcal{R}_0^H$  must be less than one ( $\mathcal{R}_0^H < 1$ ). Thus, the HIV-only submodel disease-free equilibrium is locally asymptotically stable if  $\mathcal{R}_0^H < 1$ .  $\square$

From a biological perspective, Theorem 2 indicates that if the HIV basic reproduction number is below one, it is feasible to eradicate HIV from the population, provided that the initial sizes of the subpopulations in the HIV-only submodel fall within the basin of attraction of  $\chi_0^H$ . This implies that small deviations from the disease-free state will decrease over time, allowing the system to return to the disease-free equilibrium. To ensure that the elimination of HIV is not influenced by the initial subpopulation sizes, it is essential to establish the global asymptotic stability of the HIV disease-free equilibrium.

### 3.1.4 | Global Stability of the HIV-Only Disease-Free Equilibrium

To investigate the global stability of the HIV-only submodel disease-free equilibrium, we used technique implemented by Castillo-Chavez and Feng in [43]. Thus, the HIV-only submodel (6) can be rewritten in the form

$$\begin{aligned} \frac{dU}{dt} &= \mathcal{L}(U, V), \\ \frac{dV}{dt} &= \mathcal{K}(U, V), \end{aligned} \quad (10)$$

where  $U = \{S\}$  represents the uninfected compartment  $U \in \mathbb{R}_+^1$  and  $V = \{I_H, A_H, T_H\}$  represents the infected compartments  $V \in \mathbb{R}_+^3$ .  $\chi_0^H = (U^*, 0)$  represents the disease-free equilibrium of the system.

$\chi_0^H$  is a globally asymptotically stable equilibrium for the HIV-only submodel if it satisfies the conditions  $\mathcal{T}_1$  and  $\mathcal{T}_2$  below:

$$\begin{aligned} \mathcal{T}_1 : \quad & \text{For } \frac{dU}{dt} = \mathcal{L}(U^*, 0), \text{ where } U^* \\ & \text{is globally asymptotically stable,} \\ \mathcal{T}_2 : \quad & \text{For } \frac{dV}{dt} = \mathcal{M}_V \mathcal{K}(U^*, 0)V - \hat{\mathcal{K}}(U, V), \hat{\mathcal{K}}(U, V) \\ & \geq 0 \quad \forall \mathcal{L}, \mathcal{K} \in \Omega_1, \end{aligned} \quad (11)$$

where  $\mathcal{M}_V \mathcal{K}(U^*, 0)$  is the Jacobian matrix of  $\mathcal{K}(U, V)$  taken in  $(I_H, A_H, T_H)$  and evaluated at  $(U^*, 0) = \left(\frac{\pi}{\theta}, 0, 0, 0\right)$ . If the system (10) satisfies condition  $\mathcal{T}_1$  and  $\mathcal{T}_2$  above, then the following theorem holds.

**Theorem 3.** *The equilibrium point  $(U^*, 0)$  of the system (10) is globally asymptotically stable if  $\mathcal{R}_0^H \leq 1$ , and condition  $\mathcal{T}_1$  and  $\mathcal{T}_2$  are satisfied.*

*Proof.* From HIV-only submodel system (6), we obtained  $\mathcal{L}(U, V)$  and  $\mathcal{K}(U, V)$ :

$$\mathcal{L}(U, V) = \left[ (1 - \varepsilon_1 I_H) \pi - \frac{(1-rz)\beta_H (I_H + c_1 A_H + c_2 T_H) S}{N} - \theta S \right],$$

$$\mathcal{K}(U, V) = \begin{bmatrix} \frac{(1-rz)\beta_H (I_H + c_1 A_H + c_2 T_H) S}{N} + \varepsilon_1 \pi I_H - (\eta + \sigma_1 + \theta) I_H \\ \eta I_H - (\sigma_2 + \delta_H + \theta) A_H \\ \sigma_1 I_H + \sigma_2 A_H - (\phi_1 \delta_H + \theta) T_H \end{bmatrix}.$$

Now, we consider  $\frac{dU}{dt} = \mathcal{L}(U^*, 0)$  the reduced system from condition  $\mathcal{T}_1$ :

$$\frac{dS}{dt} = \pi - \theta S \quad (12)$$

$U^* = \left(\frac{\pi}{\theta}\right)$  is a globally asymptotically stable equilibrium point for the reduced system  $\frac{dU}{dt} = \mathcal{L}(U, 0)$  in (12). We note that this asymptotic dynamics is independent of the initial condition in  $\Omega_1$ . Therefore, the convergence of the solution of the reduced system (12) is global in  $\Omega_1$ . Hence, we compute

$$\begin{aligned} & \mathcal{M}_V \mathcal{K}(U^*, 0) \\ &= \begin{bmatrix} (1-rz)\beta_H + \varepsilon_1 \pi - (\eta + \sigma_1 + \theta) & (1-rz)\beta_H c_1 & (1-rz)\beta_H c_2 \\ \eta & -(\sigma_2 + \delta_H + \theta) & 0 \\ \sigma_1 & \sigma_2 & -(\phi_1 \delta_H + \theta) \end{bmatrix}, \\ & \hat{\mathcal{K}}(U, V) = \begin{bmatrix} (1-rz)\beta_H (I_H + c_1 A_H + c_2 T_H) \left(1 - \frac{S}{N}\right) \\ 0 \\ 0 \end{bmatrix}. \end{aligned}$$

Clearly,  $\hat{\mathcal{K}}(U, V) \geq 0$  for all  $\mathcal{L}, \mathcal{K} \in \Omega_1$  because  $S \leq N$ . Thus, this prove that the HIV-only disease-free equilibrium is globally asymptotically stable whenever  $\mathcal{R}_0^H \leq 1$ .  $\square$

### 3.1.5 | Endemic Equilibrium of the HIV-Only Submodel

In this section, we will determine the conditions necessary for the existence of an equilibrium where HIV infection is endemic in the population. This situation arises when at least one of the infected variables is nonzero (i.e.,  $I_H \neq 0$ ,  $A_H \neq 0$ , or  $T_H \neq 0$ ). To analyze the endemic equilibrium point, we will solve the equations of the HIV-only submodel in terms of the “force of infection,” represented by

$$\lambda_H^{**} = \frac{(1 - rz)\beta_H(I_H^{**} + c_1 A_H^{**} + c_2 T_H^{**})}{N^{**}} \quad (13)$$

where

$$N^{**} = S^{**} + I_H^{**} + A_H^{**} + T_H^{**}.$$

Setting the right-hand sides of the equations of the HIV-only submodel (6) to zero (at steady state), we obtained

$$\begin{aligned} S^{**} &= \frac{\pi(K_1 - \varepsilon_1 \pi)}{\lambda_H^{**} K_1 + \theta(K_1 - \varepsilon_1 \pi)}, \\ I_H^{**} &= \frac{\lambda_H^{**} \pi}{\lambda_H^{**} K_1 + \theta(K_1 - \varepsilon_1 \pi)}, \\ A_H^{**} &= \frac{\lambda_H^{**} \pi \eta}{K_2(\lambda_H^{**} K_1 + \theta(K_1 - \varepsilon_1 \pi))}, \\ T_H^{**} &= \frac{\lambda_H^{**} \pi(\sigma_1 K_2 + \eta \sigma_2)}{K_2 K_3(\lambda_H^{**} K_1 + \theta(K_1 - \varepsilon_1 \pi))}. \end{aligned} \quad (14)$$

Substituting Equation (14) into Equation (13) and simplifying, we obtained

$$\mathcal{H}(\lambda_H^{**}) = E_1 \lambda_H^{**2} + E_2 \lambda_H^{**} = 0 \quad (15)$$

where

$$\begin{aligned} E_1 &= \pi(K_1 K_2 + \eta K_3 + \sigma_1 K_2 + \eta \sigma_2), \\ E_2 &= \pi K_1 K_2 K_3 (1 - \mathcal{R}_0^H). \end{aligned} \quad (16)$$

The solution to the quadratic equation in (15) is  $\lambda_{H1}^{**} = 0$  and  $\lambda_{H2}^{**} = -\frac{\pi K_1 K_2 K_3 (1 - \mathcal{R}_0^H)}{\pi(K_1 K_2 + \eta K_3 + \sigma_1 K_2 + \eta \sigma_2)}$ . The root  $\lambda_{H1}^{**} = 0$  corresponds to the disease-free equilibrium. Furthermore root  $\lambda_{H2}^{**} > 0$  if  $\mathcal{R}_0^H > 1$  and  $\lambda_{H2}^{**} < 0$  if  $\mathcal{R}_0^H < 1$ . This confirms the existence of a unique positive endemic equilibrium when  $\mathcal{R}_0^H > 1$ . Thus, this result is summarized below.

**Theorem 4.** *The HIV-only submodel (6) has a unique positive endemic equilibrium whenever  $\mathcal{R}_0^H > 1$  and no endemic equilibrium otherwise.*

## 3.2 | HBV-Only Submodel

The HBV-only submodel is obtained by setting the HIV and the co-infection compartments to zero (i.e.,  $I_H = A_H = T_H = I_{HAB} = I_{HCB} = I_{AAB} = I_{ACB} = T_{HB} = 0$ ) in the HIV and HBV

co-infection model (1). Thus, the HBV-only submodel is given by

$$\begin{aligned} \frac{dS}{dt} &= (1 - \varepsilon_2 I_{AB})\pi - \lambda_B S - (\alpha + \theta)S + \gamma V_B, \\ \frac{dV_B}{dt} &= \alpha S - (\gamma + \theta)V_B, \\ \frac{dI_{AB}}{dt} &= \lambda_B S + \varepsilon_2 \pi I_{AB} + e_9 \lambda_B R - (\psi + \tau_1 + \delta_B + \theta)I_{AB}, \\ \frac{dI_{CB}}{dt} &= \psi I_{AB} - (\tau_2 + \delta_B + \theta)I_{CB}, \\ \frac{dT_B}{dt} &= \tau_1 I_{AB} + \tau_2 I_{CB} - (q + \phi_2 \delta_B + \theta)T_B, \\ \frac{dR}{dt} &= q T_B - (e_9 \lambda_B + \theta)R, \end{aligned} \quad (17)$$

where

$$\lambda_B = \frac{(1 - rz)\beta_B(I_{AB} + I_{CB})}{N}.$$

It can be shown that the closed region

$$\begin{aligned} \Omega_2 = \{ (S, V_B, I_{AB}, I_{CB}, T_B, R) \in \mathbb{R}_+^6 : \\ S + V_B + I_{AB} + I_{CB} + T_B + R \leq \frac{\pi}{\theta} \} \end{aligned}$$

is positively invariant. Hence, it is adequate to consider the dynamics of the HBV-only submodel in  $\Omega_2$ .

### 3.2.1 | The Disease-Free Equilibrium of the HBV-Only Submodel (DFEB)

The HBV disease-free equilibrium is a steady state where there is no HBV infection in the population. This is obtained by equating the right-hand side of the HBV-only submodel (17) to zero and setting the infected variables to zero (i.e.,  $I_{AB} = I_{CB} = T_B = 0$ ). Therefore, the disease-free equilibrium of the HBV-only submodel is given by

$$\begin{aligned} \chi_0^B &= (S^*, V_B^*, I_{AB}^*, I_{CB}^*, T_B^*, R^*) \\ &= \left( \frac{\pi(\gamma + \theta)}{\theta(\alpha + \gamma + \theta)}, \frac{\alpha \pi}{\theta(\alpha + \gamma + \theta)}, 0, 0, 0, 0 \right). \end{aligned} \quad (18)$$

### 3.2.2 | HBV Basic Reproduction Number

The HBV basic reproduction number, denoted as  $\mathcal{R}_0^B$ , is a vital parameter that governs the transmission of HBV within a population. It represents the expected number of secondary infections generated by a single HBV-infected individual introduced into a completely susceptible population. Understanding  $\mathcal{R}_0^B$  is essential for predicting the potential spread of the disease and for implementing effective control measures. When  $\mathcal{R}_0^B$  exceeds 1, it indicates a likelihood of an outbreak, whereas a value below 1 suggests that the disease may not be able to sustain transmission in the population. The HBV basic reproduction number can be calculated using the next generation operator method, as detailed in [41]. Following the methodology in [41], the nonnegative matrix  $\mathcal{F}$  for new infections and the nonsingular matrix  $\mathcal{V}$

for the remaining transition terms at the HBV-only disease-free equilibrium are defined as follows:

$$\mathcal{F} = \begin{bmatrix} \frac{(1-rz)\beta_B S^*}{S^*+V_B^*} + \varepsilon_2 \pi & \frac{(1-rz)\beta_B S^*}{S^*+V_B^*} & 0 \\ 0 & 0 & 0 \\ 0 & 0 & 0 \end{bmatrix}, \text{ and}$$

$$\mathcal{V} = \begin{bmatrix} (\psi + \tau_1 + \delta_B + \theta) & 0 & 0 \\ -\psi & (\tau_2 + \delta_B + \theta) & 0 \\ -\tau_1 & -\tau_2 & (q + \phi_2 \delta_B + \theta) \end{bmatrix}.$$

Hence, it follows from [41] that  $\mathcal{R}_0^B = \rho(\mathcal{F}\mathcal{V}^{-1})$ , where  $\rho$  is the spectral radius or largest eigenvalue of the matrix  $\mathcal{F}\mathcal{V}^{-1}$ .

Thus,

$$\mathcal{R}_0^B = \frac{(1-rz)\beta_B(\gamma + \theta)(\psi + (\tau_2 + \delta_B + \theta))}{(\alpha + \gamma + \theta)(\psi + \tau_1 + \delta_B + \theta)(\tau_2 + \delta_B + \theta)} + \frac{\varepsilon_2 \pi}{(\psi + \tau_1 + \delta_B + \theta)}. \quad (19)$$

### 3.2.3 | Local Stability of the HBV Disease-Free Equilibrium

**Theorem 5.** *The disease-free equilibrium ( $\chi_0^B$ ) of the HBV-only submodel (17) is locally asymptotically stable if  $\mathcal{R}_0^B < 1$  and unstable if  $\mathcal{R}_0^B > 1$ .*

*Proof.* We analyzed the local stability of the disease-free equilibrium of the HBV-only submodel by obtaining the Jacobian matrix of the HBV-only submodel (17) and evaluating at the HBV disease-free equilibrium, given by

$$\mathcal{J}(\chi_0^B) = \begin{bmatrix} -u_1 & \gamma & -\left(\frac{(1-rz)\beta_B u_2}{(\alpha + \gamma + \theta)} + \varepsilon_2 \pi\right) & -\frac{(1-rz)\beta_B u_2}{(\alpha + \gamma + \theta)} & 0 & 0 \\ \alpha & -u_2 & 0 & 0 & 0 & 0 \\ 0 & 0 & \frac{(1-rz)\beta_B u_2}{(\alpha + \gamma + \theta)} + \varepsilon_2 \pi - u_3 & \frac{(1-rz)\beta_B u_2}{(\alpha + \gamma + \theta)} & 0 & 0 \\ 0 & 0 & \psi & -u_4 & 0 & 0 \\ 0 & 0 & \tau_1 & \tau_2 & -u_5 & 0 \\ 0 & 0 & 0 & 0 & q & -\theta \end{bmatrix},$$

where  $u_1 = \alpha + \theta$ ,  $u_2 = \gamma + \theta$ ,  $u_3 = \psi + \tau_1 + \delta_B + \theta$ ,  $u_4 = \tau_2 + \delta_B + \theta$ , and  $u_5 = q + \phi_2 \delta_B + \theta$ .

The eigenvalues of the Jacobian matrix  $\mathcal{J}(\chi_0^B)$  are  $\lambda_1 = -\theta$ ,  $\lambda_2 = -u_5$  and the roots of the characteristic polynomial given below:

$$\mathcal{Q}(\lambda) = \lambda^4 + \Phi_1 \lambda^3 + \Phi_2 \lambda^2 + \Phi_3 \lambda + \Phi_4 \quad (20)$$

where

$$\Phi_1 = u_1 + u_2 + u_3 + u_4 - \left(\frac{(1-rz)\beta_B u_2}{(\alpha + \gamma + \theta)} + \varepsilon_2 \pi\right),$$

$$\Phi_2 = u_1(u_2 + u_3 + u_4) + u_2(u_3 + u_4) + u_3 u_4 + \alpha \gamma - \frac{(1-rz)\beta_B u_2(\psi + u_1 + u_2 + u_4)}{(\alpha + \gamma + \theta)}$$

$$\varepsilon_2 \pi(u_1 + u_2 + u_4),$$

$$\Phi_3 = u_1 u_2 (u_3 + u_4) + u_3 u_4 (u_1 + u_2) + \alpha \gamma (\varepsilon_2 \pi - u_3) - \varepsilon_2 \pi (u_1 u_2 + u_1 u_4 + u_2 u_4) - \frac{(1-rz)\beta_B u_2 (\psi (u_1 + u_2) + u_1 (u_2 + u_4) + u_2 u_4 - \alpha \gamma)}{(\alpha + \gamma + \theta)},$$

$$\Phi_4 = \theta u_3 u_4 (\alpha + \gamma + \theta) (1 - \mathcal{R}_0^B).$$

By applying the Routh-Hurwitz criterion [42] to the polynomial in Equation (20), which states that all roots of the characteristic polynomial  $\mathcal{Q}(\lambda)$  have negative real parts if  $\Phi_1 > 0$ ,  $\Phi_3 > 0$ ,  $\Phi_4 > 0$ , and  $\Phi_1 \Phi_2 \Phi_3 > \Phi_3^2 + \Phi_1^2 \Phi_4$ . For all this condition to be satisfied,  $\mathcal{R}_0^B$  must be less than one ( $\mathcal{R}_0^B < 1$ ). Thus, the HBV-only submodel disease-free equilibrium is locally asymptotically stable if  $\mathcal{R}_0^B < 1$ .  $\square$

### 3.2.4 | HBV Endemic Equilibrium

Before exploring the global asymptotic stability of the disease-free equilibrium for the HBV-only submodel (17), it is important to determine the potential number of equilibrium solutions that the model can exhibit. To do this, we will identify the conditions necessary for the existence of an equilibrium where HBV infection is endemic in the population. This situation arises when at least one of the infected HBV variables is nonzero (i.e.,  $I_{AB} \neq 0$ ,  $I_{CB} \neq 0$ , or  $T_B \neq 0$ ). Thus, to analyze the endemic equilibrium point, we will solve the equations of the HBV-only submodel in terms of the “force of infection,” represented by

$$\lambda_B^{**} = \frac{(1-rz)\beta_B(I_{AB}^{**} + I_{CB}^{**})}{N^{**}} \quad (21)$$

where

$$N^{**} = S^{**} + I_{AB}^{**} + I_{CB}^{**} + T_B^{**} + R^{**}.$$

Setting the right-hand side of the equations of the HBV-only submodel (17) to zero, we obtained

$$S^{**} = \frac{\pi u_2 u_4 u_5 (e_9 \lambda_B^{**} + \theta) (u_3 - \varepsilon_2 \pi) - e_9 \lambda_B^{**} \pi q u_2 (\tau_1 u_4 + \tau_2 \psi)}{(e_9 \lambda_B^{**} + \theta) ((\lambda_B^{**} u_2 + u_1 u_2 - \alpha \gamma) (u_3 - \varepsilon_2 \pi) u_4 u_5 + \lambda_B^{**} \varepsilon_2 \pi u_2 u_4 u_5) - Z_1},$$

$$V_B^{**} = \frac{\pi \alpha u_4 u_5 (e_9 \lambda_B^{**} + \theta) (u_3 - \varepsilon_2 \pi) - e_9 \lambda_B^{**} \pi \alpha q (\tau_1 u_4 + \tau_2 \psi)}{(e_9 \lambda_B^{**} + \theta) ((\lambda_B^{**} u_2 + u_1 u_2 - \alpha \gamma) (u_3 - \varepsilon_2 \pi) u_4 u_5 + \lambda_B^{**} \varepsilon_2 \pi u_2 u_4 u_5) - Z_1},$$

$$I_{AB}^{**} = \frac{\lambda_B^{**} \pi u_2 u_4 u_5 (e_9 \lambda_B^{**} + \theta)}{(e_9 \lambda_B^{**} + \theta) ((\lambda_B^{**} u_2 + u_1 u_2 - \alpha \gamma) (u_3 - \varepsilon_2 \pi) u_4 u_5 + \lambda_B^{**} \varepsilon_2 \pi u_2 u_4 u_5) - Z_1},$$

$$I_{CB}^{**} = \frac{\lambda_B^{**} \pi \psi u_2 u_5 (e_9 \lambda_B^{**} + \theta)}{(e_9 \lambda_B^{**} + \theta) ((\lambda_B^{**} u_2 + u_1 u_2 - \alpha \gamma) (u_3 - \varepsilon_2 \pi) u_4 u_5 + \lambda_B^{**} \varepsilon_2 \pi u_2 u_4 u_5) - Z_1},$$

$$T_B^{**} = \frac{\lambda_B^{**} \pi u_2 (e_9 \lambda_B^{**} + \theta) (\tau_1 u_4 + \tau_2 \psi)}{(e_9 \lambda_B^{**} + \theta) ((\lambda_B^{**} u_2 + u_1 u_2 - \alpha \gamma) (u_3 - \varepsilon_2 \pi) u_4 u_5 + \lambda_B^{**} \varepsilon_2 \pi u_2 u_4 u_5) - Z_1},$$

$$R^{**} = \frac{\lambda_B^{**} \pi q u_2 (\tau_1 u_4 + \tau_2 \psi)}{(e_9 \lambda_B^{**} + \theta) ((\lambda_B^{**} u_2 + u_1 u_2 - \alpha \gamma) (u_3 - \varepsilon_2 \pi) u_4 u_5 + \lambda_B^{**} \varepsilon_2 \pi u_2 u_4 u_5) - Z_1}, \quad (22)$$

where

$$Z_1 = e_9 \lambda_B^{**} q (\lambda_B^{**} u_2 + u_1 u_2 - \alpha \gamma) (\tau_1 u_4 + \tau_2 \psi).$$

Substituting Equation (22) into Equation (21), we obtained

$$\mathcal{E}(\lambda_B^{**}) = (m_1 \lambda_B^{**2} + m_2 \lambda_B^{**} + m_3) \lambda_B^{**} = 0 \quad (23)$$

where

$$\begin{aligned} m_1 &= \pi e_9 u_2 (u_4 u_5 + \psi u_5 + \tau_1 u_4 + \tau_2 \psi), \\ m_2 &= \pi e_9 u_4 u_5 (\alpha + u_2) (u_3 - \varepsilon_2 \pi) + \pi \theta u_2 u_5 (\psi + u_4) \\ &\quad + \pi (\tau_1 u_4 + \tau_2 \psi) (u_2 (q + \theta) - e_9 q (\alpha + u_2)) - \\ &\quad \pi e_9 u_2 u_5 (1 - r\varphi) \beta_B (\psi + u_4), \\ m_3 &= \pi \theta u_3 u_4 u_5 (\alpha + u_2) (1 - \mathcal{R}_0^B). \end{aligned}$$

The solution of  $\mathcal{C}(\lambda_B^{**})$  are  $\lambda_B^{**} = 0$  and  $m_1 \lambda_B^{**2} + m_2 \lambda_B^{**} + m_3 = 0$ . Here,  $\lambda_B^{**} = 0$  represents the HBV-only disease-free equilibrium point, and its stability has been previously examined. On the other hand,  $m_1 \lambda_B^{**2} + m_2 \lambda_B^{**} + m_3 = 0$  represents the HBV-only endemic equilibrium. The structure of the polynomial  $\mathcal{C}(\lambda_B^{**})$  suggests the occurrence of a backward bifurcation. This phenomenon is typically characterized by the coexistence of a stable HBV disease-free equilibrium and a stable endemic equilibrium, even when the associated reproduction number of the HBV-only submodel is less than one. Backward bifurcation has been observed in various epidemiological models, as documented in studies such as [44–47]. From a biological perspective, the implication of backward bifurcation is that achieving the basic reproduction number below one ( $\mathcal{R}_0^B < 1$ ) may not be sufficient for effectively controlling the HBV infection within the population. The public health implication of this phenomenon is significant: While it is necessary for the reproduction number ( $\mathcal{R}_0^B$ ) to be less than one, this condition alone is no longer adequate for effective disease control. In essence, the backward bifurcation characteristic of the HBV-only submodel (19) complicates efforts to manage HBV effectively within the population. It can be seen from (23) that  $m_1 > 0$  (because all the model parameters are nonnegative). Furthermore,  $m_3 > 0$  whenever  $\mathcal{R}_0^B < 1$ , and  $m_3 > 0$  if  $\mathcal{R}_0^B > 1$ . Hence, the number of possible positive real roots of the polynomial  $\mathcal{C}(\lambda_B^{**})$  depends on the sign of  $m_2$  and  $m_3$ . Therefore, there are three cases we have to consider of  $m_1 \lambda_B^{**2} + m_2 \lambda_B^{**} + m_3 = 0$ :

1. If  $m_2 < 0$  and  $m_3 = 0$  or  $m_2^2 - 4m_1 m_3 = 0$ , then  $\mathcal{C}(\lambda_B^{**})$  has a unique endemic equilibrium point (i.e. one positive root), and there is no possibility of backward bifurcation.
2. If  $m_2 < 0$ ,  $m_3 > 0$ , and  $m_2^2 - 4m_1 m_3 > 0$ , then  $\mathcal{C}(\lambda_B^{**})$  has two endemic equilibrium (i.e., two positive roots), and therefore, there is possibility of the occurrence of backward bifurcation.
3. Otherwise, there is none.

Thus, the above examination leads to the following theorem.

**Theorem 6.** *The HBV-only submodel (17) has*

- i. Precisely one unique endemic equilibrium if  $m_3 < 0$  (i.e.,  $\mathcal{R}_0^B > 1$ ).
- ii. Precisely one unique endemic equilibrium if  $m_2 < 0$  and  $m_3 = 0$  or  $m_2^2 - 4m_1 m_3 = 0$ .
- iii. Precisely two endemic equilibria if  $m_3 > 0$  (i.e.,  $\mathcal{R}_0^B < 1$ ),  $m_2 < 0$ , and  $m_2^2 - 4m_1 m_3 > 0$ .
- iv. No endemic equilibrium otherwise.

From case iii, the HBV-only submodel exhibits a backward bifurcation that occurs when multiple endemic equilibrium exists if and only if  $\mathcal{R}_0^B < 1$ .

### 3.2.5 | Possibility of the Existence of Backward Bifurcation

The existence of the backward bifurcation is explored through the application of the center manifold theory, a method popularized by Castillo-Chavez and Song in [46].

**Theorem 7.** *The HBV-only submodel (17) exhibits backward bifurcation at  $\mathcal{R}_0^B = 1$ , whenever  $a > 0$ .*

*Proof.* To apply the center manifold theorem, we will carry out some modifications to the HBV-only submodel variables. Let  $S = x_1$ ,  $V_B = x_2$ ,  $I_{AB} = x_3$ ,  $I_{CB} = x_4$ ,  $T_B = x_5$ , and  $R = x_6$ . Using the vector notation  $x = (x_1, x_2, x_3, \dots, x_6)^T$  and  $\frac{dx}{dt} = F(x)$ , with  $F = (f_1, f_2, f_3, \dots, f_6)^T$ . Therefore, the HBV-only submodel (17) becomes

$$\begin{aligned} \frac{dx_1}{dt} &\equiv f_1 = (1 - \varepsilon_2 x_3) \pi - \frac{(1 - rz) \beta_B (x_3 + x_4) x_1}{x_1 + x_2 + x_3 + x_4 + x_5 + x_6} \\ &\quad - (\alpha + \theta) x_1 + \gamma x_2, \\ \frac{dx_2}{dt} &\equiv f_2 = \alpha x_1 - (\gamma + \theta) x_2, \\ \frac{dx_3}{dt} &\equiv f_3 = \frac{(1 - rz) \beta_B (x_3 + x_4) x_1}{x_1 + x_2 + x_3 + x_4 + x_5 + x_6} \\ &\quad + \varepsilon_2 \pi x_3 + \frac{e_9 (1 - rz) \beta_B (x_3 + x_4) x_6}{x_1 + x_2 + x_3 + x_4 + x_5 + x_6} \\ &\quad - (\psi + \tau_1 + \delta_B + \theta) x_3, \\ \frac{dx_4}{dt} &\equiv f_4 = \psi x_3 - (\tau_2 + \delta_B + \theta) x_4, \\ \frac{dx_5}{dt} &\equiv f_5 = \tau_1 x_3 + \tau_2 x_4 - (q + \phi_2 \delta_B + \theta) x_5, \\ \frac{dx_6}{dt} &\equiv f_6 = q x_5 - \frac{e_9 (1 - rz) \beta_B (x_3 + x_4) x_6}{x_1 + x_2 + x_3 + x_4 + x_5 + x_6} - \theta x_6. \end{aligned} \quad (24)$$

We considered the HBV transmission rate ( $\beta_B$ ) as the bifurcation parameter. Solving for  $\beta_B = \beta_B^*$  from  $\mathcal{R}_0^B = 1$ , we obtained

$$\beta_B^* = \frac{(\alpha + \gamma + \theta)(\psi + \tau_1 + \delta_B + \theta)(\tau_2 + \delta_B + \theta) - \varepsilon_2 \pi (\alpha + \gamma + \theta)(\tau_2 + \delta_B + \theta)}{(1 - rz)(\gamma + \theta)(\psi + (\tau_2 + \delta_B + \theta))} \quad (25)$$

Evaluating the Jacobian of the transformed system (24) at the HBV disease-free equilibrium ( $\chi_0^B$ ) with  $\beta_B = \beta_B^*$ , we obtained

$$\begin{aligned} &\mathcal{J}(\chi_0^B)|_{\beta_B = \beta_B^*} \\ &= \begin{bmatrix} -u_1 & \gamma & -\left(\frac{(1-rz)\beta_B^* u_2}{(\alpha+\gamma+\theta)} + \varepsilon_2 \pi\right) & -\frac{(1-rz)\beta_B^* u_2}{(\alpha+\gamma+\theta)} & 0 & 0 \\ \alpha & -u_2 & 0 & 0 & 0 & 0 \\ 0 & 0 & \frac{(1-rz)\beta_B^* u_2}{(\alpha+\gamma+\theta)} + \varepsilon_2 \pi - u_3 & \frac{(1-rz)\beta_B^* u_2}{(\alpha+\gamma+\theta)} & 0 & 0 \\ 0 & 0 & \psi & -u_4 & 0 & 0 \\ 0 & 0 & \tau_1 & \tau_2 & -u_5 & 0 \\ 0 & 0 & 0 & 0 & q & -\theta \end{bmatrix}, \end{aligned}$$

where  $u_1 = \alpha + \theta$ ,  $u_2 = \gamma + \theta$ ,  $u_3 = \psi + \tau_1 + \delta_B + \theta$ ,  $u_4 = \tau_2 + \delta_B + \theta$ , and  $u_5 = q + \phi_2 \delta_B + \theta$ .

The Jacobian matrix  $J(\chi_0^B)|_{\beta_B=\beta_B^*}$  has a simple zero eigenvalue (a center), and all other eigenvalues have negative real part (hence, the center manifold theorem can be applied [45, 46]); the right eigenvector,  $w = (w_1, w_2, w_3, w_4, w_5, w_6)^T$ , associated with the simple zero eigenvalue, can be obtained from  $J(\chi_0^B)|_{\beta_B=\beta_B^*}w = 0$ , given by

$$\begin{aligned} u_1w_1 + \gamma w_2 - \left( \frac{(1-rz)\beta_B^*u_2}{(\alpha+\gamma+\theta)} + \varepsilon_2\pi \right) w_3 - \left( \frac{(1-rz)\beta_B^*u_2}{(\alpha+\gamma+\theta)} \right) w_4 &= 0 \\ \alpha w_1 - u_2w_2 &= 0, \\ \left( \frac{(1-rz)\beta_B^*u_2}{(\alpha+\gamma+\theta)} + \varepsilon_2\pi - u_3 \right) w_3 + \left( \frac{(1-rz)\beta_B^*u_2}{(\alpha+\gamma+\theta)} \right) w_4 &= 0 \\ \psi w_3 - u_4w_4 &= 0 \\ \tau_1w_3 + \tau_2w_4 - u_5w_5 &= 0 \\ qw_5 - \theta w_6 &= 0. \end{aligned} \tag{26}$$

From the above equation (26), we obtained

$$\begin{aligned} w_1 &= \frac{u_2w_2}{\alpha}, w_2 = w_2 > 0, w_3 = w_3 > 0, w_4 = -\frac{((1-rz)\beta_B^*u_2 + (\alpha+\gamma+\theta)(\varepsilon_2\pi - u_3 - \psi))w_3}{(1-rz)\beta_B^*u_2 + (\alpha+\gamma+\theta)u_4}, \\ w_5 &= \frac{(\tau_1((1-rz)\beta_B^*u_2 + (\alpha+\gamma+\theta)u_4) - \tau_2((1-rz)\beta_B^*u_2 + (\alpha+\gamma+\theta)(\varepsilon_2\pi - u_3 - \psi)))w_3}{((1-rz)\beta_B^*u_2 + (\alpha+\gamma+\theta)u_4)u_5}, \\ w_6 &= \frac{q(\tau_1((1-rz)\beta_B^*u_2 + (\alpha+\gamma+\theta)u_4) - \tau_2((1-rz)\beta_B^*u_2 + (\alpha+\gamma+\theta)(\varepsilon_2\pi - u_3 - \psi)))w_3}{((1-rz)\beta_B^*u_2 + (\alpha+\gamma+\theta)u_4)u_5\theta}. \end{aligned}$$

Similarly, the left eigenvector,  $v = (v_1, v_2, v_3, v_4, v_5, v_6)$ , satisfying  $v \cdot w = 1$ , associated with the simple zero eigenvalues, can be obtained from  $vJ(\chi_0^B)|_{\beta_B=\beta_B^*} = 0$ , given by

$$\begin{aligned} -u_1v_1 + \alpha v_2 &= 0 \\ \gamma v_1 - u_2v_2 &= 0 \\ -\left( \frac{(1-rz)\beta_B^*u_2}{(\alpha+\gamma+\theta)} + \varepsilon_2\pi \right) v_1 &+ \left( \frac{(1-rz)\beta_B^*u_2}{(\alpha+\gamma+\theta)} + \varepsilon_2\pi - u_3 \right) v_3 + \psi v_4 + \tau_1v_5 = 0 \\ -\left( \frac{(1-rz)\beta_B^*u_2}{(\alpha+\gamma+\theta)} \right) v_1 &+ \left( \frac{(1-rz)\beta_B^*u_2}{(\alpha+\gamma+\theta)} \right) v_3 - u_4v_4 + \tau_2v_5 = 0 \\ -u_5v_5 + qv_6 &= 0 \\ -\theta v_6 &= 0. \end{aligned} \tag{27}$$

Solving the above equation (27), we obtained

$$\begin{aligned} v_1 = v_1 > 0, v_2 &= \frac{(\gamma + u_1)v_1}{(\alpha + \gamma + \theta)}, v_3 = v_3 > 0, \\ v_4 &= \frac{\varepsilon_2\pi v_1 + (u_3 - \varepsilon_2\pi)v_3}{\psi + u_4}, v_5 = v_6 = 0. \end{aligned}$$

Because  $v_5 = v_6 = 0$  for  $k = 1, 2, 3, 4, 5, 6$ , the only nonzero partial derivatives of  $f_1, f_2, f_3, \dots, f_6$  evaluated at the HBV disease-free

equilibrium  $(\chi_0^B)$  are

$$\begin{aligned} \frac{\partial^2 f_1}{\partial x_1 \partial x_3} &= \frac{\partial^2 f_1}{\partial x_3 \partial x_1} = \frac{\partial^2 f_1}{\partial x_1 \partial x_4} = \frac{\partial^2 f_1}{\partial x_4 \partial x_1} \\ &= -\frac{(1-rz)\beta_B\theta}{\pi} + \frac{(1-rz)\beta_B\theta(\gamma+\theta)}{\pi(\alpha+\gamma+\theta)}, \\ \frac{\partial^2 f_3}{\partial x_1 \partial x_3} &= \frac{\partial^2 f_3}{\partial x_3 \partial x_1} = \frac{\partial^2 f_3}{\partial x_1 \partial x_4} = \frac{\partial^2 f_3}{\partial x_4 \partial x_1} \\ &= \frac{(1-rz)\beta_B\theta}{\pi} - \frac{(1-rz)\beta_B\theta(\gamma+\theta)}{\pi(\alpha+\gamma+\theta)}, \\ \frac{\partial^2 f_1}{\partial x_3^2} &= \frac{\partial^2 f_1}{\partial x_4^2} = \frac{2(1-rz)\beta_B\theta(\gamma+\theta)}{\pi(\alpha+\gamma+\theta)}, \frac{\partial^2 f_3}{\partial x_3^2} \\ &= \frac{\partial^2 f_3}{\partial x_4^2} = -\frac{2(1-rz)\beta_B\theta(\gamma+\theta)}{\pi(\alpha+\gamma+\theta)} \\ \frac{\partial^2 f_1}{\partial x_2 \partial x_3} &= \frac{\partial^2 f_1}{\partial x_3 \partial x_2} = \frac{\partial^2 f_1}{\partial x_2 \partial x_4} = \frac{\partial^2 f_1}{\partial x_4 \partial x_2} \end{aligned}$$

$$\begin{aligned} &= \frac{(1-rz)\beta_B\theta(\gamma+\theta)}{\pi(\alpha+\gamma+\theta)}, \\ \frac{\partial^2 f_1}{\partial x_3 \partial x_5} &= \frac{\partial^2 f_1}{\partial x_5 \partial x_3} = \frac{\partial^2 f_1}{\partial x_4 \partial x_5} = \frac{\partial^2 f_1}{\partial x_5 \partial x_4} \\ &= \frac{(1-rz)\beta_B\theta(\gamma+\theta)}{\pi(\alpha+\gamma+\theta)}, \\ \frac{\partial^2 f_1}{\partial x_3 \partial x_6} &= \frac{\partial^2 f_1}{\partial x_6 \partial x_3} = \frac{\partial^2 f_1}{\partial x_4 \partial x_6} = \frac{\partial^2 f_1}{\partial x_6 \partial x_4} \\ &= \frac{(1-rz)\beta_B\theta(\gamma+\theta)}{\pi(\alpha+\gamma+\theta)}, \\ \frac{\partial^2 f_3}{\partial x_2 \partial x_3} &= \frac{\partial^2 f_3}{\partial x_3 \partial x_2} = \frac{\partial^2 f_3}{\partial x_2 \partial x_4} = \frac{\partial^2 f_3}{\partial x_4 \partial x_2} \\ &= -\frac{(1-rz)\beta_B\theta(\gamma+\theta)}{\pi(\alpha+\gamma+\theta)}, \\ \frac{\partial^2 f_3}{\partial x_3 \partial x_5} &= \frac{\partial^2 f_3}{\partial x_5 \partial x_3} = \frac{\partial^2 f_3}{\partial x_4 \partial x_5} = \frac{\partial^2 f_3}{\partial x_5 \partial x_4} \\ &= -\frac{(1-rz)\beta_B\theta(\gamma+\theta)}{\pi(\alpha+\gamma+\theta)}, \\ \frac{\partial^2 f_3}{\partial x_3 \partial x_6} &= \frac{\partial^2 f_3}{\partial x_6 \partial x_3} = \frac{\partial^2 f_3}{\partial x_4 \partial x_6} = \frac{\partial^2 f_3}{\partial x_6 \partial x_4} \\ &= -\frac{(1-rz)\beta_B\theta(\gamma+\theta)}{\pi(\alpha+\gamma+\theta)}, \\ \frac{\partial^2 f_1}{\partial x_3 \partial x_4} &= \frac{\partial^2 f_1}{\partial x_4 \partial x_3} = \frac{2(1-rz)\beta_B\theta(\gamma+\theta)}{\pi(\alpha+\gamma+\theta)}, \frac{\partial^2 f_3}{\partial x_3 \partial x_4} \\ &= \frac{\partial^2 f_3}{\partial x_4 \partial x_3} = -\frac{2(1-rz)\beta_B\theta(\gamma+\theta)}{\pi(\alpha+\gamma+\theta)} \end{aligned}$$

$$\begin{aligned} \frac{\partial^2 f_1}{\partial x_3 \partial \beta_B^*} &= \frac{\partial^2 f_1}{\partial x_4 \partial \beta_B^*} = -\frac{(1-rz)(\gamma+\theta)}{\alpha+\gamma+\theta}, \frac{\partial^2 f_3}{\partial x_3 \partial \beta_B^*} \\ &= \frac{\partial^2 f_3}{\partial x_4 \partial \beta_B^*} = \frac{(1-rz)(\gamma+\theta)}{\alpha+\gamma+\theta}. \end{aligned} \quad (28)$$

Thus, the bifurcation coefficient

$$\begin{aligned} a = & \frac{2(v_1 - v_3)w_2w_3(1-rz)\beta_B^*\theta u_2(1 - ((1-rz)\beta_B^*u_2 + (\alpha+\gamma+\theta)(\epsilon_2\pi - u_3 - \psi)))}{((1-rz)\beta_B^*u_2 + (\alpha+\gamma+\theta)u_4)\pi} \left( \frac{\gamma+\theta}{\alpha+\gamma+\theta} - 1 \right) \\ & + \frac{2(v_1 - v_3)w_3^2(1-rz)\beta_B^*\theta(\gamma+\theta)}{(\alpha+\gamma+\theta)\pi} + \frac{2v_1(u_5w_2 + \tau_1w_3)w_3(1-rz)\beta_B^*\theta(\gamma+\theta)}{(\alpha+\gamma+\theta)\pi u_5} + \\ & \frac{2(v_1 - v_3)w_3^2(1-rz)\beta_B^*\theta(\gamma+\theta)((1-rz)\beta_B^*u_2 + (\alpha+\gamma+\theta)(\epsilon_2\pi - u_3 - \psi))^2}{((1-rz)\beta_B^*u_2 + (\alpha+\gamma+\theta)u_4)^2(\alpha+\gamma+\theta)\pi} \\ & \frac{2v_1(u_5w_2 + (\tau_1 + \tau_2)w_3)w_3(1-rz)\beta_B^*\theta(\gamma+\theta)((1-rz)\beta_B^*u_2 + (\alpha+\gamma+\theta)(\epsilon_2\pi - u_3 - \psi))}{((1-rz)\beta_B^*u_2 + (\alpha+\gamma+\theta)u_4)(\alpha+\gamma+\theta)\pi u_5} + \\ & \frac{2v_1w_3^2(q+\theta)\tau_2(1-rz)\beta_B^*\theta(\gamma+\theta)((1-rz)\beta_B^*u_2 + (\alpha+\gamma+\theta)(\epsilon_2\pi - u_3 - \psi))^2}{((1-rz)\beta_B^*u_2 + (\alpha+\gamma+\theta)u_4)^2(\alpha+\gamma+\theta)\pi\theta u_5} \\ & \frac{2v_1w_3^2(\tau_2 + \tau_1)q(1-rz)\beta_B^*\theta(\gamma+\theta)((1-rz)\beta_B^*u_2 + (\alpha+\gamma+\theta)(\epsilon_2\pi - u_3 - \psi))}{((1-rz)\beta_B^*u_2 + (\alpha+\gamma+\theta)u_4)(\alpha+\gamma+\theta)\pi\theta u_5} + \\ & \frac{2v_1w_3^2q\tau_1(1-rz)\beta_B^*\theta(\gamma+\theta)}{(\alpha+\gamma+\theta)\pi\theta u_5} - \frac{2v_3(\theta u_5w_2 + (\theta+q)\tau_1w_3)w_3(1-rz)\beta_B^*\theta(\gamma+\theta)}{(\alpha+\gamma+\theta)\pi\theta u_5} + \\ & \frac{2v_3(u_5w_2 + (\tau_1 + \tau_2)w_3)w_3(1-rz)\beta_B^*\theta(\gamma+\theta)((1-rz)\beta_B^*u_2 + (\alpha+\gamma+\theta)(\epsilon_2\pi - u_3 - \psi))}{((1-rz)\beta_B^*u_2 + (\alpha+\gamma+\theta)u_4)(\alpha+\gamma+\theta)\pi u_5} \\ & \frac{2v_3w_3^2(q+\theta)\tau_2(1-rz)\beta_B^*\theta(\gamma+\theta)((1-rz)\beta_B^*u_2 + (\alpha+\gamma+\theta)(\epsilon_2\pi - u_3 - \psi))^2}{((1-rz)\beta_B^*u_2 + (\alpha+\gamma+\theta)u_4)^2(\alpha+\gamma+\theta)\pi\theta u_5} \\ & \frac{2v_3w_3^2(\tau_2 + \tau_1)q(1-rz)\beta_B^*\theta(\gamma+\theta)((1-rz)\beta_B^*u_2 + (\alpha+\gamma+\theta)(\epsilon_2\pi - u_3 - \psi))}{((1-rz)\beta_B^*u_2 + (\alpha+\gamma+\theta)u_4)(\alpha+\gamma+\theta)\pi\theta u_5} + \\ & \frac{4(v_3 - v_1)w_3^2(1-rz)\beta_B^*\theta(\gamma+\theta)((1-rz)\beta_B^*u_2 + (\alpha+\gamma+\theta)(\epsilon_2\pi - u_3 - \psi))}{((1-rz)\beta_B^*u_2 + (\alpha+\gamma+\theta)u_4)(\alpha+\gamma+\theta)\pi}, \end{aligned} \quad (29)$$

$$\begin{aligned} b = & \frac{(v_1 - v_3)w_3(1-rz)(\gamma+\theta)((1-rz)\beta_B^*u_2 + (\alpha+\gamma+\theta)(\epsilon_2\pi - u_3 - \psi))}{((1-rz)\beta_B^*u_2 + (\alpha+\gamma+\theta)u_4)(\alpha+\gamma+\theta)} \\ & + \frac{(v_3 - v_1)w_3(1-rz)(\gamma+\theta)}{(\alpha+\gamma+\theta)}. \end{aligned} \quad (30)$$

Given that the bifurcation coefficient  $b$  is positive, Theorem 4.1 in [46] indicates that the HBV-only submodel demonstrates a backward bifurcation at  $\mathcal{R}_0^B = 1$ , provided that the bifurcation coefficient  $a$  is also positive.  $\square$

### 3.2.6 | Global Stability of the HBV-Only Disease-Free Equilibrium: Special Case

Some primary causes of backward bifurcation include imperfect vaccination, vector-borne diseases, and the reinfection of

recovered individuals [44, 45]. Models that account for reinfection typically lose their backward bifurcation property when the reinfection parameters are set to zero. Therefore, we will investigate the impact of the reinfection parameter ( $e_9$ ) on the backward bifurcation phenomenon of the HBV-only submodel (17). To do this, we will set the reinfection parameter to zero (i.e.,  $e_9 = 0$ ) in the HBV-only sub-

model (17) in the absence of reinfection can be reformulated as follows:

$$\begin{aligned} \frac{dG}{dt} &= Q(G, H), \\ \frac{dH}{dt} &= P(G, H), \end{aligned} \quad (31)$$

where  $G = \{S, V_B, R\}$  and  $H = \{I_{AB}, I_{CB}, T_B\}$  where  $G$  represents the uninfected compartment  $G \in \mathbb{R}_+^3$  and  $H$  represents the infected compartments  $H \in \mathbb{R}_+^3$ .  $\chi_0^B = (G^*, 0)$  represents the HBV disease-free equilibrium of the system.

$\chi_0^B$  is a globally asymptotically stable equilibrium for the HBV-only submodel if it satisfies the conditions  $\mathcal{S}_1$  and  $\mathcal{S}_2$  below:

$$\begin{aligned} \mathcal{S}_1 : \quad & \frac{dG}{dt} = Q(G^*, 0), \text{ where } G^* \text{ is the DFE,} \\ \mathcal{S}_2 : \quad & \frac{dH}{dt} = \mathcal{D}_H \mathcal{P}(G, 0)H - \hat{\mathcal{P}}(G, H), \hat{\mathcal{P}}(G, H) \geq 0 \quad \forall G, H \in \Omega_2, \end{aligned} \quad (32)$$

where  $\mathcal{D}_H \mathcal{P}(G^*, 0)$  is the Jacobian matrix of  $\mathcal{P}(G, H)$  taken in  $(I_{AB}, I_{CB}, T_B)$  and evaluated at  $(G^*, 0) = \left( \frac{\pi(\gamma+\theta)}{\theta(\alpha+\gamma+\theta)}, \frac{\alpha\pi}{\theta(\alpha+\gamma+\theta)}, 0, 0, 0, 0 \right)$ . If the system (31) satisfies condition  $\mathcal{S}_1$  and  $\mathcal{S}_2$  above, then the following theorem holds:

**Theorem 8.** *The equilibrium point  $(G^*, 0)$  of the system (31) is globally asymptotically stable if  $\mathcal{R}_0^B \leq 1$ , and conditions  $\mathcal{S}_1$  and  $\mathcal{S}_2$  are satisfied.*

*Proof.* From HBV-only submodel system (17), we obtained  $Q(U, V)$  and  $\mathcal{P}(U, V)$ :

$$\begin{aligned} Q(G, H) &= \begin{bmatrix} (1 - \varepsilon_2 I_{AB})\pi - \frac{(1-rz)\beta_B(I_{AB}+I_{CB})S}{N} - (\alpha + \theta)S + \gamma V_B \\ \alpha S - (\gamma + \theta)V_B \\ qT_B - \theta R \end{bmatrix}, \\ \mathcal{P}(G, H) &= \begin{bmatrix} \frac{(1-rz)\beta_B(I_{AB}+I_{CB})S}{N} + \varepsilon_2 \pi I_{AB} - (\psi + \tau_1 + \delta_B + \theta)I_{AB} \\ \psi I_{AB} - (\tau_2 + \delta_B + \theta)I_{CB} \\ \tau_1 I_{AB} + \tau_2 I_{CB} - (q + \phi_2 \delta_B + \theta)T_B \end{bmatrix}. \end{aligned}$$

Now, we consider  $\frac{dG}{dt} = Q(G^*, 0)$  the reduced system from condition  $\mathcal{S}_1$ :

$$\begin{aligned} \frac{dS}{dt} &= \pi - (\alpha + \theta)S + \gamma V_B, \\ \frac{dV_B}{dt} &= \alpha S - (\alpha + \theta)V_B, \\ \frac{dR}{dt} &= 0. \end{aligned} \quad (33)$$

$G^* = \left( \frac{\pi(\gamma+\theta)}{\theta(\alpha+\gamma+\theta)}, \frac{\alpha\pi}{\theta(\alpha+\gamma+\theta)}, 0 \right)$  is a globally asymptotically stable equilibrium point for the reduced system  $\frac{dG}{dt} = Q(G, 0)$  in (33). We note that this asymptotic dynamics is independent of the initial condition in  $\Omega_2$ . Therefore, the convergence of the solution of the reduced system (33) is global in  $\Omega_2$ . Hence, we compute

$$\mathcal{D}_H \mathcal{P}(G, 0) = \begin{bmatrix} \frac{(1-rz)\beta_B(\gamma+\theta)}{(\alpha+\gamma+\theta)} + \varepsilon_2 \pi - (\psi + \tau_1 + \delta_B + \theta) & \frac{(1-rz)\beta_B(\gamma+\theta)}{(\alpha+\gamma+\theta)} & 0 \\ \psi & -(\tau_2 + \delta_B + \theta) & 0 \\ \tau_1 & \tau_2 & -(q + \phi_2 \delta_B + \theta) \end{bmatrix},$$

$$\hat{\mathcal{P}}(G, H) = \begin{bmatrix} (1 - rz)\beta_B(I_{AB} + I_{CB}) \left( \frac{(\gamma+\theta)}{(\alpha+\gamma+\theta)} - \frac{S}{N} \right) \\ 0 \\ 0 \end{bmatrix}.$$

Thus, because  $\frac{S}{N} \leq \frac{(\gamma+\theta)}{(\alpha+\gamma+\theta)}$ , then  $\hat{\mathcal{P}}(G, H) \geq 0$  for  $Q, \mathcal{P} \in \Omega_2$ . Hence, this prove that the HBV-only disease-free equilibrium is globally asymptotically stable whenever  $\mathcal{R}_0^B \leq 1$ .  $\square$

### 3.3 | HIV and HBV Co-Infection Model

The disease-free equilibrium of the HIV and HBV co-infection model (1), denoted by  $(\chi_0^{HB})$ , is obtained by setting all the infected variables to zero and equating the right-hand side of the HIV and HBV co-infected model (1) to zero, which is given by

$$\begin{aligned} \chi_0^{HB} &= (S^*, I_H^*, A_H^*, T_H^*, V_B^*, I_{AB}^*, I_{CB}^*, T_B^*, R^*, \\ & \quad I_{HAB}^*, I_{HCB}^*, I_{AAB}^*, I_{ACB}^*, T_{HB}^*) \\ &= \left( \frac{\pi(\gamma + \theta)}{\theta(\alpha + \gamma + \theta)}, 0, 0, 0, \frac{\alpha\pi}{\theta(\alpha + \gamma + \theta)}, 0, 0, 0, 0, 0, 0, 0, 0, 0, 0 \right). \end{aligned} \quad (34)$$

Similar to the cases discussed in Sections 3.1.2 and 3.2.2 for the HIV-only and HBV-only submodels, we can demonstrate, using the next generation operator method outlined in [41], that the basic reproduction number for the HIV-HBV co-infection model (1), denoted as  $\mathcal{R}_0^{HB}$ , is given by

$$\mathcal{R}_0^{HB} = \max \left\{ \frac{(\gamma + \theta)\mathcal{R}_0^H}{(\alpha + \gamma + \theta)}, \mathcal{R}_0^B \right\} \quad (35)$$

**Theorem 9.** *The disease-free equilibrium of the HIV and HBV co-infection model (1) is locally asymptotically stable if  $\mathcal{R}_0^{HB} < 1$  and unstable whenever  $\mathcal{R}_0^{HB} > 1$ .*

*Proof.* The proof follows a similar approach to that of the HIV-only and HBV-only submodels.  $\square$

Likewise, as observed in the HBV-only submodel, the complete HIV and HBV co-infection model (1) also exhibits the phenomenon of backward bifurcation.

**Theorem 10.** *The HIV and HBV co-infection model (1) undergoes backward bifurcation at  $\mathcal{R}_0^{HB} = 1$ , whenever  $a > 0$ .*

The proof is in Appendix A.

### 3.4 | Sensitivity Analysis of the Basic Reproduction Numbers

In this section, we shall carry out the sensitivity analysis on the basic parameters that constitute the HIV-only and HBV-only

basic reproduction numbers, in order to identify parameters that can impact the basic reproduction numbers. Sensitivity analysis notifies us on how significant each parameter is to the disease transmission. We shall employ the approach presented in [43]. Following the approach in [43], we use the normalized forward sensitivity index of a variable, “ $\mathcal{E}$ ,” that depends differentially on the parameter, “ $\varphi$ ,” defined as

$$\mathcal{E} \nabla_{\varphi} = \frac{\partial \mathcal{E}}{\partial \varphi} \times \frac{\varphi}{\mathcal{E}} \quad (36)$$

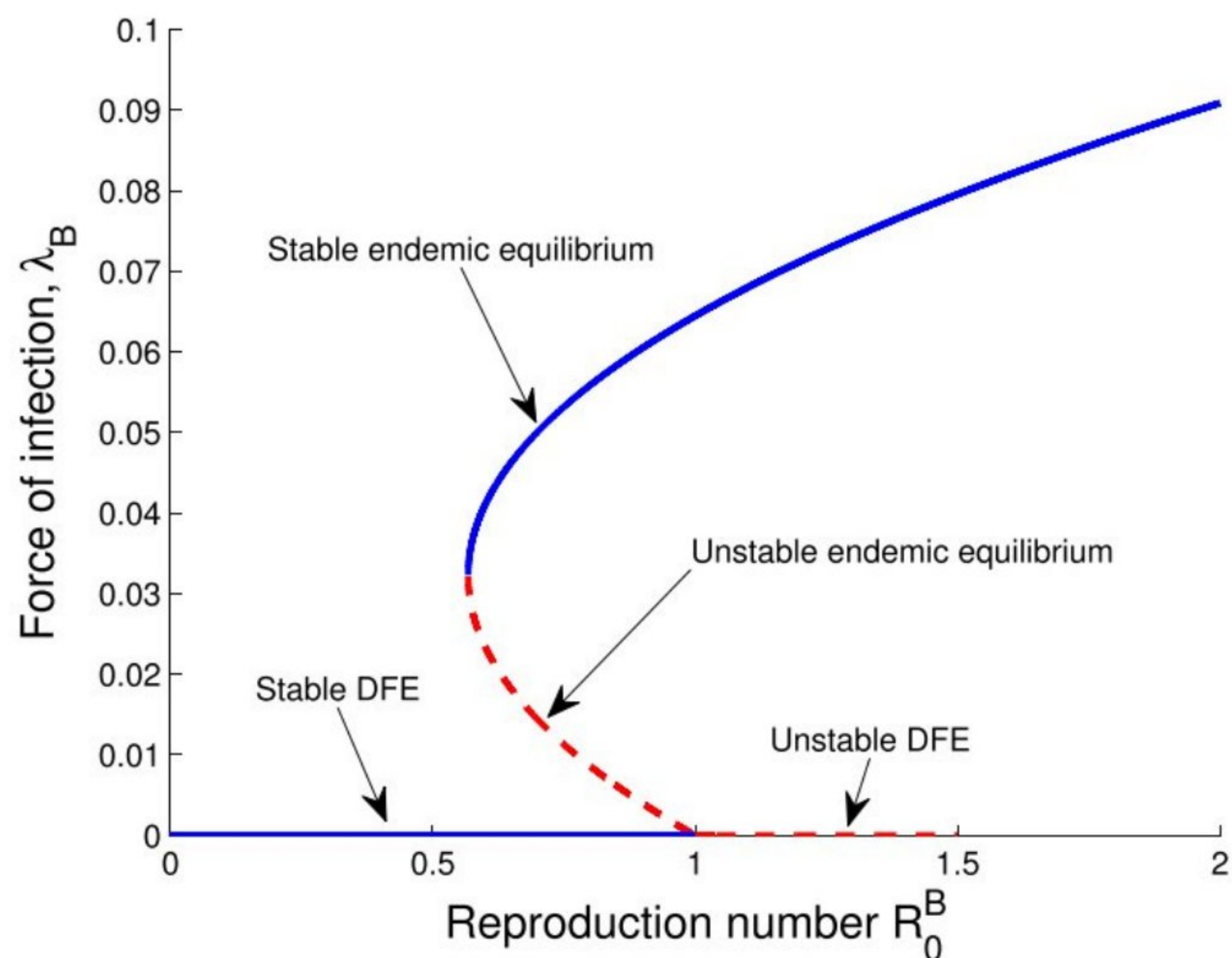


**FIGURE 2** | Bifurcation diagram. [Colour figure can be viewed at [wileyonlinelibrary.com](https://onlinelibrary.wiley.com)]

Hence, the sensitivity index of the basic reproduction number of the HIV-only submodel (8) and the HBV-only submodel (19) with respect to the parameter, “ $\varphi$ ,” are given by

$$\mathcal{R}_0^H \nabla_{\varphi} = \frac{\partial \mathcal{R}_0^H}{\partial \varphi} \times \frac{\varphi}{\mathcal{R}_0^H}, \quad \text{and} \quad \mathcal{R}_0^B \nabla_{\varphi} = \frac{\partial \mathcal{R}_0^B}{\partial \varphi} \times \frac{\varphi}{\mathcal{R}_0^B} \quad (37)$$

Firstly, we compute the sensitivity indices of the HIV-only submodel (8) basic parameters.

$$\mathcal{R}_0^H \nabla_{\beta_H} = \frac{(1 - rz) \left( (\sigma_2 + \delta_H + \theta)(\phi_1 \delta_H + \theta) + c_1 \eta (\phi_1 \delta_H + \theta) + c_2 (\sigma_1 (\sigma_2 + \delta_H + \theta) + \eta \sigma_2) \right)}{(\eta + \sigma_1 + \theta)(\sigma_2 + \delta_H + \theta)(\phi_1 \delta_H + \theta)} \times \frac{\beta_H (\eta + \sigma_1 + \theta)(\sigma_2 + \delta_H + \theta)(\phi_1 \delta_H + \theta)}{(1 - rz) \beta_H \left( (\sigma_2 + \delta_H + \theta)(\phi_1 \delta_H + \theta) + c_1 \eta (\phi_1 \delta_H + \theta) + c_2 (\sigma_1 (\sigma_2 + \delta_H + \theta) + \eta \sigma_2) \right) + y \varepsilon_1 \pi},$$

where  $y = (\sigma_2 + \delta_H + \theta)(\phi_1 \delta_H + \theta)$ .

We have

$$\mathcal{R}_0^H \nabla_{\beta_H} = \frac{(1 - rz) \beta_H \left( (\sigma_2 + \delta_H + \theta)(\phi_1 \delta_H + \theta) + c_1 \eta (\phi_1 \delta_H + \theta) + c_2 (\sigma_1 (\sigma_2 + \delta_H + \theta) + \eta \sigma_2) \right)}{(1 - rz) \beta_H \left( (\sigma_2 + \delta_H + \theta)(\phi_1 \delta_H + \theta) + c_1 \eta (\phi_1 \delta_H + \theta) + c_2 (\sigma_1 (\sigma_2 + \delta_H + \theta) + \eta \sigma_2) \right) + y \varepsilon_1 \pi},$$

$$\mathcal{R}_0^H \nabla_{\beta_H} = 0.9582 \quad (38)$$

Similarly, we obtained the sensitivity index for the rest of the HIV-only basic parameters, given by

$$\begin{aligned} \mathcal{R}_0^H \nabla_r &= -0.8845, \mathcal{R}_0^H \nabla_z = -0.8845, \mathcal{R}_0^H \nabla_{\sigma_1} \\ &= -0.5468, \mathcal{R}_0^H \nabla_{\sigma_2} = -0.0439, \\ \mathcal{R}_0^H \nabla_{\eta} &= -0.1424, \mathcal{R}_0^H \nabla_{\delta_H} = -0.0031, \mathcal{R}_0^H \nabla_{c_1} \\ &= 0.0488, \mathcal{R}_0^H \nabla_{c_2} = 0.2343, \end{aligned}$$

$$\begin{aligned} \mathcal{R}_0^H \nabla_{\theta} &= -0.2638, \mathcal{R}_0^H \nabla_{\varepsilon_1} = 0.0418, \mathcal{R}_0^H \nabla_{\pi} \\ &= -0.0418. \end{aligned}$$

In similar reasoning, we obtained the sensitivity indices of the basic parameters of the HBV-only submodel (19), given by (Figure 2)

$$\begin{aligned} \mathcal{R}_0^B \nabla_{\beta_B} &= 0.9773, \mathcal{R}_0^B \nabla_r = -0.9021, \mathcal{R}_0^B \nabla_z \\ &= -0.9021, \mathcal{R}_0^B \nabla_{\alpha} = -0.7540, \\ \mathcal{R}_0^B \nabla_{\gamma} &= 0.4245, \mathcal{R}_0^B \nabla_{\psi} = 0.5279, \mathcal{R}_0^B \nabla_{\tau_1} \\ &= -0.7218, \mathcal{R}_0^B \nabla_{\tau_2} = -0.6094, \\ \mathcal{R}_0^B \nabla_{\delta_B} &= -0.1108, \mathcal{R}_0^B \nabla_{\varepsilon_2} = 0.0227, \mathcal{R}_0^B \nabla_{\pi} \\ &= 0.0227, \mathcal{R}_0^B \nabla_{\theta} = 0.2436. \end{aligned}$$

### 3.4.1 | Interpretation of the Sensitivity Indices

The bar chart of the sensitivity indices of the basic reproduction for the HIV and HBV submodels with respect to the basic parameters are depicted in Figures 3 and 4, respectively. Those parameters that have positive indices for the HIV and HBV submodels have great impact on the spread of the diseases in the community if their values are increasing. Due to the fact that the basic reproduction number increases as their values increases. Conversely, when the parameters with negative indices rise in value, they play a role in alleviating disease burdens, leading to a decrease in the basic reproduction numbers.

### 3.5 | Impact of HIV on HBV Infection

In this section, we shall investigate the impact of HIV infection on the transmission of HBV using the approached described in [26].

Firstly, we will express the basic reproduction number of the HBV ( $\mathcal{R}_0^B$ ) in terms of the basic reproduction number of HIV ( $\mathcal{R}_0^H$ ). To do this, we expressed the parameter  $\pi$  (because it is common for both HIV and HBV equilibrium points) in Equation (8) in terms of  $\mathcal{R}_0^H$ , we obtained

$$\mathcal{R}_0^H = \frac{(1 - rz) \beta_H (K_2 K_3 + c_1 \eta K_3 + c_2 (\sigma_1 K_2 + \eta \sigma_2))}{K_1 K_2 K_3} + \frac{\varepsilon_1 \pi}{K_1},$$

where  $K_1 = \eta + \sigma_1 + \theta$ ,  $K_2 = \sigma_2 + \delta_H + \theta$ , and  $K_3 = \phi_1 \delta_H + \theta$ . Solving for  $\pi$ , we have

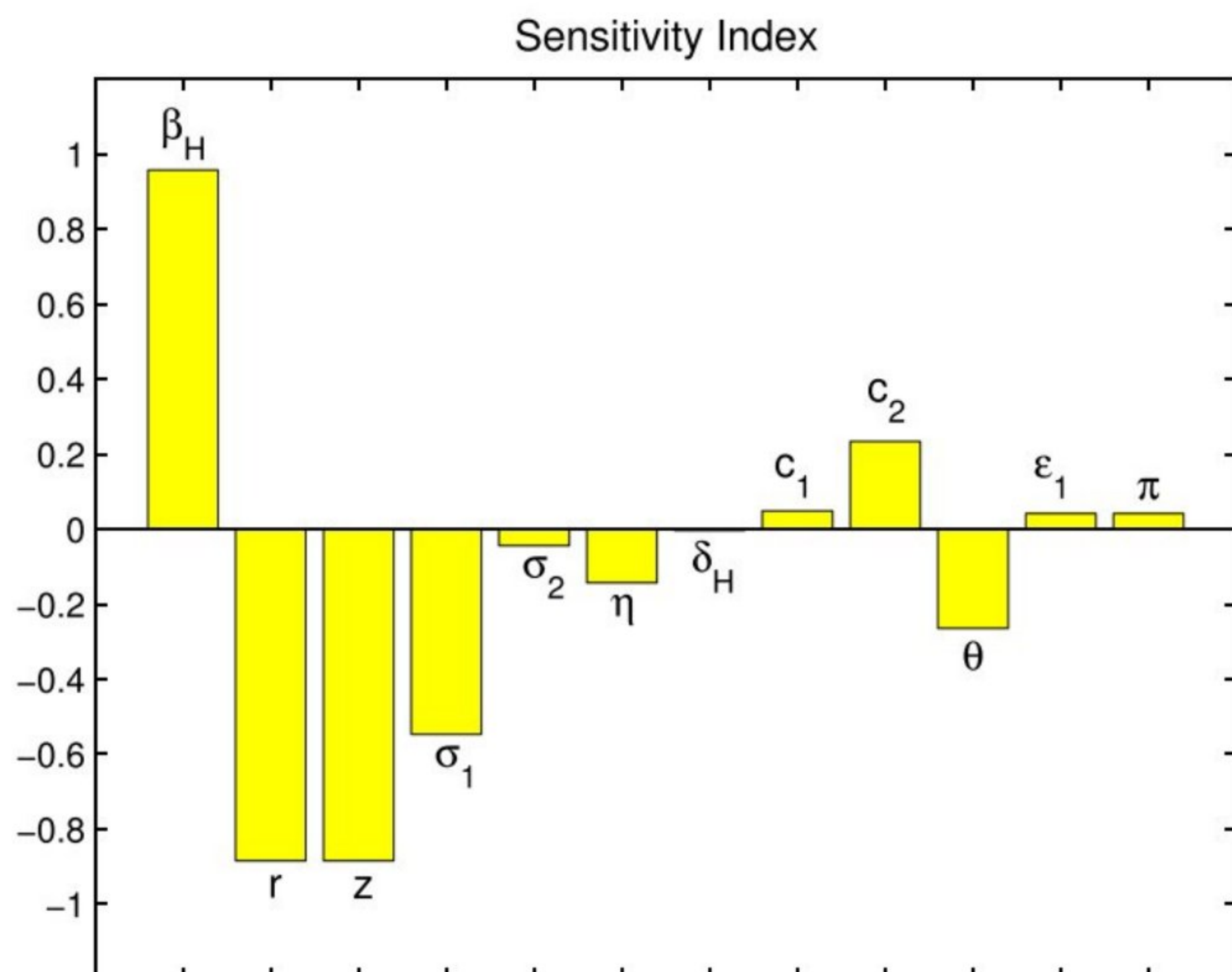


**FIGURE 3** | Sensitivity index of the HIV basic reproduction number. [Colour figure can be viewed at [wileyonlinelibrary.com](https://onlinelibrary.wiley.com)]

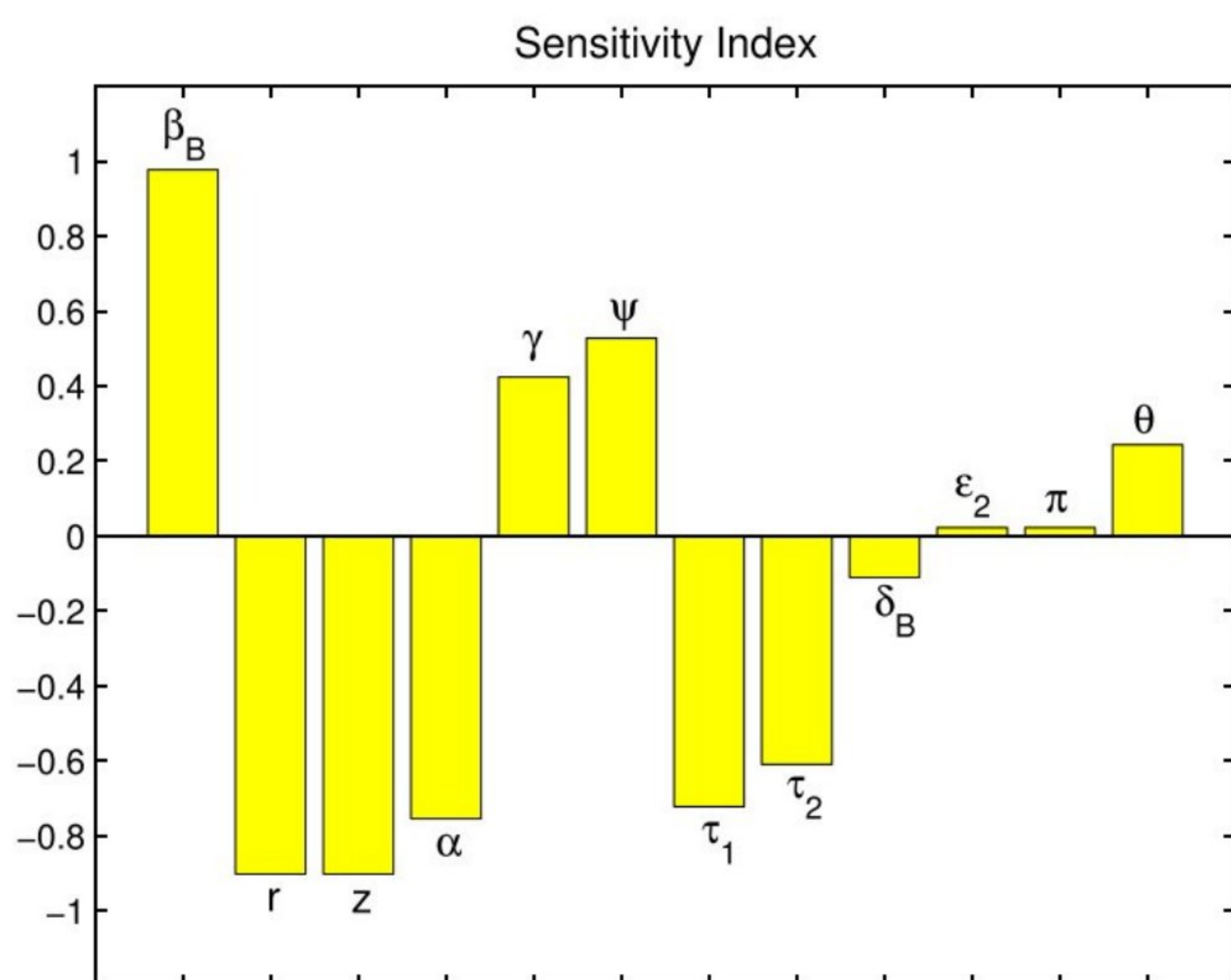


**FIGURE 4** | Sensitivity index of the HBV basic reproduction number. [Colour figure can be viewed at [wileyonlinelibrary.com](https://onlinelibrary.wiley.com)]

$$\pi = \frac{\mathcal{R}_0^H K_1 K_2 K_3 - (1 - r\varphi)\beta_H(K_2 K_3 + c_1 \eta K_3 + c_2(\sigma_1 K_2 + \eta \sigma_2))}{\varepsilon_1 K_2 K_3} \quad (39)$$

Substituting the expression of  $\pi$  in Equation (39) into the HBV basic reproduction number ( $\mathcal{R}_0^B$ ) in (19), we obtained  $\mathcal{R}_0^B$  in terms of  $\mathcal{R}_0^H$ , given as

$$\mathcal{R}_0^B = \frac{(1 - rz)\beta_B u_2 (\psi + u_4)}{(\alpha + \gamma + \theta)u_3 u_4} + \frac{\mathcal{R}_0^H \varepsilon_2 K_1 K_2 K_3 - (1 - rz)\beta_H \varepsilon_2 (K_2 K_3 + c_1 \eta K_3 + c_2(\sigma_1 K_2 + \eta \sigma_2))}{\varepsilon_1 K_2 K_3 u_3} \quad (40)$$

where  $u_1 = \alpha + \theta$ ,  $u_2 = \gamma + \theta$ ,  $u_3 = \psi + \tau_1 + \delta_B + \theta$ ,  $u_4 = \tau_2 + \delta_B + \theta$ , and  $u_5 = q + \phi_2 \delta_B + \theta$ .

Taking the partial derivatives of  $\mathcal{R}_0^B$  in (40) with respect to  $\mathcal{R}_0^H$ , we have

$$\frac{\partial \mathcal{R}_0^B}{\partial \mathcal{R}_0^H} = \frac{\varepsilon_2 K_1}{\varepsilon_1 u_3} > 0 \quad (41)$$

Thus, it is observed that the partial derivative of  $\mathcal{R}_0^B$  with respect to  $\mathcal{R}_0^H$  in (41) is positive. Hence, this result implies that an increase in HIV infection within the population will enhance the transmission of HBV positively.

### 3.6 | Impact of HBV on HIV Infection

Similarly, we investigated the impact of HBV infection on the transmission of HIV, using the same approach in the previous section. We expressed the basic reproduction number of HIV ( $\mathcal{R}_0^H$ ) in terms of the basic reproduction number of HBV ( $\mathcal{R}_0^B$ ); then, we expressed the parameter  $\pi$  in Equation (19) in terms of  $\mathcal{R}_0^B$ ; we have that

$$\mathcal{R}_0^B = \frac{(1 - rz)\beta_B u_2 (\psi + u_4)}{(\alpha + u_2)u_3 u_4} + \frac{\varepsilon_2 \pi}{u_3},$$

where  $u_1 = \alpha + \theta$ ,  $u_2 = \gamma + \theta$ ,  $u_3 = \psi + \tau_1 + \delta_B + \theta$ ,  $u_4 = \tau_2 + \delta_B + \theta$ , and  $u_5 = q + \phi_2 \delta_B + \theta$ .

We obtained  $\pi$  as

$$\pi = \frac{\mathcal{R}_0^B (\alpha + u_2) u_3 u_4 - (1 - rz)\beta_B u_2 (\psi + u_4)}{(\alpha + u_2)\varepsilon_2 u_4} \quad (42)$$

Substituting the expression of  $\pi$  in Equation (42) into the HIV basic reproduction number ( $\mathcal{R}_0^H$ ) in (8), we obtained  $\mathcal{R}_0^H$  in terms of  $\mathcal{R}_0^B$ , given as

$$\mathcal{R}_0^H = \frac{(1 - rz)\beta_H (K_2 K_3 + c_1 \eta K_3 + c_2(\sigma_1 K_2 + \eta \sigma_2))}{K_1 K_2 K_3} + \frac{\mathcal{R}_0^B (\alpha + u_2)\varepsilon_1 u_3 u_4 - (1 - rz)\beta_B \varepsilon_1 u_2 (\psi + u_4)}{(\alpha + u_2)\varepsilon_2 u_4 K_1}, \quad (43)$$

where  $K_1 = \eta + \sigma_1 + \theta$ ,  $K_2 = \sigma_2 + \delta_H + \theta$ , and  $K_3 = \phi_1 \delta_H + \theta$ .

Taking the partial derivatives of  $\mathcal{R}_0^H$  in (43) with respect to  $\mathcal{R}_0^B$ , we have

$$\frac{\partial \mathcal{R}_0^H}{\partial \mathcal{R}_0^B} = \frac{\varepsilon_1 u_3}{\varepsilon_2 K_1} > 0 \quad (44)$$

Similarly, it is observed that the partial derivative of  $\mathcal{R}_0^H$  with respect to  $\mathcal{R}_0^B$  in (44) is positive. Therefore, this result indicates that an increase in HBV infection within the population will significantly increase the transmission of HIV positively.

## 4 | Numerical Simulation

In this section, we shall simulate the HIV and HBV co-infection model numerically using parameter values in Table 2, in order to illustrate some of the analytic results obtained in the study. We

**TABLE 2** | Parameter values.

Parameter	Value	Source
$\pi$	0.0685	[48]
$\theta$	0.007765	[49]
$\varepsilon_1$	0.4	[26]
$\varepsilon_2$	0.2	[23]
$\varepsilon_3$	0.07	Assumed
$\alpha$	0.06	[50]
$\beta_B$	0.9416	Fitted
$\beta_H$	0.85	Fitted
$\gamma$	0.01	[50]
$r$	0.6	[51]
$z$	0.8	[51]
$\sigma_1$	0.2031	Fitted
$\sigma_2$	0.3693	Fitted
$\eta$	0.07	[26]
$c_1$	0.4	[26]
$c_2$	0.01	[26]
$\delta_H$	0.01	[26]
$\psi$	0.3292	Fitted
$\tau_1$	0.9	Fitted
$\tau_2$	0.0593	Fitted
$\delta_B$	0.01	[28]
$\phi_1$	0.001	[26]
$\phi_2$	0.003	Fitted
$q$	0.12	Fitted
$\mu$	0.1737	Fitted
$\omega_1$	0.3	Assumed
$\omega_2$	0.6	[30]
$\omega_3$	0.5	Assumed
$\omega_4$	0.4	Assumed
$e_1, e_2, e_3$	0.3, 0.1, 0.4	Assumed
$e_4, e_5, e_6$	0.2, 0.1, 0.5	Assumed
$e_7, e_8, e_9$	0.4, 0.32, 0.2	Assumed
$\nu$	0.47	Assumed
$\kappa$	0.5	Assumed
$\xi_1$	0.2	Assumed
$\xi_2$	0.4	Assumed
$\delta_{HAB}$	0.001	[30]
$\delta_{HCB}$	0.06	Assumed
$\delta_{AAB}$	0.005	[52]
$\delta_{ACB}$	0.2165	Assumed
$\delta_{THB}$	0.001	[30]
$d$	0.5	Assumed
$p$	0.3	Assumed

**TABLE 3** | Yearly reported cases of acute HBV in the United State from 2006 to 2021.

Year	Reported cases
2006	4713
2007	4519
2008	4029
2009	3371
2010	3350
2011	2903
2012	2895
2013	3050
2014	2791
2015	3370
2016	3218
2017	3409
2018	3322
2019	3192
2020	2157
2021	2045

shall be utilizing the ODE solver coded in MATLAB for the model simulation (Table 3).

We perform the model data fitting for the HIV and HBV co-infection model with the yearly cumulative cases of new HIV infection and the yearly cumulative reported cases of acute HBV infection in the United states from 2006 to 2022, in order to validate our model (Figures 5 and 6). The HIV yearly data in the United State were sourced from AIDSvu [53], and the yearly HBV acute data were sourced from [54–56] (Table 4). The model data fitting was carried out using the fmincon algorithm in the MATLAB optimization tool box [57]. This method employs the least square approach, known for its efficiency and reliability. The goal is to align the observed data set,  $Y_i$ , with the estimated values,  $X_i$ , aiming to minimize the sum of the squares errors (SSE), expressed mathematically as (Table 5)

$$SSE = \sum_{i=1}^k (Y_i - X_i)^2 \quad (45)$$

#### 4.1 | Discussion of Results

Figure 7 is the simulation of the contour plots of the HIV basic reproduction. Figure 7b,c depicts the contour plot of the HIV basic reproduction number ( $\mathcal{R}_0^H$ ) as a function of the compliance rate to condom usage ( $r$ ) and the treatment rate of HIV-only-infected individuals with no clinical symptoms of AIDS ( $\sigma_1$ ), and the contour plot of the HIV basic reproduction number ( $\mathcal{R}_0^H$ ) as a function of the compliance rate to condom usage ( $r$ ) and the treatment rate of HIV-only-infected individuals with clinical symptoms of AIDS ( $\sigma_2$ ). It is observed in Figure 7b,c that as the compliance rate to condom usage ( $r$ ) and the treatment rates ( $\sigma_1$  and  $\sigma_2$ ) increases, the HIV basic reproduction number

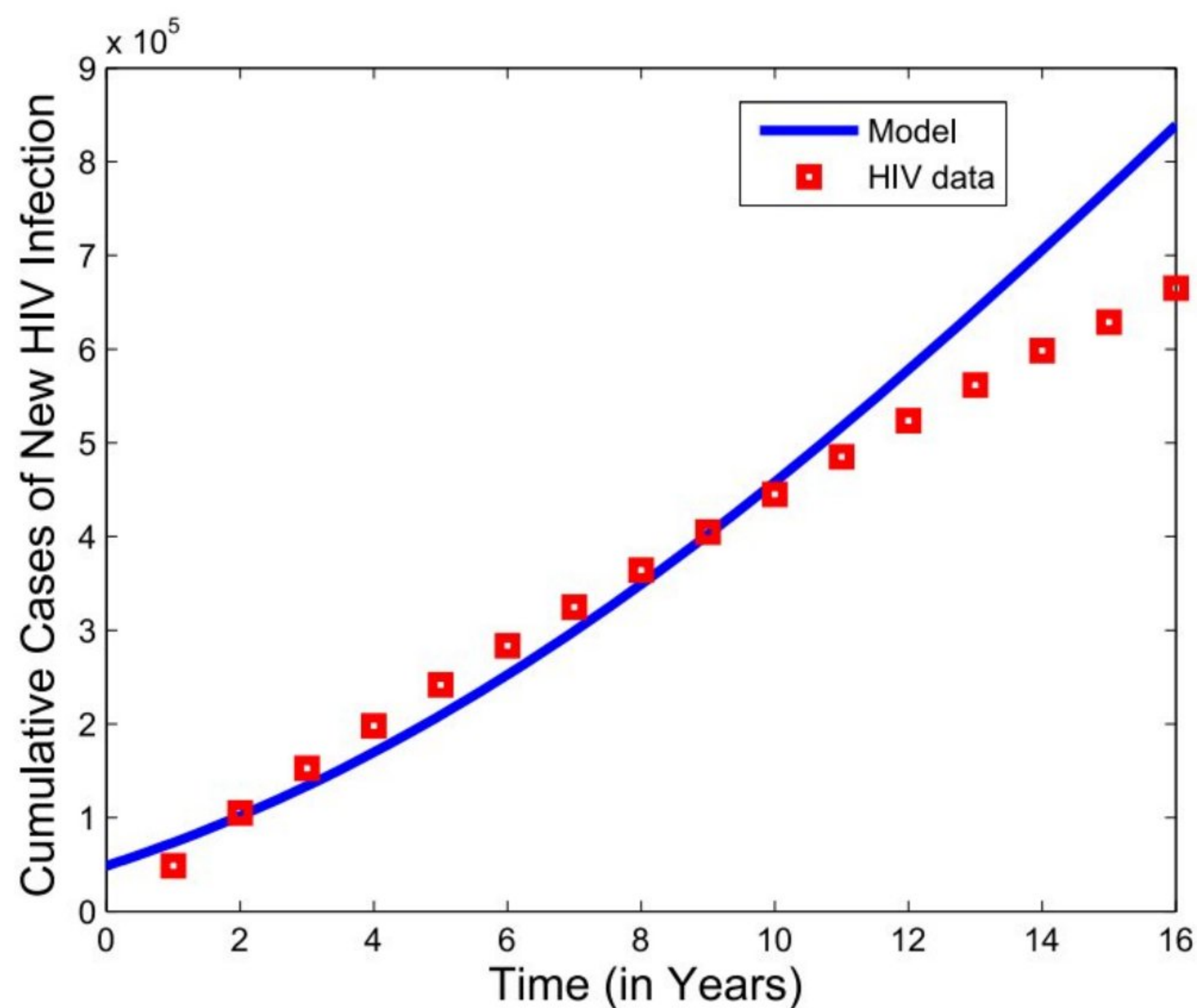


**FIGURE 5** | Data fitting of the cumulative new cases of HIV infection. [Colour figure can be viewed at [wileyonlinelibrary.com](https://onlinelibrary.wiley.com)]

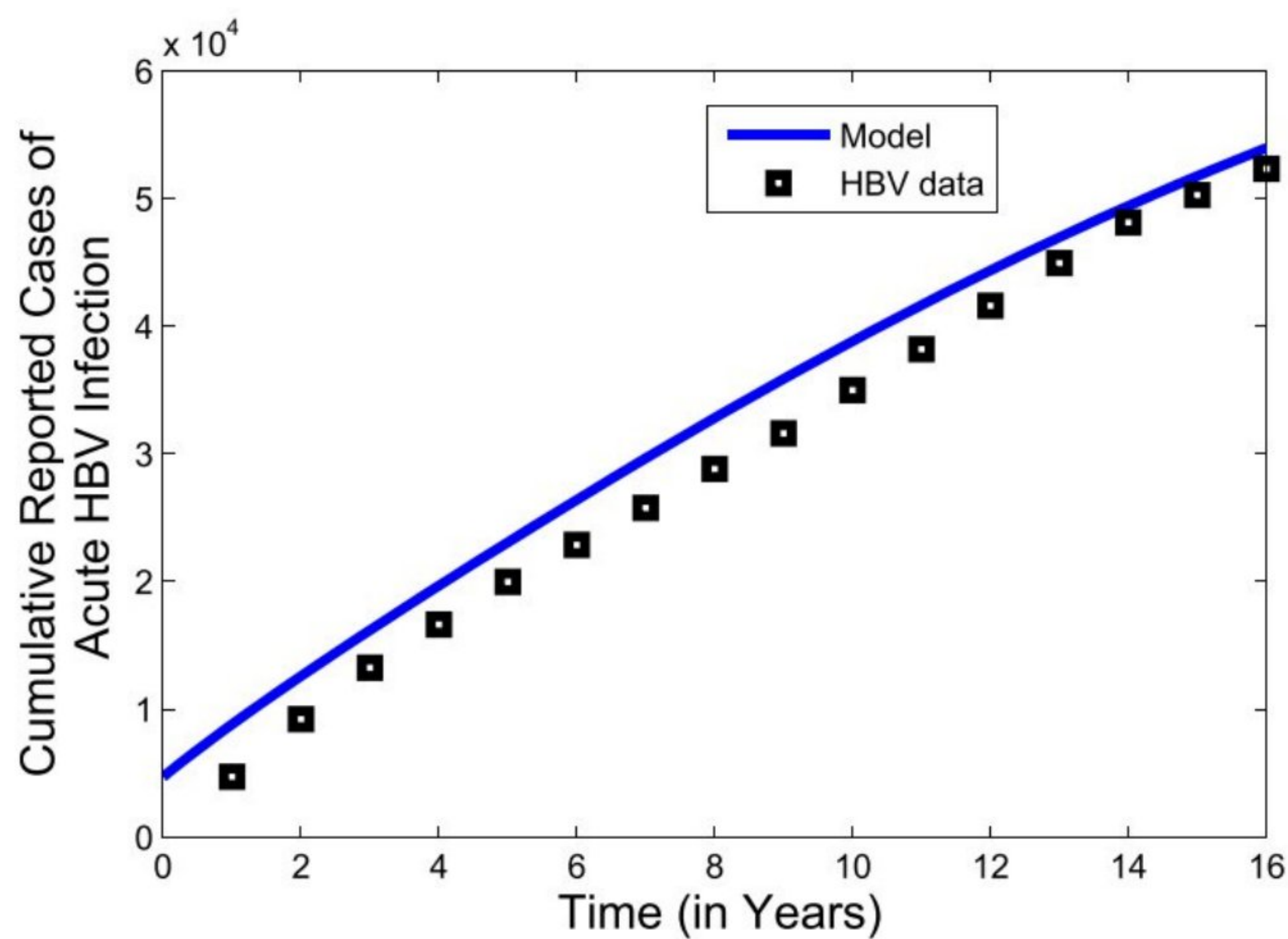


**FIGURE 6** | Data fitting of the cumulative reported cases of acute HBV infection. [Colour figure can be viewed at [wileyonlinelibrary.com](https://onlinelibrary.wiley.com)]

decreases. Similar result is observed in Figure 7a, for the contour plot of the HIV basic reproduction number ( $\mathcal{R}_0^H$ ) as a function of the treatment rates ( $\sigma_1$ ) and ( $\sigma_2$ ). These results align seamlessly with the results from the sensitivity analysis of the HIV basic reproduction in Section 3.4. Figure 8 depicts the simulations of the contour plots of the HBV basic reproduction number. Figure 8b,c is the contour plots of the HBV basic reproduction number ( $\mathcal{R}_0^B$ ) as a function of the compliance rate to condom usage ( $r$ ) and the treatment rate of HBV acute-infected individuals ( $\tau_1$ ) and as a function of the compliance rate to condom usage ( $r$ ) and treatment rate of chronic HBV-infected individuals ( $\tau_2$ ). It is observed in Figure 8b that if the compliance rate to condom usage ( $r$ ) and acute HBV treatment rate ( $\tau_1$ ) is stepped up to 80%, the HBV basic reproduction number ( $\mathcal{R}_0^B$ ) will be reduced to 0.6. In Figure 8c, if the compliance rate to condom usage ( $r$ ) and chronic HBV treatment rate ( $\tau_2$ ) is increased to 60%, the HBV basic reproduction number ( $\mathcal{R}_0^B$ ) will be reduced to 0.4. Figure 8d is the contour plot of the HBV basic reproduction number ( $\mathcal{R}_0^B$ )

**TABLE 4** | Yearly reported cases of new HIV infection in the United State from 2006 to 2021 from AIDSvu.

Year	Reported cases
2006	48,600
2007	56,300
2008	47,821
2009	45,315
2010	43,662
2011	41,831
2012	41,009
2013	39,715
2014	40,470
2015	40,285
2016	39,962
2017	38,775
2018	37,736
2019	36,817
2020	30,575
2021	36,126

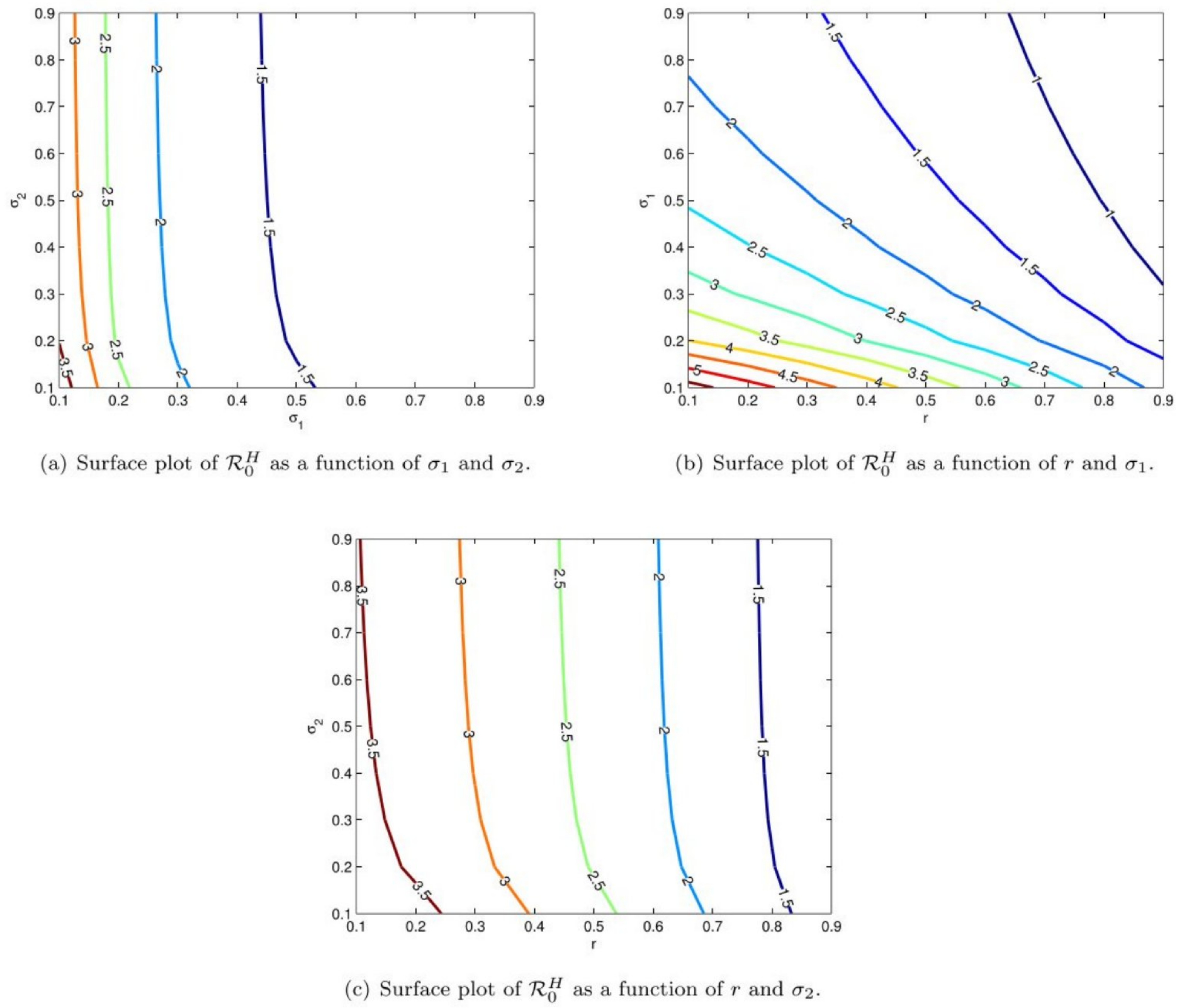
**TABLE 5** | Values of the impact of one disease on the other.

$\frac{\partial \mathcal{R}_0^B}{\partial \mathcal{R}_0^H}$	0.1131
$\frac{\partial \mathcal{R}_0^H}{\partial \mathcal{R}_0^B}$	8.8439

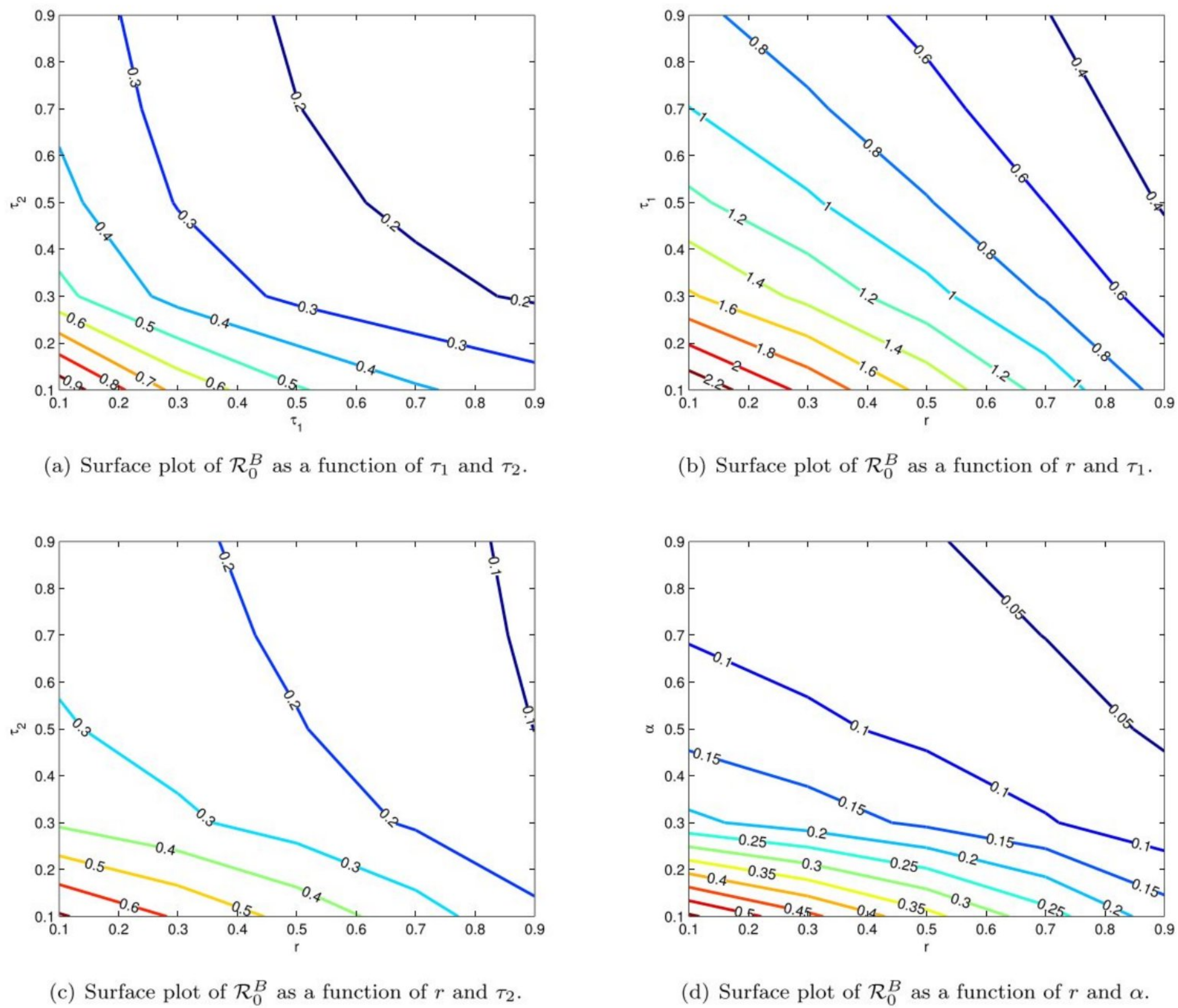
as a function of the compliance rate to condom usage ( $r$ ) and the HBV vaccination rate ( $\alpha$ ). It is observed in Figure 8d that if the compliance rate to condom usage ( $r$ ) and the HBV vaccination rate ( $\alpha$ ) is stepped up to 70%, the HBV basic reproduction number ( $\mathcal{R}_0^B$ ) will be brought to 0.15. Figure 8a is the contour plot of the HBV basic reproduction number ( $\mathcal{R}_0^B$ ) as a function of the acute HBV treatment rate ( $\tau_1$ ) and the chronic HBV treatment rate ( $\tau_2$ ). It is observed that if the HBV treatment rates  $\tau_1$  and  $\tau_2$  are increased to 80%, the HBV basic reproduction number ( $\mathcal{R}_0^B$ ) will be reduced to 0.3.

Figure 9 is the simulation of the cumulative new cases of HIV infection when the HIV basic reproduction number is less than one ( $\mathcal{R}_0^H = 0.3604$ ). In Figure 9a-c, it is observed that when the values of the compliance rate to the usage of condom ( $r$ ), and the treatment rates of HIV-infected individuals ( $\sigma_1$  and  $\sigma_2$ ) increases, the cumulative new cases of HIV decrease. Furthermore, if the compliance rate to condom usage ( $r$ ) can be stepped up 70%, the treatment rate ( $\sigma_1$ ) to 70%, and the treatment rate ( $\sigma_2$ ) to 90%, the cumulative new cases of HIV will be reduced below 60,000, 53,000, and 60,000, respectively, within 10 years.

Similarly, Figure 10 depicts the simulation of the cumulative new cases of HBV infection when the HBV basic reproduction number is less than one ( $\mathcal{R}_0^B = 0.4789$ ). In Figure 10a, it is observed that if the compliance rate to condom usage ( $r$ ) is increased to 70%, the cumulative new cases of HBV will be reduced below



**FIGURE 7** | Surface plots of the HIV basic reproduction number. [Colour figure can be viewed at [wileyonlinelibrary.com](http://wileyonlinelibrary.com)]



**FIGURE 8** | Surface plots of the HBV basic reproduction number. [Colour figure can be viewed at [wileyonlinelibrary.com](http://wileyonlinelibrary.com)]

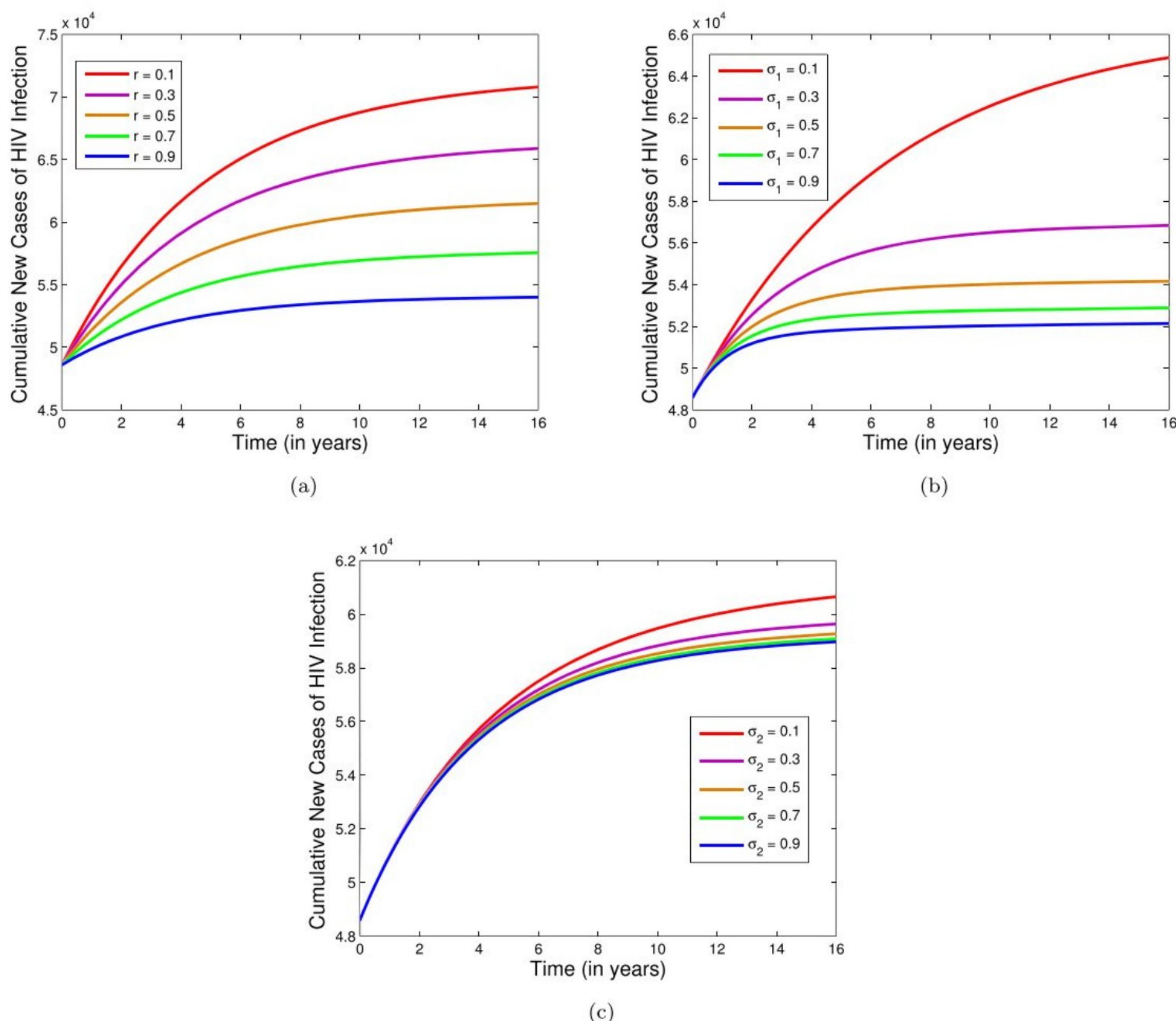


**FIGURE 9** | Simulations of full model (1) showing the plots for (a) the effect of  $r$  on the cumulative new cases of HIV; (b) the effect of  $\sigma_1$  on the cumulative new cases of HIV; and (c) the effect of  $\sigma_2$  on the cumulative new cases of HIV, for the case when  $\mathcal{R}_0^H < 1$  while varying the treatment rates and condom usage rate. Parameter values used are as in Table 2 with  $\beta_H = 0.1$  (so that  $\mathcal{R}_0^H = 0.3604$ ). The values of the HIV reproduction number when the treatment rates and condom usage rate are varied can be found in Tables 6-8. [Colour figure can be viewed at [wileyonlinelibrary.com](https://onlinelibrary.wiley.com)]

**TABLE 6** | The values of the HIV reproduction number when the treatment rates and condom usage rate are varied.

$r$	$\mathcal{R}_0^H$
0.1	0.5625
0.3	0.4817
0.5	0.4008
0.7	0.3199
0.9	0.2391

**TABLE 7** | The values of the HIV reproduction number when the treatment rates and condom usage rate are varied.

$\sigma_1$	$\mathcal{R}_0^H$
0.1	0.5306
0.3	0.2851
0.5	0.2095
0.7	0.1729
0.9	0.1512

50,000 within 10 years. In Figure 10d, it is observed that if the vaccination rate ( $\alpha$ ) is stepped up to 50%, the cumulative new cases of HIV will be reduced below 12,000 within 14 years. In Figure 10b, it is observed that if the treatment rate ( $\tau_1$ ) for acute HBV-infected individuals is stepped up to 70%, the cumulative new cases of HBV infection will decrease to below 60,000 in 12 years. Furthermore, in Figure 10c, it is the treatment rate of chronic HBV-infected individuals ( $\tau_2$ ) is increased to 50%, the cumulative new cases of HBV will decrease below 20,000 within 10 years.

**TABLE 8** | The values of the HIV reproduction number when the treatment rates and condom usage rate are varied.

$\sigma_2$	$\mathcal{R}_0^H$
0.1	0.3892
0.3	0.3631
0.5	0.3572
0.7	0.3545
0.9	0.3531

Figure 11 is the simulation of the effect of the treatment rate ( $\sigma_1$ ) on HIV on infected individuals with no clinical symptoms of AIDS ( $I_H(t)$ ), the effect of the treatment rate ( $\sigma_1$ ) on HIV on

infected individuals with clinical symptoms of AIDS ( $A_H(t)$ ), the effect of the treatment rate ( $\tau_1$ ) on HBV on infected individuals with acute infection ( $I_{AB}(t)$ ), the effect of the treatment rate ( $\tau_1$ )

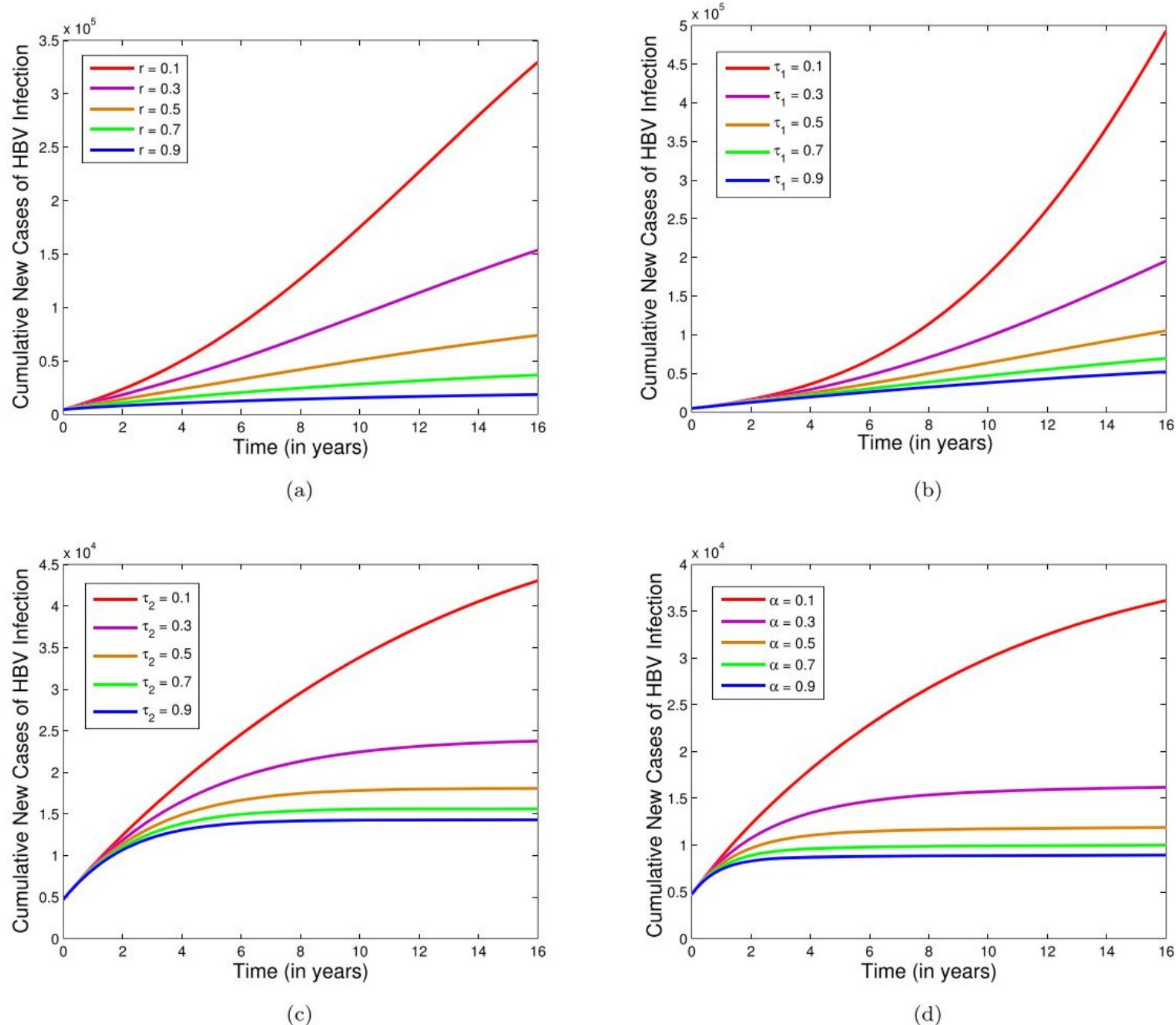


**FIGURE 10** | Simulations of full model (1) showing the plots for (a) the effect of  $r$  on the cumulative new cases of HBV; (b) the effect of  $\tau_1$  on the cumulative new cases of HBV; (c) the effect of  $\tau_2$  on the cumulative new cases of HBV; and (d) the effect of  $\alpha$  on the cumulative new cases of HBV, for the case when  $\mathcal{R}_0^B < 1$  while varying the treatment rates, condom usage rate, and vaccination rate. Parameter values used are as in Table 2 (so that  $\mathcal{R}_0^B = 0.4789$ ). The values of the HBV reproduction number when the treatment rates, condom usage rate, and vaccination rate are varied can be found in Tables 9-11. [Colour figure can be viewed at [wileyonlinelibrary.com](https://onlinelibrary.wiley.com)]

on HBV on infected individuals with chronic infection ( $I_{CB}(t)$ ), the effect of the vaccination rate ( $\alpha$ ) on HBV on infected individuals with acute infection ( $I_{AB}(t)$ ), and the effect of the vaccination rate ( $\alpha$ ) on HBV on infected individuals with chronic infection ( $I_{CB}(t)$ ), using parameter values in Table 2 with  $\beta_H = 0.1$  (so that  $\mathcal{R}_0^H = 0.3604$  and  $\mathcal{R}_0^B = 0.4789$ ). Figure 11 illustrates the convergence to the local stability of the disease-free equilibrium in line with Theorems 2 and 5.

Figure 12 depicts the simulation of the infected individuals with both HIV (not showing clinical symptoms of AIDS) and acute HBV infection ( $I_{HAB}(t)$ ), infected individuals with both HIV (not

**TABLE 9** | The values of the HBV reproduction number when the treatment rates, condom usage rate, and vaccination rate are varied.

$r$	$\mathcal{R}_0^B$
0.1	0.8427
0.3	0.6972
0.5	0.5517
0.7	0.4062
0.9	0.2607

**TABLE 10** | The values of the HBV reproduction number when the treatment rates, condom usage rate, and vaccination rate are varied.

$\tau_1$	$\mathcal{R}_0^B$
0.1	1.3361
0.3	0.9231
0.5	0.7051
0.7	0.5704
0.9	0.4789

**TABLE 11** | The values of the HBV reproduction number when the treatment rates, condom usage rate, and vaccination rate are varied.

$\tau_2$	$\mathcal{R}_0^B$
0.1	0.3465
0.3	0.1887
0.5	0.1528
0.7	0.1369
0.9	0.1279

showing clinical symptoms of AIDS) and chronic HBV infection ( $I_{HCB}(t)$ ), infected individuals with both HIV (showing clinical symptoms of AIDS) and acute HBV infection ( $I_{AAB}(t)$ ), and

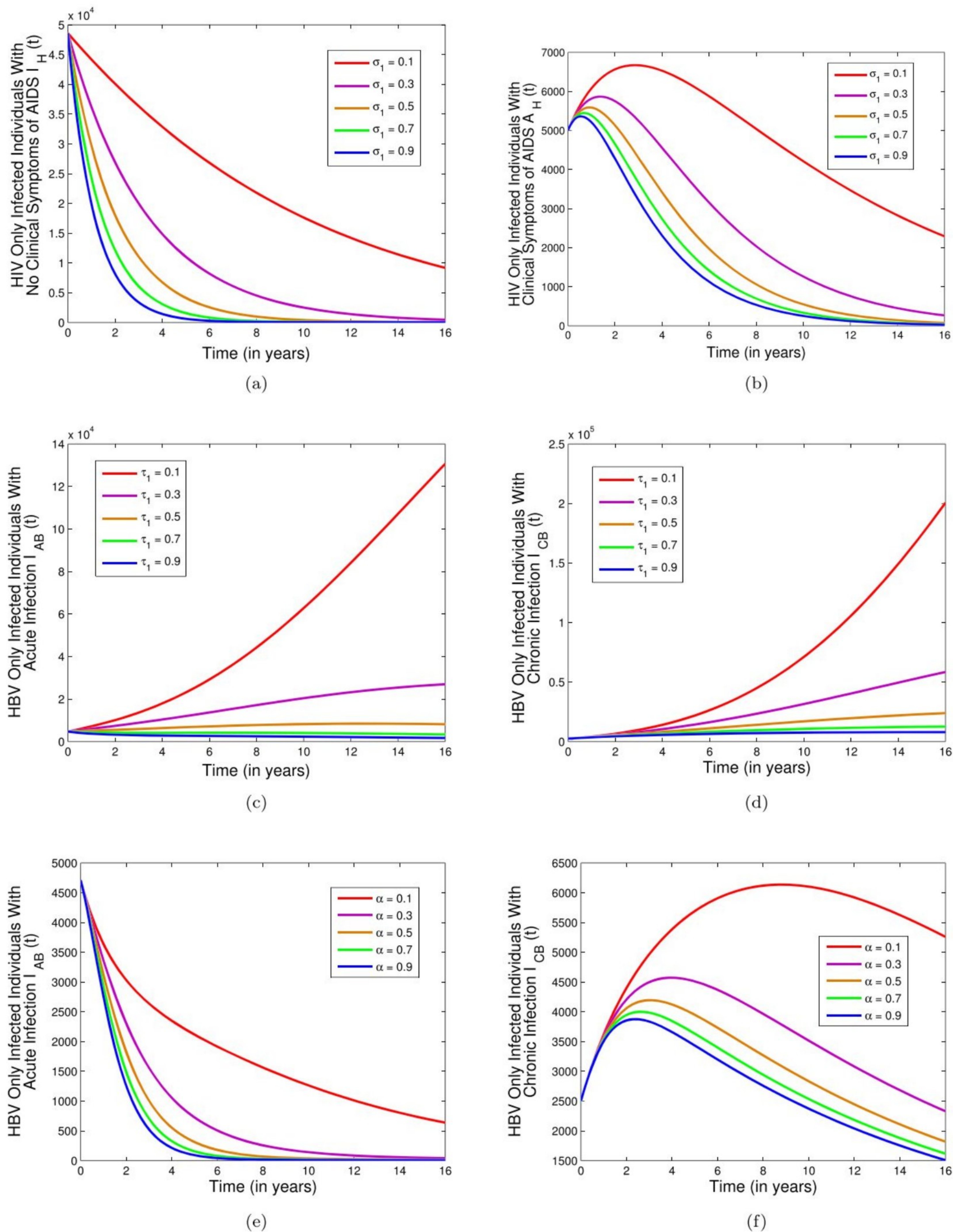


**FIGURE 11** | Simulations of full model (1) showing the plots for (a) the effect of  $\sigma_1$  on HIV-only-infected individuals with no clinical symptoms of AIDS; (b) the effect of  $\sigma_1$  on HIV-only-infected individuals with clinical symptoms of AIDS; (c) the effect of  $\tau_1$  on HBV-only-infected individuals with acute infection; (d) the effect of  $\tau_1$  on HBV-only-infected individuals with chronic infection; (e) the effect of  $\alpha$  on HBV-only-infected individuals with acute infection; and (f) the effect of  $\alpha$  on HBV-only-infected individuals with chronic infection, for the case when  $\mathcal{R}_0^B < 1$  and  $\mathcal{R}_0^H < 1$  while varying the treatment rates and vaccination rate. Parameter values used are as in Table 2 with  $\beta_H = 0.1$  (so that  $\mathcal{R}_0^H = 0.3604$  and  $\mathcal{R}_0^B = 0.4789$ ). The values of the HIV reproduction number and HBV reproduction number when the treatment rates and vaccination rate are varied can be found in Tables 6-11. [Colour figure can be viewed at [wileyonlinelibrary.com](http://wileyonlinelibrary.com)]

infected individuals with both HIV (showing clinical symptoms of AIDS) and chronic HBV infection ( $I_{ACB}(t)$ ), using parameter values in Table 2 with  $\beta_H = 0.1$  (so that  $\mathcal{R}_0^H = 0.3604$  and  $\mathcal{R}_0^B = 0.4789$ ) while varying the treatment rates of the co-infected compartments. Figure 12 illustrates the convergence

of the HIV and HBV co-infection to the local stability of the disease-free equilibrium in line with Theorem 9. Additionally, increasing the treatment rates of the respective co-infected compartments reduces the burden of HIV and HBV co-infection (Table 12).

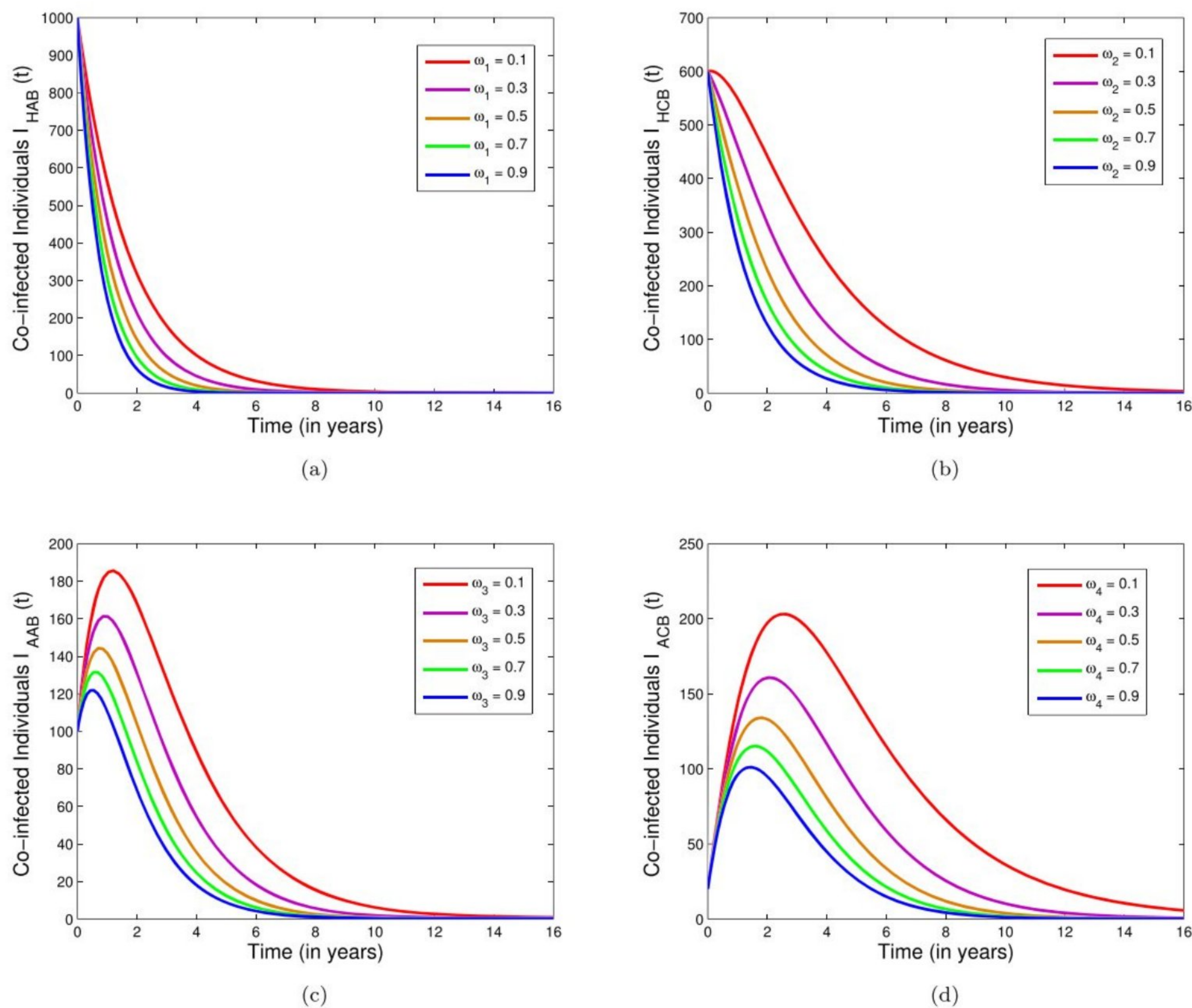


**FIGURE 12** | Simulations of full model (1) showing the plots for (a) the effect of  $\omega_1$  on the co-infected class  $I_{HAB}$ ; (b) the effect of  $\omega_2$  on the co-infected class  $I_{HCB}$ ; (c) the effect of  $\omega_3$  on the co-infected class  $I_{AAB}$ ; and (d) the effect of  $\omega_4$  on the co-infected class  $I_{ACB}$ , for the case when  $\mathcal{R}_0^B < 1$  and  $\mathcal{R}_0^H < 1$  while varying the treatment rates. Parameter values used are as in Table 2 with  $\beta_H = 0.1$  (so that  $\mathcal{R}_0^H = 0.3604$ ,  $\mathcal{R}_0^B = 0.4789$ , and  $\mathcal{R}_0^{HB} = 0.4789$ ). [Colour figure can be viewed at [wileyonlinelibrary.com](https://onlinelibrary.wiley.com)]

**TABLE 12** | The values of the HBV reproduction number when the treatment rates, condom usage rate, and vaccination rate are varied.

$\alpha$	$\mathcal{R}_0^B$
0.1	0.3183
0.3	0.1218
0.5	0.0771
0.7	0.0573
0.9	0.0461

**TABLE 13** | The values of the HIV reproduction number when the treatment rates and condom usage rate are varied.

$r$	$\mathcal{R}_0^H$
0.1	4.0497
0.3	3.3624
0.5	2.6750
0.7	1.9877
0.9	1.3004

Figure 13 is the simulation of the effect of the treatment rate of HIV-only-infected individuals showing clinical symptoms of AIDS ( $\sigma_2$ ) on the prevalence of HIV-only-infected individuals with no clinical symptoms of AIDS ( $I_H(t)$ ) and HIV-only-infected individuals with clinical symptoms of AIDS ( $A_H(t)$ ), and the effects of the treatment rate of chronic HBV-only-infected individuals ( $\tau_2$ ) on the prevalence of HBV-only-infected individuals with acute infection ( $I_{AB}(t)$ ) and HBV-only-infected individuals with chronic infection ( $I_{CB}(t)$ ), when the HIV and HBV basic reproduction number is less than one ( $\mathcal{R}_0^H = 0.3604$  and  $\mathcal{R}_0^B = 0.4789$ ). It is observed in Figure 13a that increasing the HIV treatment rate ( $\sigma_2$ ) has very little effect in reducing the prevalence of

**TABLE 14** | The values of the HIV reproduction number when the treatment rates and condom usage rate are varied.

$\sigma_1$	$\mathcal{R}_0^H$
0.1	3.3538
0.3	1.8792
0.5	1.4255
0.7	1.2051
0.9	1.0749

HIV. In Figure 13b, it is observed that if the HIV treatment rate ( $\sigma_2$ ) is increased to 70%, the number of HIV-only-infected individuals showing clinical symptoms of AIDS will reduce to below



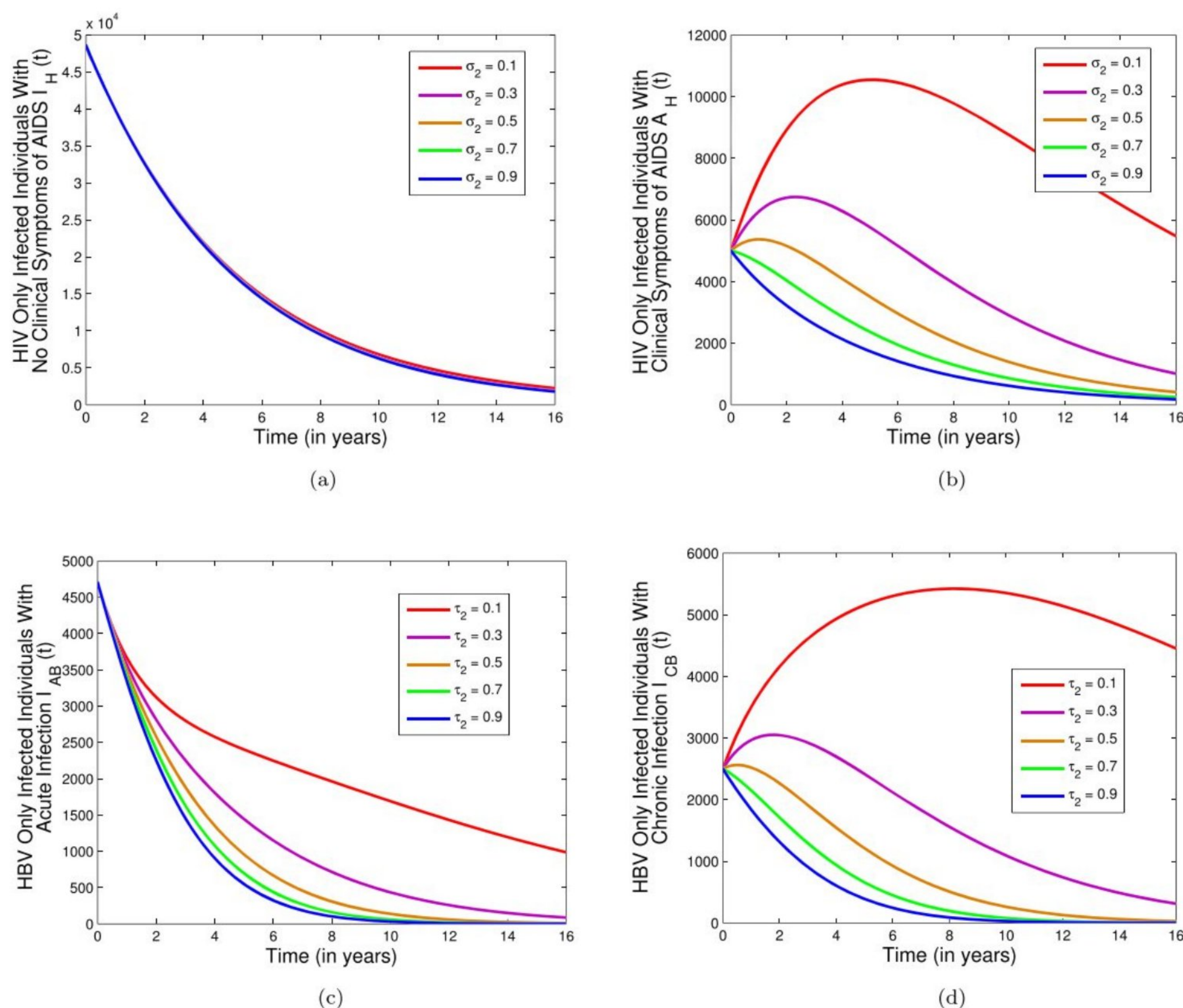


**FIGURE 13** | Simulations of full model (1) showing the plots for (a) the effect of  $\sigma_2$  on HIV-only-infected individuals with no clinical symptoms of AIDS; (b) the effect of  $\sigma_2$  on HIV-only-infected individuals with clinical symptoms of AIDS; (c) the effect of  $\tau_2$  on HBV-only-infected individuals with acute infection; and (d) the effect of  $\tau_2$  on HBV-only-infected individuals with chronic infection, for the case when  $R_0^B < 1$  and  $R_0^H < 1$  while varying the treatment rates. Parameter values used are as in Table 2 with  $\beta_H = 0.1$  (so that  $R_0^H = 0.3604$  and  $R_0^B = 0.4789$ ). The values of the HIV reproduction number and HBV reproduction number when the treatment rates are varied can be found in Tables 15 and 18. [Colour figure can be viewed at [wileyonlinelibrary.com](https://onlinelibrary.wiley.com)]

**TABLE 15** | The values of the HIV reproduction number when the treatment rates and condom usage rate are varied.

$\sigma_2$	$R_0^H$
0.1	2.5768
0.3	2.3548
0.5	2.3043
0.7	2.2819
0.9	2.2693

**TABLE 16** | The values of the HBV reproduction number when the treatment rates, condom usage rate, and vaccination rate are varied.

$r$	$R_0^B$
0.1	2.6531
0.3	2.1925
0.5	1.7319
0.7	1.2713
0.9	0.8107

2000 within 6 years. In Figure 13c,d, it is observed that if the HBV treatment rate ( $\tau_2$ ) is stepped up to 70%, the prevalence of acute

**TABLE 17** | The values of the HBV reproduction number when the treatment rates, condom usage rate, and vaccination rate are varied.

$\tau_1$	$R_0^B$
0.1	2.9706
0.3	2.3868
0.5	1.9948
0.7	1.7134
0.9	1.5016

**TABLE 18** | The values of the HBV reproduction number when the treatment rates, condom usage rate, and vaccination rate are varied.

$\tau_2$	$R_0^B$
0.1	1.0356
0.3	0.4802
0.5	0.3538
0.7	0.2979
0.9	0.2663

and chronic HBV will decrease to below 500 and 1000, respectively, within 6 years.

Figure 14 is the simulation of the cumulative new cases of HIV infection when the HIV basic reproduction number is greater than one ( $\mathcal{R}_0^H = 2.3314$ ). It is observed in Figure 14a-c that if the compliance rate to condom usage ( $r$ ) can be stepped up to 70%, the treatment rate ( $\sigma_1$ ) to 70%, and the treatment rate ( $\sigma_2$ ) to 90%, the values of the cumulative new cases of HIV will be reduced to below 5,000,000, 300,000, and 800,000 within 16 years. Figure 15 is the simulations of the effect of the compliance rate to the usage of condom ( $r$ ), treatment rates of acute and chronic HBV-infected individuals ( $\tau_1$  and  $\tau_2$ ), and the HBV vaccination rate ( $\alpha$ ) on the cumulative new cases of HBV infection, for the case when the HBV basic reproduction number is greater than one. In Figure 15a, it is observed that if the compliance rate to the usage of condom ( $r$ ) is stepped up to 70%, the cumulative

new cases of HBV infection will be reduced to below 100,000 within 16 years. In Figure 15b, it is observed that if the treatment rate for acute HBV-infected individuals ( $\tau_1$ ) is increased to 90%, the cumulative new cases of HBV infection will significantly be reduced to below 100,000 within 12 years. It is also observed in Figure 15c that if the treatment rate for chronic HBV-infected individuals ( $\tau_2$ ) is stepped up to 70%, the cumulative new cases of HBV infection will be below 20,000 within 16 years. In Figure 15d, it is observed that when the HBV vaccination rate ( $\alpha$ ) is increased to 70%, the cumulative new cases of HBV infection will be within 11,000 in 16 years.

Figure 16 is the simulation of the effect of the treatment rate ( $\sigma_1$ ) on HIV on infected individuals with no clinical symptoms of AIDS ( $I_H(t)$ ), the effect of the treatment rate ( $\sigma_1$ ) on HIV on infected individuals with clinical symptoms of AIDS ( $A_H(t)$ ), the effect of the treatment rate ( $\tau_1$ ) on HBV on infected individuals with acute infection ( $I_{AB}(t)$ ), the effect of the treatment rate ( $\tau_1$ ) on HBV on infected individuals with chronic infection ( $I_{CB}(t)$ ), the effect of the vaccination rate ( $\alpha$ ) on HBV on infected individuals with acute infection ( $I_{AB}(t)$ ), and the effect of the vaccination rate ( $\alpha$ ) on HBV on infected individuals with chronic infection ( $I_{CB}(t)$ ), using parameter values in Table 2 with  $\gamma = 0.05$  and  $\psi = 0.7$  (so that  $\mathcal{R}_0^H = 2.3314$  and  $\mathcal{R}_0^B = 1.5016$ ). Figure 16 illustrates the convergence to the endemic equilibrium while varying the treatment rates of the respective infected compartments ( $\sigma_1$

**TABLE 19** | The values of the HBV reproduction number when the treatment rates, condom usage rate, and vaccination rate are varied.

$\alpha$	$\mathcal{R}_0^B$
0.1	1.1221
0.3	0.4974
0.5	0.3207
0.7	0.2373
0.9	0.1887

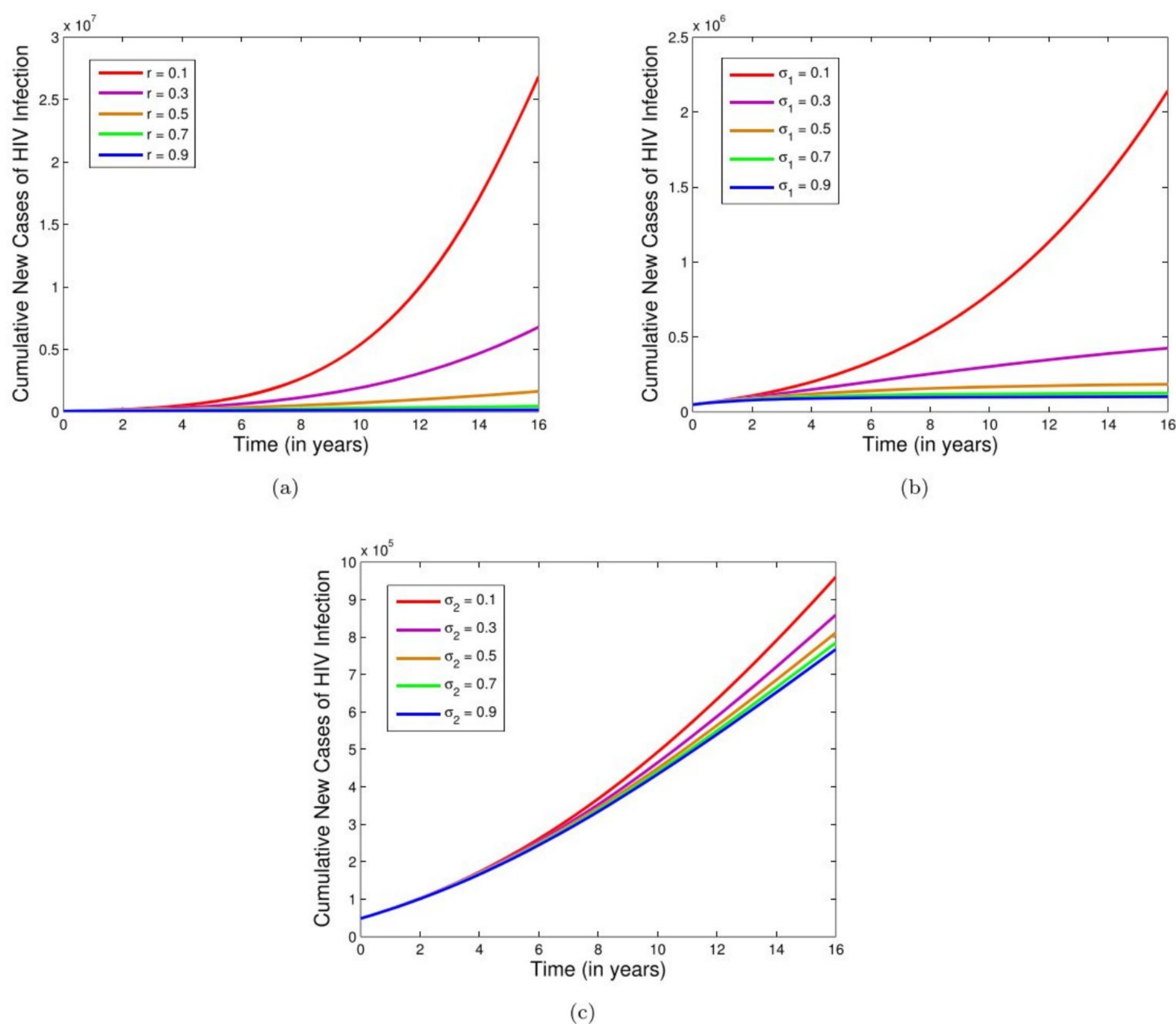


**FIGURE 14** | Simulations of full model (1) showing the plots for (a) the effect of  $r$  on the cumulative new cases of HIV; (b) the effect of  $\sigma_1$  on the cumulative new cases of HIV; and (c) the effect of  $\sigma_2$  on the cumulative new cases of HIV, for the case when  $\mathcal{R}_0^H > 1$  while varying the treatment rates and condom usage rate. Parameter values used are as in Table 2 (so that  $\mathcal{R}_0^H = 2.3314$ ). The values of the HIV reproduction number when the treatment rates and condom usage rate are varied can be found in Tables 13-15. [Colour figure can be viewed at [wileyonlinelibrary.com](https://onlinelibrary.wiley.com)]

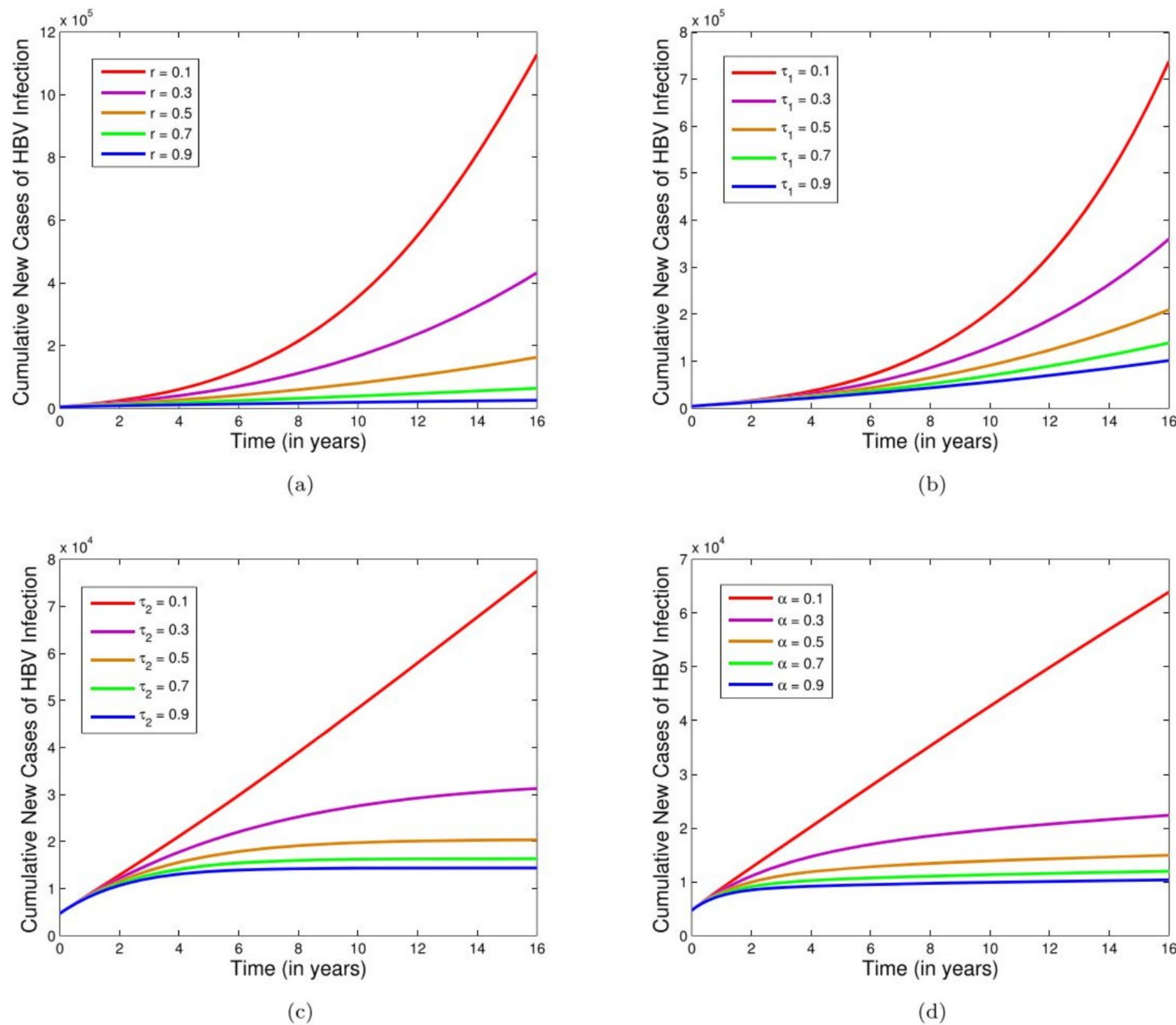


**FIGURE 15** | Simulations of full model (1) showing the plots for (a) the effect of  $r$  on the cumulative new cases of HBV; (b) the effect of  $\tau_1$  on the cumulative new cases of HBV; (c) the effect of  $\tau_2$  on the cumulative new cases of HBV; and (d) the effect of  $\alpha$  on the cumulative new cases of HBV, for the case when  $\mathcal{R}_0^B > 1$  while varying the treatment rates, condom usage rate and vaccination rate. Parameter values used are as in Table 2 with  $\gamma = 0.05$  and  $\psi = 0.7$  (so that  $\mathcal{R}_0^B = 1.5016$ ). The values of the HBV reproduction number when the treatment rates, condom usage rate, and vaccination rate are varied can be found in Tables 16–19. [Colour figure can be viewed at [wileyonlinelibrary.com](https://onlinelibrary.wiley.com/doi/10.1111/j.11754.1154)]

and  $\tau_1$ ) and the HBV vaccination rate ( $\alpha$ ). It is observed that an increase in the treatment rates and vaccination rate reduces the number of infected individuals of both diseases.

Figure 17 is the simulation of the infected individuals with both HIV (not showing clinical symptoms of AIDS) and acute HBV infection ( $I_{HAB}(t)$ ), infected individuals with both HIV (not showing clinical symptoms of AIDS) and chronic HBV infection ( $I_{HCB}(t)$ ), infected individuals with both HIV (showing clinical symptoms of AIDS) and acute HBV infection ( $I_{AAB}(t)$ ), and infected individuals with both HIV (showing clinical symptoms of AIDS) and chronic HBV infection ( $I_{ACB}(t)$ ), using parameter values in Table 2 with  $\gamma = 0.05$  and  $\psi = 0.7$  (so that  $\mathcal{R}_0^H =$  and  $\mathcal{R}_0^B = 1.5016$ , thus  $\mathcal{R}_0^{HB} = 1.5016 > 1$ ). Figure 17 illustrates the convergence to the endemic equilibrium of the HIV and HBV co-infection while varying the treatment rate rates of the respective co-infected compartments. It is observed that in the presence of the endemicity of HIV and HBV co-infection, increasing the treatment rates of the co-infected compartments will significantly reduce the burden of the co-infection of HIV and HBV. Figure 18 depicts the simulation of the effect of the treatment rate of the HIV-only-infected individuals (showing clinical symptoms of AIDS) ( $\sigma_2$ ) on the HIV-only-infected individuals not showing clinical symptoms of AIDS ( $I_H(t)$ ), HIV-only-infected individu-

als showing clinical symptoms of AIDS ( $A_H(t)$ ), and the effect of the treatment rate of chronic HBV-infected individuals ( $\tau_2$ ) on the acute HBV-only-infected individuals ( $I_{AB}(t)$ ), for the case when  $\mathcal{R}_0^H > 1$  and  $\mathcal{R}_0^B > 1$  using parameter values in Table 2 with  $\gamma = 0.05$  and  $\psi = 0.7$  (so that  $\mathcal{R}_0^H = 2.3314$  and  $\mathcal{R}_0^B = 1.5016$ ). It is observed in Figure 18a–d that increasing the treatment rates  $\sigma_2$  and  $\tau_2$  significantly reduces the prevalence of infected individuals with HIV and HBV infection, respectively.

Figures 19 and 20 depict the simulations of the effect of the vaccination rate against HBV ( $\alpha$ ) on HIV-infected individuals. In Figure 19a,b, it is observed that when the HIV basic reproduction number is less than unity, the vaccination rate against HBV ( $\alpha$ ) has minimal effect in reducing the number of HIV-infected individuals showing and not showing clinical symptoms of AIDS when the rate is increasing. In Figure 20a,b, it is observed that when the HIV basic reproduction number exceed 1, and the vaccination rate against HBV is stepped up to 70%, the number of individuals infected with HIV not showing clinical symptoms of AIDS will be reduced below 50,000 with 12 years; furthermore, the number of individual infected with HIV showing clinical symptoms of AIDS will be reduced below 10,000 within 12 years.

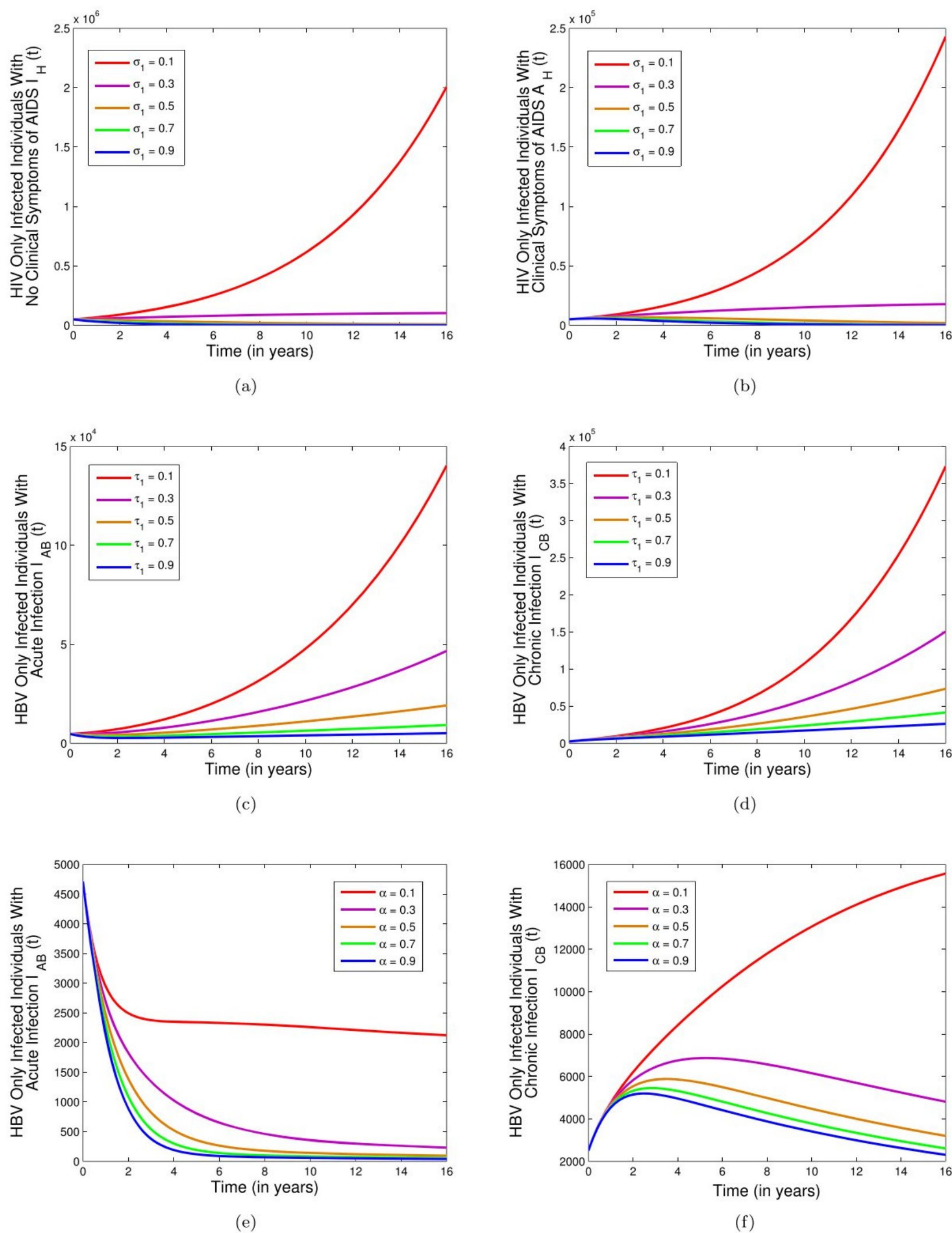


**FIGURE 16** | Simulations of full model (1) showing the plots for (a) the effect of  $\sigma_1$  on HIV-only-infected individuals with no clinical symptoms of AIDS; (b) the effect of  $\sigma_1$  on HIV-only-infected individuals with clinical symptoms of AIDS; (c) the effect of  $\tau_1$  on HBV-only-infected individuals with acute infection; (d) the effect of  $\tau_1$  on HBV-only-infected individuals with chronic infection; (e) the effect of  $\alpha$  on HBV-only-infected individuals with acute infection; and (f) the effect of  $\alpha$  on HBV-only-infected individuals with chronic infection, for the case when  $\mathcal{R}_0^B < 1$  and  $\mathcal{R}_0^H < 1$  while varying the treatment rates and vaccination rate Parameter values used are as in Table 2 with  $\gamma = 0.05$  and  $\psi = 0.7$  (so that  $\mathcal{R}_0^H = 2.3314$  and  $\mathcal{R}_0^B = 1.5016$ ). The values of the HIV reproduction number and HBV reproduction number when the treatment rates and vaccination rate are varied can be found in Tables 13, 17, and 19. [Colour figure can be viewed at [wileyonlinelibrary.com](https://onlinelibrary.wiley.com)]

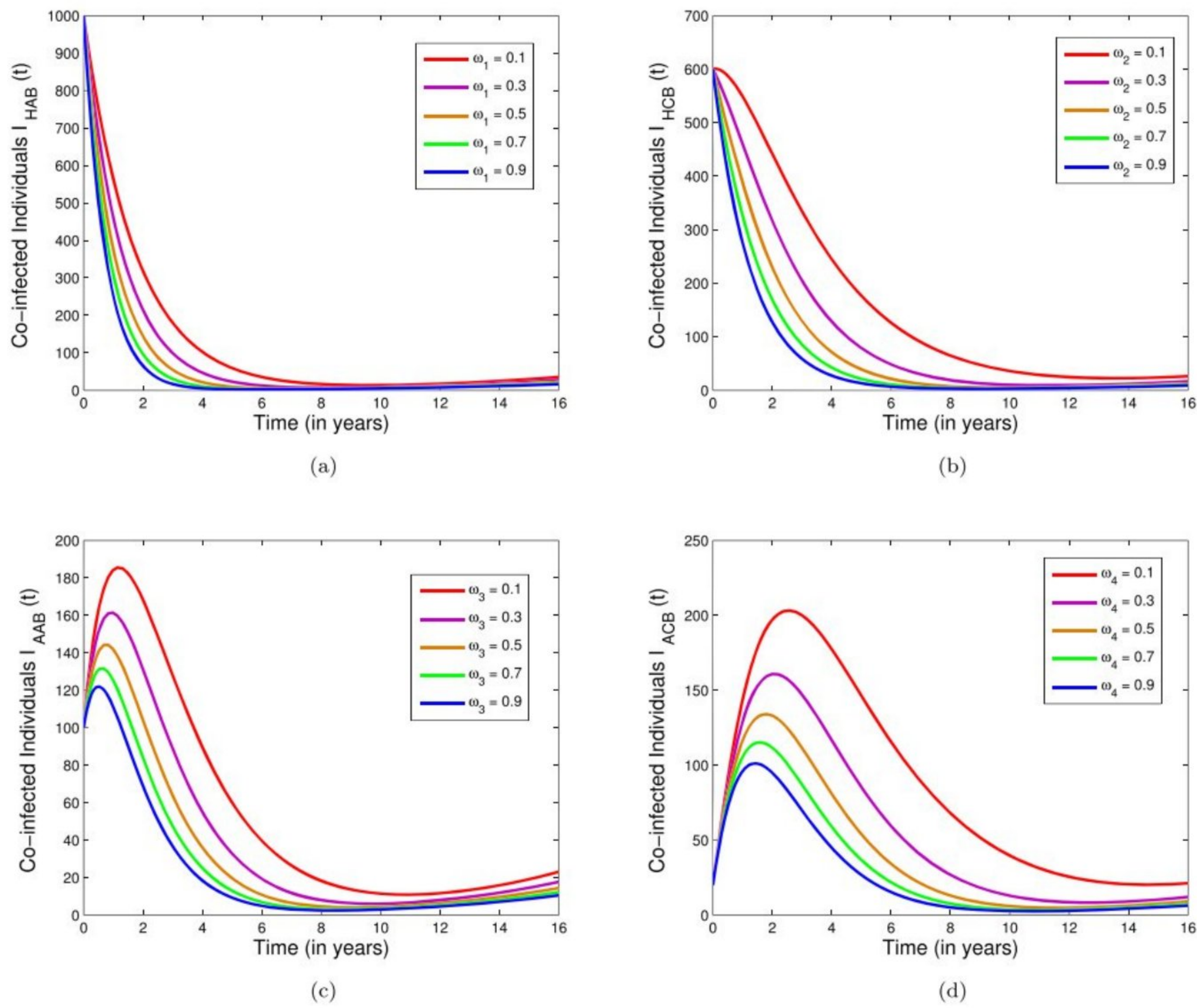


**FIGURE 17** | Simulations of full model (1) showing the plots for (a) the effect of  $\omega_1$  on the co-infected class  $I_{HAB}$ ; (b) the effect of  $\omega_2$  on the co-infected class  $I_{HCB}$ ; (c) the effect of  $\omega_3$  on the co-infected class  $I_{AAB}$ ; and (d) the effect of  $\omega_4$  on the co-infected class  $I_{ACB}$ , for the case when  $\mathcal{R}_0^B < 1$  and  $\mathcal{R}_0^H < 1$  while varying the treatment rates. Parameter values used are as in Table 2 with  $\gamma = 0.05$  and  $\psi = 0.7$  (so that  $\mathcal{R}_0^H = 2.3314$  and  $\mathcal{R}_0^B = 1.5016$ ). [Colour figure can be viewed at [wileyonlinelibrary.com](http://wileyonlinelibrary.com)]

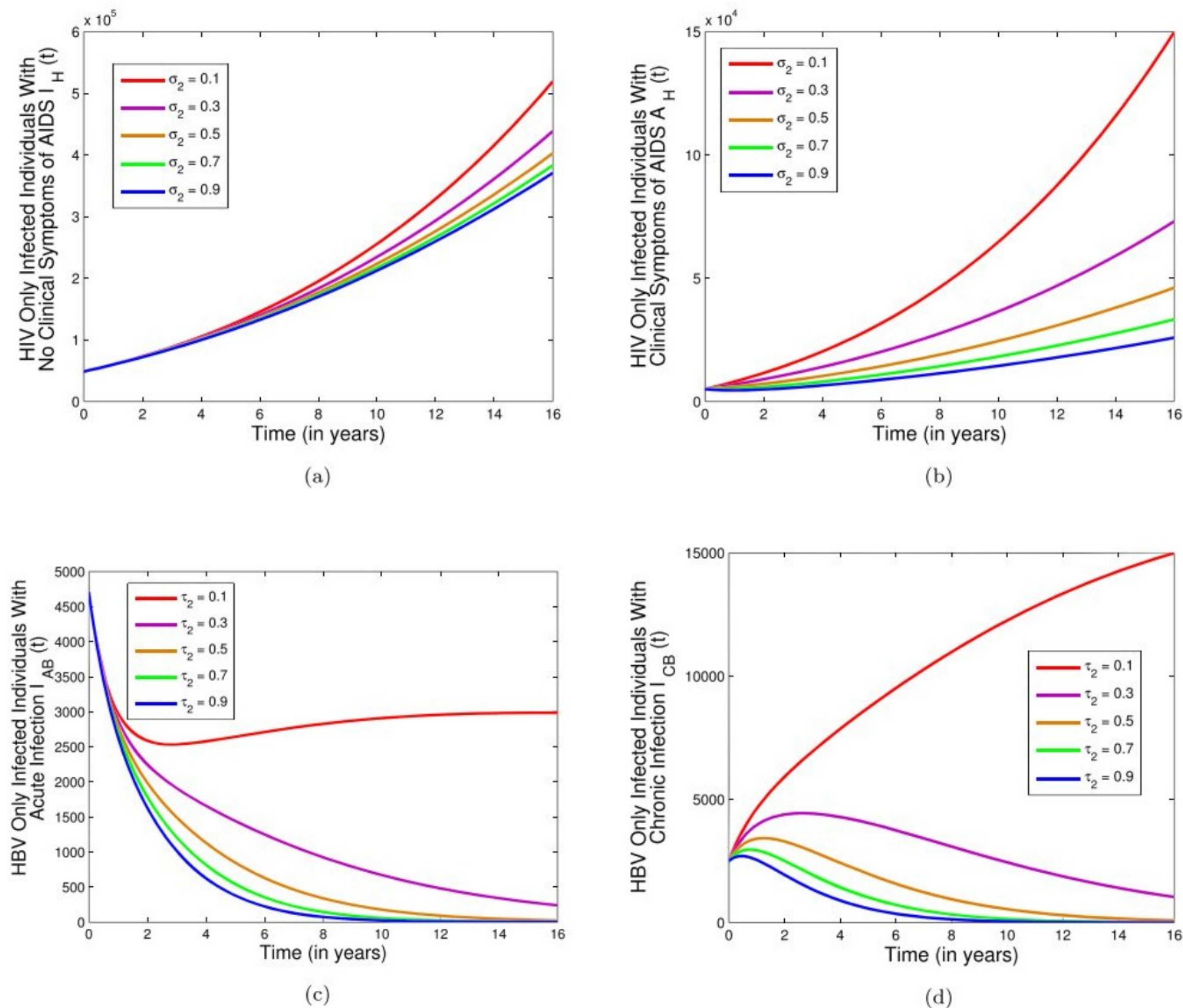


**FIGURE 18** | Simulations of full model (1) showing the plots for (a) the effect of  $\sigma_2$  on HIV-only-infected individuals with no clinical symptoms of AIDS; (b) the effect of  $\sigma_2$  on HIV-only-infected individuals with clinical symptoms of AIDS; (c) the effect of  $\tau_2$  on HBV-only-infected individuals with acute infection; and (d) the effect of  $\tau_2$  on HBV-only-infected individuals with chronic infection, for the case when  $\mathcal{R}_0^B > 1$  and  $\mathcal{R}_0^H > 1$  while varying the treatment rates. Parameter values used are as in Table 2 with  $\gamma = 0.05$  and  $\psi = 0.7$  (so that  $\mathcal{R}_0^H = 2.3314$  and  $\mathcal{R}_0^B = 1.5016$ ). The values of the HBV reproduction number when the treatment rates, condom usage rate, and vaccination rate are varied can be found in Tables 4-6. [Colour figure can be viewed at [wileyonlinelibrary.com](http://wileyonlinelibrary.com)]

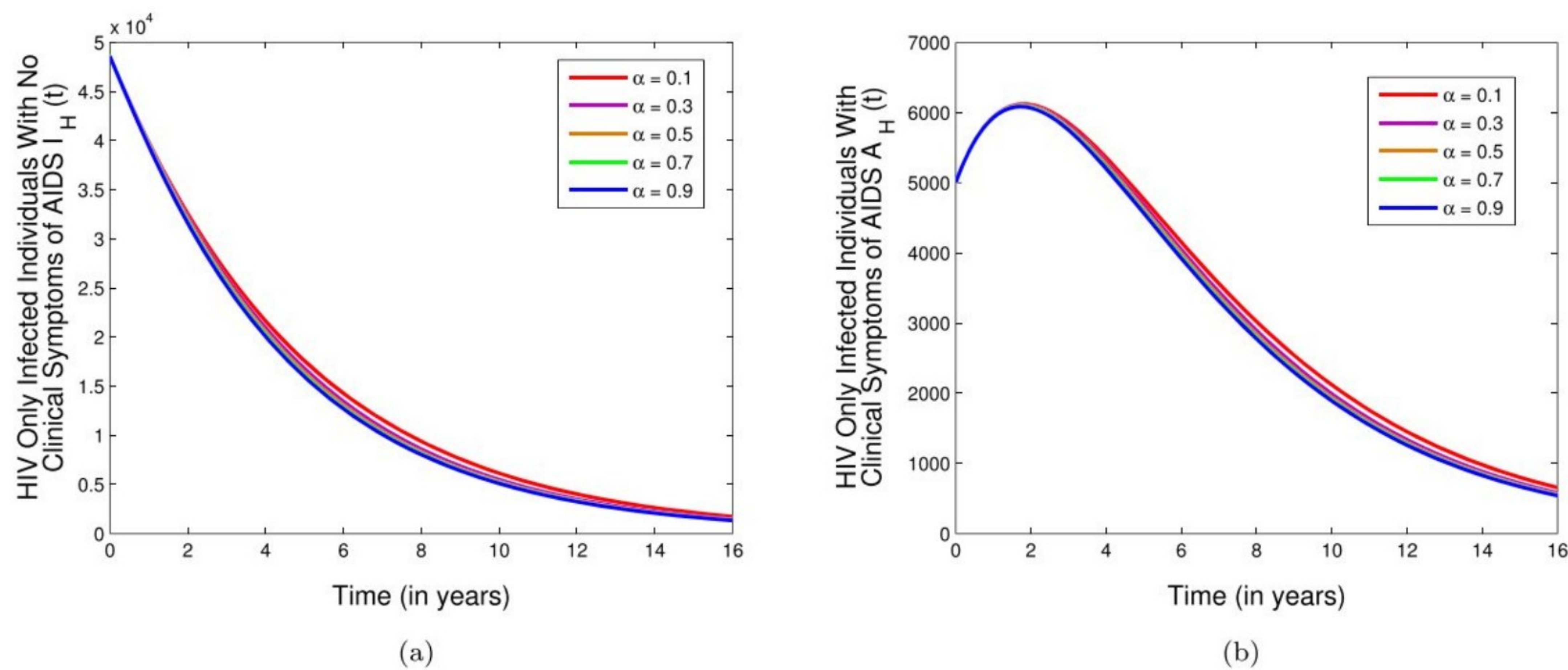


**FIGURE 19** | Simulations of full model (1) showing the plots for (a) the effect of  $\alpha$  on HIV-only-infected individuals with no clinical symptoms of AIDS and (b) the effect of  $\alpha$  on HIV-only-infected individuals with clinical symptoms of AIDS, for the case when  $\mathcal{R}_0^B < 1$ . Parameter values used are as in Table 2 (so that  $\mathcal{R}_0^B = 0.4789$ ). [Colour figure can be viewed at [wileyonlinelibrary.com](https://onlinelibrary.wiley.com/doi/10.1002/mma.11154)]

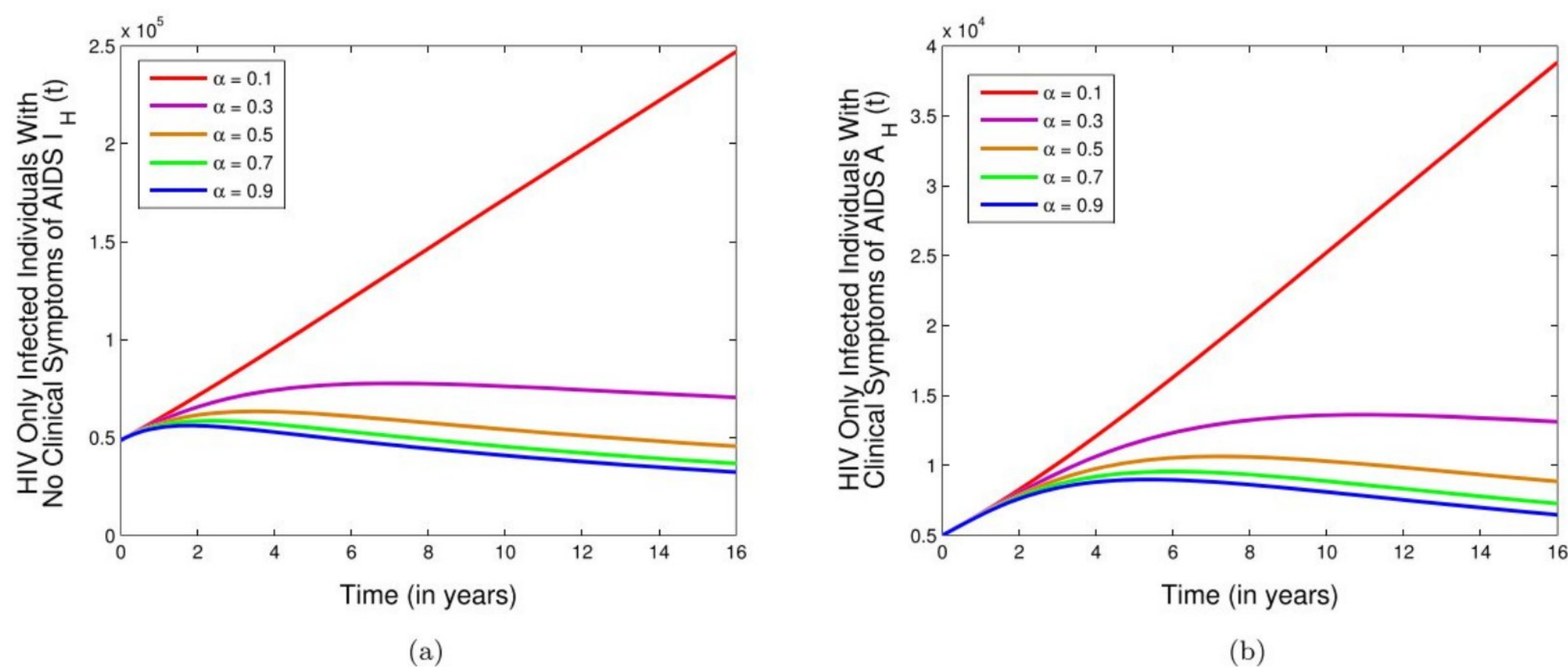


**FIGURE 20** | Simulations of full model (1) showing the plots for (a) the effect of  $\alpha$  on HIV-only-infected individuals with no clinical symptoms of AIDS and (b) the effect of  $\alpha$  on HIV-only-infected individuals with clinical symptoms of AIDS, for the case when  $\mathcal{R}_0^B > 1$ . Parameter values used are as in Table 2 with  $\gamma = 0.05$  and  $\psi = 0.7$  (so that  $\mathcal{R}_0^B = 1.5016$ ). [Colour figure can be viewed at [wileyonlinelibrary.com](https://onlinelibrary.wiley.com/terms-and-conditions)]

## 5 | Conclusion

This paper presents a deterministic mathematical model to investigate the transmission dynamics of HIV and HBV co-infection, incorporating factors such as infection from birth or migration, HBV vaccination, and reinfection after recovery from HBV. We first conducted a qualitative analysis of two submodels: one for HIV alone and another for HBV alone. Using the next generation operator method, we calculated the basic reproduction numbers for these submodels and assessed the local stability of their disease-free equilibrium. The findings indicate that the HIV-only submodel achieves a globally stable disease-free equilibrium when the basic reproduction number for HIV is below one. In contrast, the HBV-only submodel exhibits backward bifurcation even when its basic reproduction number is less than one. To further explore this phenomenon, we applied center manifold theory, demonstrating that the comprehensive model for HIV and HBV co-infection also experiences backward bifurcation. Additionally, we conducted a sensitivity analysis on the basic reproduction numbers of both submodels to determine the impact

of various parameters on the transmission dynamics of HIV and HBV. Our theoretical analysis was further validated through numerical simulations of the complete co-infection model. The key findings of this study include the following:

1. The HIV-only submodel disease-free equilibrium is globally asymptotically stable when the HIV-only basic reproduction number is less than one.
2. The HBV-only submodel undergoes the phenomenon of backward bifurcation when the HBV-associated reproduction number is less than unity. Consequently, the bifurcation property complicates the effective control of HBV infection in the population when the reproduction number is less than unity.
3. Under the assumption of no reinfection, the HBV-only submodel achieves global stability at the disease-free equilibrium if its reproduction number is less than one.

4. It is shown using the center manifolds theory that the full HIV and HBV co-infection model exhibits the occurrence of backward bifurcation.
5. The sensitivity analysis of the HIV-only and HBV-only sub-models' basic reproduction numbers indicates that the top rank parameters that greatly influenced the HIV and HBV transmission are HIV transmission rate ( $\beta_H$ ), HBV transmission rate ( $\beta_B$ ), waning rate of HBV vaccination ( $\gamma$ ), progression rate from  $I_{AB}$  to  $I_{CB}$  class ( $\psi$ ), recruitment rate ( $\pi$ ), fraction of individuals that are infected with HIV and HBV from birth or migration ( $\epsilon_1$  and  $\epsilon_2$ ), modification parameter that accounts for increase in infectiousness for individual showing clinical symptoms of AIDS ( $c_1$ ), modification parameter that accounts for decrease in HIV infectiousness for individuals receiving HIV treatment ( $c_2$ ), and natural death rate ( $\theta$ ).
6. Our findings suggest that an increase in one disease positively impacts the spread of the other. Notably, HBV infection has a greater influence on the transmission of HIV than vice versa, indicating a stronger relationship in how HBV facilitates the spread of HIV compared to the influence of HIV on HBV transmission.
7. The outcome of the numerical simulations indicates that enhancing compliance with condom use, improving treatment rates for both diseases, and increasing the HBV vaccination rate significantly reduce HIV, HBV, and their co-infection.

Based on the findings of this study, the following recommendations are provided for policymakers in the healthcare sector to effectively address and curb the spread of HIV, HBV, and their co-infection:

1. Comprehensive awareness and education company should target both the general and at-risk populations to increase awareness about the transmission of HIV and HBV. The programs should cover safer sexual practices, the importance of vaccination, and the dangers of needle sharing.
2. All infants should be vaccinated against HBV at birth, as well as unvaccinated adults who are at high risk. Including those co-infected with HIV.
3. Healthcare providers should strictly adhere to infection control protocols, including the use of gloves, sterilization of medical equipment, and proper disposal of sharp objects to prevent accidental exposure to both viruses.
4. Individuals in high-risk category such as sexually active people with multiple partners and MSM should undergo regular HIV and HBV testing. Individuals diagnosed with either HIV or HBV should also be tested for the other virus because co-infection is common.

This study can be extended in numerous ways:

1. By reformulating the HIV and HBV co-infection model and incorporating time-dependent optimal control strategies and carrying out the cost-effectiveness analysis of the control strategies.

2. The HIV and HBV co-infection model can be reformulated as a Caputo based and Atangana-Baleanu-based fractional-order model and solved numerically.

#### Author Contributions

**Festus Abiodun Oguntolo:** conceptualization, funding acquisition. **Olumuyiwa James Peter:** validation, conceptualization, investigation, software, formal analysis, data curation, methodology. **Dipo Aldila:** conceptualization, funding acquisition. **Ghaniyyat Bolanle Balogun:** visualization, formal analysis. **Aminat Olabisi Ajiboye:** funding acquisition, investigation, writing – original draft. **Benjamin Idoko Omede:** writing – original draft, project administration, visualization.

#### Conflicts of Interest

The authors declare no conflicts of interest.

#### Data Availability Statement

Data used to support the findings of this study are included in the article. The authors used parameter values whose sources are from the literature as shown in Table 2.

#### References

1. P. M. Sharp and B. H. Hahn, "Origins of HIV and the AIDS Pandemic," *Cold Spring Harbor Perspectives in Medicine* 1, no. 1 (2011): a006841.
2. E. Kumah, D. S. Boakye, R. Boateng, and E. Agyei, "Advancing the Global Fight Against HIV/Aids: Strategies, Barriers, and the Road to Eradication," *Annals of Global Health* 89, no. 1 (2023): 83.
3. A. Kapila, S. Chaudhary, R. B. Sharma, H. Vashist, S. S. Sisodia, and A. Gupta, "A Review on: HIV AIDS," *Indian Journal of Pharmaceutical and Biological Research* 4, no. 3 (2016): 69–73.
4. WHO, "Fact Sheet Report on HIV/AIDS," (2022), <https://www.who.int/news-room/fact-sheets/detail/hiv-aids>.
5. J. Pattyn, G. Hendrickx, A. Vorsters, and P. Van Damme, "Hepatitis B Vaccines," *Journal of Infectious Diseases* 224, no. Supplement\_4 (2021): S343–S351.
6. A. Kuiper, A. J. Gehring, and M. Isogawa, "Mechanisms of HBV Immune Evasion," *Antiviral Research* 179 (2020): 104816.
7. T. Pollicino and G. Caminiti, "HBV-Integration Studies in the Clinic: Role in the Natural History of Infection," *Viruses* 13, no. 3 (2021): 368.
8. J. H. MacLachlan and B. C. Cowie, "Hepatitis B Virus Epidemiology," *Cold Spring Harbor Perspectives in Medicine* 5, no. 5 (2015): a021410.
9. V. Papastergiou, R. Lombardi, D. MacDonald, and E. A. Tsochatzis, "Global Epidemiology of Hepatitis B Virus (HBV) Infection," *Current Hepatology Reports* 14 (2015): 171–178.
10. R. P. Beasley and L. Y. Hwang, "Postnatal Infectivity of Hepatitis B Surface Antigen-Carrier Mothers," *Journal of Infectious Diseases* 147, no. 2 (1983): 185–190.
11. M. Guvenir and A. Arikan, "Hepatitis B Virus: From Diagnosis to Treatment," *Polish Journal of Microbiology* 69, no. 4 (2020): 391–399.
12. N. A. Terrault, A. S. Lok, B. J. McMahon, et al., "Update on Prevention, Diagnosis, and Treatment of Chronic Hepatitis B: AASLD 2018 Hepatitis B Guidance," *Hepatology* 67, no. 4 (2018): 1560–1599.
13. R. W. de Almeida, M. P. Espírito-Santo, P. S. F. Sousa, A. J. de Almeida, E. Lampe, and L. L. Lewis-Ximenez, "Hepatitis B Virus DNA Stability in Plasma Samples Under Short-Term Storage at 42°C," *Brazilian Journal of Medical and Biological Research* 48, no. 6 (2015): 553–556.

14. P. Van Damme, "Long-Term Protection After Hepatitis B Vaccine," *Journal of Infectious Diseases* 214, no. 1 (2016): 1–3.
15. A. Babaei, H. Jafari, and A. Liya, "Mathematical Models of HIV/AIDS and Drug Addiction in Prisons," *European Physical Journal Plus* 135, no. 5 (2020): 1–12.
16. F. A. Wodajo and T. T. Mekonnen, "Effect of Intervention of Vaccination and Treatment on the Transmission Dynamics of HBV Disease: A Mathematical Model Analysis," *Journal of Mathematics* 2022, no. 1 (2022): 9968832.
17. F. Inayaturohmat, N. Anggriani, A. K. Supriatna, and M. H. A. Biswas, "A Systematic Literature Review of Mathematical Models for Coinfections: Tuberculosis, Malaria, and HIV/AIDS," *Journal of Multidisciplinary Healthcare* 2024 (2024): 1091–1109.
18. T. I. Chinebu, C. U. Okonkwo, T. Oyedepo, et al., "Numerical Simulation of the Intracellular Dynamics of HBV/Malaria Co-Infection With Immune Control and Treatment," *International Journal of Mathematical Analysis and Modelling* 5, no. 2 (2022): 284–313.
19. T. T. Yusuf and O. I. Idisi, "Modelling the Transmission Dynamics of HIV and HBV Co-Epidemics: Analysis and Simulation," *Mathematical Theory and Modeling* 10, no. 2 (2020): 48–77.
20. T. K. Ayele, E. F. D. Goufo, and S. Mugisha, "Mathematical Modeling of HIV/AIDS With Optimal Control: A Case Study in Ethiopia," *Results in Physics* 26 (2021): 104263.
21. O. Sharomi and A. B. Gumel, "Dynamical Analysis of a Multi-Strain Model of HIV in the Presence of Anti-Retroviral Drugs," *Journal of Biological Dynamics* 2, no. 3 (2008): 323–345.
22. E. O. Omondi, R. W. Mbogo, and L. S. Luboobi, "A Mathematical Model of HIV Transmission Between Commercial Sex Workers and Injection Drug Users," *Research in Mathematics* 9, no. 1 (2022): 2082044.
23. S. Ullah, M. A. Khan, and J. F. Gómez-Aguilar, "Mathematical Formulation of Hepatitis B Virus With Optimal Control Analysis," *Optimal Control Applications and Methods* 40, no. 3 (2019): 529–544.
24. T. Khan, G. Zaman, and M. I. Chohan, "The Transmission Dynamic and Optimal Control of Acute and Chronic Hepatitis B," *Journal of Biological Dynamics* 11, no. 1 (2017): 172–189.
25. A. Khan, R. Zarin, G. Hussain, A. H. Usman, U. W. Humphries, and J. F. Gomez-Aguilar, "Modeling and Sensitivity Analysis of HBV Epidemic Model With Convex Incidence Rate," *Results in Physics* 22 (2021): 103836.
26. B. I. Omede, B. Bolaji, O. J. Peter, A. A. Ibrahim, and F. A. Oguntolu, "Mathematical Analysis on the Vertical and Horizontal Transmission Dynamics of HIV and Zika Virus Co-Infection," *Franklin Open* 2023 (2023): 100064.
27. A. Nwankwo and D. Okuonghae, "Mathematical Analysis of the Transmission Dynamics of HIV Syphilis Co-Infection in the Presence of Treatment for Syphilis," *Bulletin of Mathematical Biology* 80, no. 3 (2018): 437–492.
28. E. E. Endashaw and T. T. Mekonnen, "Modeling the Effect of Vaccination and Treatment on the Transmission Dynamics of Hepatitis B Virus and HIV/AIDS Coinfection," *Journal of Applied Mathematics* 2022, no. 1 (2022): 5246762.
29. M. A. Ullah, N. Raza, A. Omame, and M. S. Alqarni, "A New Co-Infection Model for HBV and HIV With Vaccination and Asymptomatic Transmission Using Actual Data From Taiwan," *Physica Scripta* 99, no. 6 (2024): 065254.
30. E. E. Endashaw, D. M. Gebru, and H. T. Alemneh, "Coinfection Dynamics of HBV/HIV/AIDS With Mother to Child Transmission and Medical Interventions," *Computational and Mathematical Methods in Medicine* 2022, no. 1 (2022): 4563577.
31. M. K. James, C. G. Ngari, S. Karanja, and R. Muriungi, "Modeling HIV-HBV Co-infection Dynamics: Stochastic Differential Equations and Matlab Simulation With Euler-Maruyama Numerical Method," *Asian Research Journal of Mathematics* 20, no. 7 (2024): 49–69.
32. S. W. Teklu and A. H. Workie, "HIV/AIDS and HBV Co-Infection With Optimal Control Strategies and Cost-Effectiveness Analyses Using Integer Order Model," *Scientific Reports* 15 (2025): 4004, <https://doi.org/10.1038/s41598-024-83442-z>.
33. S. W. Teklu and A. H. Workie, "A Dynamical Optimal Control Theory and Cost-Effectiveness Analyses of the HBV and HIV/AIDS Co-Infection Model," *Frontiers in Public Health* 12 (2024): 1444911, <https://doi.org/10.3389/fpubh.2024.1444911>.
34. E. E. Endashaw and T. T. Mekonnen, "Modeling the Effect of Vaccination and Treatment on the Transmission Dynamics of Hepatitis B Virus and HIV/AIDS Coinfection," *Journal of Applied Mathematics* 2022 (2022): 3105734, <https://doi.org/10.1155/2022/3105734>.
35. S. U. Khan, S. Ullah, S. Li, et al., "A Novel Simulation-Based Analysis of a Stochastic HIV Model With the Time Delay Using High Order Spectral Collocation Technique," *Scientific Reports* 14 (2024): 7961, <https://doi.org/10.1038/s41598-024-57073-3>.
36. S. W. Teklu and T. T. Mekonnen, "HIV/AIDS-Pneumonia Coinfection Model With Treatment at Each Infection Stage: Mathematical Analysis and Numerical Simulation," *Journal of Applied Mathematics* 2021 (2021): 5444605, <https://doi.org/10.1155/2021/5444605>.
37. S. W. Teklu, "Impacts of optimal control strategies on the HBV and COVID-19 co-epidemic spreading dynamics," *Scientific Reports* 14 (2024): 5328, <https://doi.org/10.1038/s41598-024-55111-8>.
38. B. I. Omede, O. J. Peter, W. Atokolo, B. Bolaji, and T. A. Ayoola, "A Mathematical Analysis of the Two-Strain Tuberculosis Model Dynamics With Exogenous Re-Infection," *Healthcare Analytics* 4 (2023): 100266.
39. V. Lakshmikantham, S. Leela, and A. A. Martynyuk, *Stability Analysis of Nonlinear Systems* (M. Dekker, 1989), 249–275.
40. H. W. Hethcote, "The Mathematics of Infectious Diseases," *SIAM Review* 42, no. 4 (2000): 599–653.
41. P. Van den Driessche and J. Watmough, "Reproduction Numbers and Sub-Threshold Endemic Equilibria for Compartmental Models of Disease Transmission," *Mathematical Biosciences* 180, no. 1–2 (2002): 29–48.
42. T. S. Hassan, E. M. Elabbasy, A. E. Matouk, R. A. Ramadan, A. T. Abdulrahman, and I. Odinaev, "Routh–Hurwitz Stability and Quasiperiodic Attractors in a Fractional-Order Model for Awareness Programs: Applications to COVID-19 Pandemic," *Discrete Dynamics in Nature and Society* 2022 (2022): 1–15.
43. C. Castillo-Chavez and Z. Feng, "Global Stability of an Age-Structure Model for TB and Its Applications to Optimal Vaccination Strategies," *Mathematical Biosciences* 151, no. 2 (1998): 135–154.
44. A. B. Gumel, "Causes of Backward Bifurcations in Some Epidemiological Models," *Journal of Mathematical Analysis and Applications* 395, no. 1 (2012): 355–365.
45. S. A. Jose, R. Raja, B. I. Omede, et al., "Mathematical Modeling on Co-Infection: Transmission Dynamics of Zika Virus and Dengue Fever," *Nonlinear Dynamics* 111, no. 5 (2023): 4879–4914.
46. C. Castillo-Chavez and B. Song, "Dynamical Models of Tuberculosis and Their Applications," *Mathematical Biosciences & Engineering* 1, no. 2 (2004): 361–404.
47. A. Omame, D. Okuonghae, R. A. Umana, and S. C. Inyama, "Analysis of a Co-Infection Model for HPV-TB," *Applied Mathematical Modelling* 77 (2020): 881–901.
48. J. A. Martin, H. C. Kung, T. J. Mathews, et al., "Annual Summary of Vital Statistics: 2006," *Pediatrics* 121, no. 4 (2008): 788–801.
49. M. Heron, D. L. Hoyert, S. L. Murphy, J. Xu, K. D. Kochanek, and B. Tejada-Vera, "Deaths: Final Data for 2006," *National Vital Statistics Reports* 57, no. 14 (2009): 1–134.

50. H. Alrabaiah, M. A. Safi, M. H. DarAssi, et al., "Optimal Control Analysis of Hepatitis B Virus With Treatment and Vaccination," *Results in Physics* 19 (2020): 103599.

51. A. B. Gumel, J. M.-S. Lubuma, O. Sharomi, and Y. A. Terefe, "Mathematics of a Sex-Structured Model for Syphilis Transmission Dynamics," *Mathematical Methods in the Applied Sciences* 41, no. 18 (2018): 8488–8513.

52. A. Omame and M. Abbas, "Modeling SARS-CoV-2 and HBV Co-Dynamics With Optimal Control," *Physica A: Statistical Mechanics and its Applications* 615 (2023): 128607.

53. AIDSvu, <https://map.aidsvu.org/profiles/nation/usa/overview>.

54. CDC Archive, "Table 3.1 Reported Cases of Acute, Hepatitis B, by State—United States, 2006–2010," <https://archive.cdc.gov/#/details?q=hepatitis/statistics/2010surveillance/table3.1&start=0&rows=10&url=https://www.cdc.gov/hepatitis/statistics/2010surveillance/table3.1.htm>.

55. CDC Archive, "Surveillance for Viral Hepatitis—United States, 2014," <https://archive.cdc.gov/details?url=https://www.cdc.gov/hepatitis/statistics/2014surveillance/index.htm>.

56. CDC, "Number of Reported Cases\* of Acute Hepatitis B Virus Infection and Estimated Infections†—United States, 2014–2021," <https://www.cdc.gov/hepatitis/statistics/2021surveillance/hepatitis-b/figure-2.1.htm>.

57. J. McCall, "Genetic Algorithms for Modelling and Optimisation," *Journal of Computational and Applied Mathematics* 184, no. 1 (2005): 205–222.

## Appendix A

### Proof of Theorem 10

*Proof.* The proof is also based on using the center manifold theory on the full HIV-HBV co-infection model (1). Similarly, we will carry out some modifications to the model variables for conveniences. Let  $S = x_1$ ,  $I_H = x_2$ ,  $A_H = x_3$ ,  $T_H = x_4$ ,  $VB = x_5$ ,  $I_{AB} = x_6$ ,  $I_{CB} = x_7$ ,  $T_B = x_8$ ,  $R = x_9$ ,  $I_{HAB} = x_{10}$ ,  $I_{HCB} = x_{11}$ ,  $I_{AAB} = x_{12}$ ,  $I_{ACB} = x_{13}$ ,  $T_{HB} = x_{14}$ . So that  $N = \sum_{i=1}^{14} x_i$ . Using the vector notation  $x = (x_1, x_2, x_3, \dots, x_{14})^T$  and  $\frac{dx}{dt} = F(x)$ , with  $F = (f_1, f_2, f_3, \dots, f_{14})^T$ . Therefore, the full HIV-HBV co-infection model system (1) becomes

$$\begin{aligned} \frac{dx_1}{dt} &\equiv f_1 = (1 - \varepsilon_1 x_2 - \varepsilon_2 x_6 - \varepsilon_3 x_{10})\pi \\ &\quad - (\lambda_H + \lambda_B)x_1 - (\alpha + \theta)x_1 + \gamma x_5, \\ \frac{dx_2}{dt} &\equiv f_2 = \lambda_H x_1 + \varepsilon_1 \pi x_2 + e_7 \lambda_H x_5 + e_8 \lambda_H x_9 \\ &\quad - e_1 \lambda_B x_2 - (\eta + \sigma_1 + \theta)x_2, \\ \frac{dx_3}{dt} &\equiv f_3 = \eta x_2 - e_2 \lambda_B x_3 - (\sigma_2 + \delta_H + \theta)x_3, \\ \frac{dx_4}{dt} &\equiv f_4 = \sigma_1 x_2 + \sigma_2 x_3 + \mu x_{14} - e_3 \lambda_B x_4 - (\phi_1 \delta_H + \theta)x_4 \\ \frac{dx_5}{dt} &\equiv f_5 = \alpha x_1 - e_7 \lambda_H x_5 - (\gamma + \theta)x_5, \\ \frac{dx_6}{dt} &\equiv f_6 = \lambda_B x_1 + \varepsilon_2 \pi x_6 - e_4 \lambda_H x_6 + e_9 \lambda_B x_9 \\ &\quad - (\psi + \tau_1 + \delta_B + \theta)x_6, \\ \frac{dx_7}{dt} &\equiv f_7 = \psi x_6 - e_5 \lambda_H x_7 - (\tau_2 + \delta_B + \theta)x_7, \\ \frac{dx_8}{dt} &\equiv f_8 = \tau_1 x_6 + \tau_2 x_7 - e_6 \lambda_H x_8 - (q + \phi_2 \delta_B + \theta)x_8, \\ \frac{dx_9}{dt} &\equiv f_9 = q x_8 - (e_8 \lambda_H + e_9 \lambda_B + \theta)x_9, \end{aligned}$$

$$\begin{aligned} \frac{dx_{10}}{dt} &\equiv f_{10} = e_1 \lambda_B x_2 + (1 - d)e_3 \lambda_B x_4 \\ &\quad + e_4 \lambda_H x_6 + (1 - p)e_6 \lambda_H x_8 + \varepsilon_3 \pi x_{10} \\ &\quad - (\nu + \omega_1 + \delta_{HAB} + \theta)x_{10}, \\ \frac{dx_{11}}{dt} &\equiv f_{11} = e_5 \lambda_H x_7 + pe_6 \lambda_H x_8 + (1 - \kappa)\nu x_{10} \\ &\quad - (\xi_1 + \omega_2 + \delta_{HCB} + \theta)x_{11}, \\ \frac{dx_{12}}{dt} &\equiv f_{12} = e_2 \lambda_B x_3 + de_3 \lambda_B x_4 + \kappa \nu x_{10} \\ &\quad - (\xi_2 + \omega_3 + \delta_{AAB} + \theta)x_{12}, \\ \frac{dx_{13}}{dt} &\equiv f_{13} = \xi_1 x_{11} + \xi_2 x_{12} - (\omega_4 + \delta_{ACB} + \theta)x_{13}, \\ \frac{dx_{14}}{dt} &\equiv f_{14} = \omega_1 x_{10} + \omega_2 x_{11} + \omega_3 x_{12} \\ &\quad + \omega_4 x_{13} - (\delta_{THB} + \mu + \theta)x_{14}, \end{aligned} \quad (A1)$$

where

$$\lambda_H = \frac{(1 - rz)\beta_H(x_2 + c_1(x_3 + x_{12} + x_{13}) + c_2(x_4 + x_{14}) + x_{10} + x_{11})}{N}, \quad \text{and}$$

$$\lambda_B = \frac{(1 - rz)\beta_B(x_6 + x_7 + x_{10} + x_{11} + x_{12} + x_{13})}{N}.$$

With

$$\begin{aligned} N &= x_1 + x_2 + x_3 + x_4 + x_5 + x_6 + x_7 + x_8 \\ &\quad + x_9 + x_{10} + x_{11} + x_{12} + x_{13} + x_{14}. \end{aligned}$$

Here, we considered the transmission probability of HBV from infected individuals to susceptible individuals ( $\beta_B$ ) as the bifurcation parameter. Solving for  $\beta_B = \beta_B^*$  from  $\mathcal{R}_0^{HB} = 1$ , we obtained

$$\beta_B^* = \frac{(\alpha + \gamma + \theta)(\psi + \tau_1 + \delta_B + \theta)(\tau_2 + \delta_B + \theta) - \varepsilon_2 \pi (\alpha + \gamma + \theta)(\tau_2 + \delta_B + \theta)}{(1 - rz)(\gamma + \theta)(\psi + (\tau_2 + \delta_B + \theta))} \quad (A2)$$

Computing the eigenvalues of the associated Jacobian of the transformed system (A1) at the disease-free equilibrium (denoted by  $\mathcal{J}(\chi_0^{HB})$ ), it can be shown that the Jacobian matrix  $\mathcal{J}(\chi_0^{HB})$  evaluated at  $\beta_B = \beta_B^*$ , denoted by  $\mathcal{J}(\chi_0^{HB})|_{\beta_B = \beta_B^*}$ , has a right eigenvector given by

$$w = (w_1, w_2, w_3, w_4, w_5, w_6, w_7, w_8, w_9, w_{10}, w_{11}, w_{12}, w_{13}, w_{14})^T,$$

where

$$\begin{aligned} w_1 &= \frac{D_5 w_5}{\alpha}, w_2 = w_2 > 0, w_3 = \frac{\eta w_2}{D_3}, \\ w_4 &= \frac{((M_H + \varepsilon_1 \pi - D_2 + \sigma_1)D_3 + (c_1 M_H + \sigma_2)\eta)w_2}{(D_4 - c_2 M_H)D_3}, \\ w_5 &= w_5 > 0, w_6 = w_6 > 0, w_7 = \frac{(M_B + \varepsilon_2 \pi + \psi - D_6)w_6}{D_7 - M_B}, \\ w_{10} &= w_{11} = w_{12} = w_{13} = w_{14} = 0, \\ w_8 &= \frac{(\tau_1(D_7 - M_B) + \tau_2(M_B + \varepsilon_2 \pi + \psi - D_6))w_6}{(D_7 - M_B)D_8}, \\ w_9 &= \frac{q(\tau_1(D_7 - M_B) + \tau_2(M_B + \varepsilon_2 \pi + \psi - D_6))w_6}{(D_7 - M_B)\theta D_8}, \end{aligned} \quad (A3)$$

where  $D_1 = \alpha + \theta$ ,  $D_2 = \eta + \sigma_1 + \theta$ ,  $D_3 = \sigma_2 + \delta_H + \theta$ ,  $D_4 = \phi_1 \delta_H + \theta$ ,  $D_5 = \gamma + \theta$ ,  $D_6 = \psi + \tau_1 + \delta_B + \theta$ ,  $D_7 = \tau_2 + \delta_B + \theta$ ,  $D_8 = q +$

$\phi_2\delta_B + \theta$ ,  $D_9 = \nu + \omega_1 + \delta_{HAB} + \theta$ ,  $D_{10} = \xi_1 + \omega_2 + \delta_{HCB} + \theta$ ,  $D_{11} = \xi_2 + \omega_3 + \delta_{AAB} + \theta$ ,  $D_{12} = \omega_4 + \delta_{ACB} + \theta$ , and  $D_{13} = \delta_{THB} + \mu + \theta$ . With

$$M_H = \frac{(1-rz)\beta_H(\gamma+\theta)}{(\alpha+\gamma+\theta)}, \text{ and } M_B = \frac{(1-rz)\beta_B(\gamma+\theta)}{(\alpha+\gamma+\theta)}.$$

Furthermore, the matrix  $J(\chi_0^{HB})|_{\beta_B=\beta_B^*}$  has a left eigenvector, given by

$$v = (v_1, v_2, v_3, v_4, v_5, v_6, v_7, v_8, v_9, v_{10}, v_{11}, v_{12}, v_{13}, v_{14}),$$

where

$$\begin{aligned} v_1 &= v_1 > 0, v_2 = v_2 > 0, v_3 = v_3 > 0, v_6 = v_6 > 0, \\ v_{13} &= v_{13} > 0, v_{14} = v_{14} > 0, v_5 = \frac{(D_1 - \gamma)v_1}{\alpha - D_5}, \\ v_4 &= \frac{(M_H + \varepsilon_1\pi + c_1M_H)v_1 - (M_H + \varepsilon_1\pi + c_1M_H - D_2)v_2 + (D_3 - \eta)v_3}{\sigma_1 + \sigma_2}, \\ v_7 &= \frac{(M_B + \varepsilon_2\pi + M_B - D_6)v_6 - (M_B + \varepsilon_2\pi + M_B)v_1}{D_7 - \psi}, v_8 = v_9 = 0, \\ v_{10} &= \frac{(M_H + \varepsilon_2\pi + M_B)v_1 - M_Hv_2 - M_Bv_6 - \omega_2v_{14}}{\varepsilon_2\pi - D_9} - \\ &\quad \frac{\kappa\nu(c_1M_Hv_2 + M_Bv_6 + \xi_2v_{13} + \omega_3v_{14} - (c_1M_H + M_B)v_1)}{(\varepsilon_2\pi - D_9)D_{11}} - \\ &\quad \frac{(1-\kappa)\nu(M_Hv_2 + M_Bv_6 + \xi_1v_{13} + \omega_2v_{14} - (M_H + M_B)v_1)}{(\varepsilon_2\pi - D_9)D_{10}}, \\ v_{11} &= \frac{M_Hv_2 + M_Bv_6 + \xi_1v_{13} + \omega_2v_{14} - (M_H + M_B)v_1}{D_{10}}, \\ v_{12} &= \frac{c_1M_Hv_2 + M_Bv_6 + \xi_2v_{13} + \omega_3v_{14} - (c_1M_H + M_B)v_1}{D_{11}}. \end{aligned} \tag{A4}$$

After conducting extensive calculations, we can demonstrate that

$$\begin{aligned} a &= -\frac{2v_1w_5(1-rz)\beta_H\theta D_5}{\pi(\alpha+\gamma+\theta)} \left( w_1 + \frac{c_1\eta w_2}{D_3} + \mathcal{S}_1w_2 \right) \\ &\quad - \frac{2v_1w_5w_6(1-rz)\beta_B\theta D_5(1+\mathcal{S}_2)}{\pi(\alpha+\gamma+\theta)} \\ &\quad + \frac{2v_1w_2^2(1-rz)\beta_H\theta D_5}{\pi(\alpha+\gamma+\theta)} + \frac{2v_1w_2w_5(1-rz)\beta_H\theta D_5}{\pi(\alpha+\gamma+\theta)} \\ &\quad + \frac{2v_1w_2^2(1-rz)\beta_H\theta D_5\eta(1+c_1)}{\pi D_3(\alpha+\gamma+\theta)} \\ &\quad + \frac{2v_1w_2^2(1-rz)\beta_H\theta D_5\eta(1+c_2)\mathcal{S}_1}{\pi(\alpha+\gamma+\theta)} \\ &\quad + \frac{2v_1w_2w_6(1-rz)(\beta_H+\beta_B)\theta D_5}{\pi(\alpha+\gamma+\theta)} \\ &\quad + \frac{2v_1w_2w_6(1-rz)(\beta_H+\beta_B)\theta D_5\mathcal{S}_2}{\pi(\alpha+\gamma+\theta)} \\ &\quad + \frac{2v_1w_2w_6(1-rz)\beta_H\theta D_5\mathcal{S}_3}{\pi(\alpha+\gamma+\theta)} \\ &\quad + \frac{2v_1w_2w_6(1-rz)\beta_H\theta D_5q\mathcal{S}_3}{\pi\theta(\alpha+\gamma+\theta)} \\ &\quad + \frac{2v_1w_2^2(1-rz)\beta_H\theta c_1\eta D_5}{\pi D_3(\alpha+\gamma+\theta)} \\ &\quad + \frac{2v_1w_2^2(1-rz)\beta_H\theta D_5(c_1+c_2)\eta\mathcal{S}_1}{\pi D_3(\alpha+\gamma+\theta)} \\ &\quad + \frac{2v_1w_2w_5(1-rz)\beta_H\theta c_1\eta D_5}{\pi K_3(\alpha+\gamma+\theta)} \\ &\quad + \frac{2v_1w_2w_6(1-rz)(\beta_Hc_1+\beta_B)\theta\eta D_5}{\pi D_3(\alpha+\gamma+\theta)} \\ &\quad + \frac{2v_1w_2w_6(1-rz)(\beta_Hc_1+\beta_B)\eta\theta D_5\mathcal{S}_2}{\pi D_3(\alpha+\gamma+\theta)} \\ &\quad + \frac{2v_1w_2w_6(1-rz)\beta_Hc_1\eta\theta D_5\mathcal{S}_3}{\pi\theta D_3(\alpha+\gamma+\theta)} \\ &\quad + \frac{2v_1w_2^2(1-rz)\beta_Hc_2\theta D_5\mathcal{S}_1^2}{\pi(\alpha+\gamma+\theta)} \\ &\quad + \frac{2v_1w_2w_5(1-rz)(\beta_Hc_2+\beta_B)\theta D_5\mathcal{S}_1\mathcal{S}_2}{\pi(\alpha+\gamma+\theta)} \\ &\quad + \frac{2v_1w_2w_6(1-rz)\beta_Hc_2\theta D_5\mathcal{S}_1\mathcal{S}_3}{\pi(\alpha+\gamma+\theta)} \\ &\quad + \frac{2v_1w_2w_6(1-rz)\beta_Hc_2q\theta D_5\mathcal{S}_1\mathcal{S}_3}{\pi\theta(\alpha+\gamma+\theta)} \\ &\quad + \frac{2v_1w_5w_6(1-rz)\beta_B\theta D_5(1+\mathcal{S}_2)}{\pi(\alpha+\gamma+\theta)} \\ &\quad + \frac{2v_1w_6^2(1-rz)\beta_B\theta D_5\mathcal{S}_2}{\pi(\alpha+\gamma+\theta)} \\ &\quad + \frac{2v_1w_6^2(1-rz)\beta_B\theta D_5\mathcal{S}_3(q+\theta)}{\pi\theta(\alpha+\gamma+\theta)} \\ &\quad + \frac{2v_1w_6^2(1-rz)\beta_B\theta D_5\mathcal{S}_2(\mathcal{S}_2+\mathcal{S}_3)}{\pi(\alpha+\gamma+\theta)} \\ &\quad + \frac{2v_1w_6^2(1-rz)\beta_B\theta q D_5\mathcal{S}_2\mathcal{S}_3}{\pi\theta(\alpha+\gamma+\theta)} \\ &\quad + \frac{2v_2w_2w_5(1-rz)\beta_H\theta D_5(D_3+c_1\eta)}{\pi D_3(\alpha+\gamma+\theta)} \\ &\quad + \frac{2v_2w_2w_5(1-rz)\beta_Hc_2\theta D_5\mathcal{S}_1}{\pi(\alpha+\gamma+\theta)} \\ &\quad - \frac{2v_2w_2^2(1-rz)\beta_H\theta D_5(D_3+(1+c_1)\eta)}{\pi D_3(\alpha+\gamma+\theta)} \\ &\quad - \frac{2v_2w_2^2(1-rz)\beta_H\theta D_5(1+c_1)\mathcal{S}_1}{\pi(\alpha+\gamma+\theta)} \\ &\quad - \frac{2v_2w_2w_5(1-rz)\beta_H\theta D_5(1-e_7)}{\pi(\alpha+\gamma+\theta)} \\ &\quad - \frac{2v_2w_2w_6(1-rz)\theta(\alpha(\beta_He_7+\beta_Be_1)+D_5(\beta_H+\beta_Be_1))}{\pi(\alpha+\gamma+\theta)} \\ &\quad - \frac{2v_2w_2w_6(1-rz)\theta\mathcal{S}_2(\alpha(\beta_He_7+\beta_Be_1)+D_5(\beta_H+\beta_Be_1))}{\pi(\alpha+\gamma+\theta)} \\ &\quad - \frac{2v_2w_2w_6(1-rz)\beta_H\theta\mathcal{S}_3(e_7\alpha+D_5)}{\pi(\alpha+\gamma+\theta)} \\ &\quad - \frac{2v_2w_2w_6(1-rz)\beta_Hq\theta\mathcal{S}_3(\alpha(e_7-e_8)+D_5(1-e_8))}{\pi\theta(\alpha+\gamma+\theta)} \\ &\quad - \frac{2v_2w_2^2(1-rz)\beta_H\theta\eta\mathcal{S}_1(c_1+c_2)(e_7\alpha+D_5)}{\pi D_3(\alpha+\gamma+\theta)} \\ &\quad - \frac{2v_2w_2^2(1-rz)\beta_H\theta(e_7\alpha+D_5)(c_1\eta^2+c_2D_3^2\mathcal{S}_1^2)}{\pi D_3^2(\alpha+\gamma+\theta)} \\ &\quad - \frac{2v_2w_2w_6(1-rz)\beta_Hc_1\theta\eta(1+\mathcal{S}_2+\mathcal{S}_3)(e_7\alpha+D_5)}{\pi D_3(\alpha+\gamma+\theta)} \end{aligned}$$

$$\begin{aligned}
 & - \frac{2v_2w_2w_5(1-rz)\beta_Hc_1\theta\eta D_5(1-e_7)}{\pi D_3(\alpha+\gamma+\theta)} \\
 & - \frac{2v_2w_2w_6(1-rz)\beta_Hc_1\theta\eta q(\alpha(e_7-e_8)+D_5(1-e_8))\mathcal{S}_3}{\pi\theta D_3(\alpha+\gamma+\theta)} \\
 & - \frac{2v_2w_2w_5(1-rz)\beta_Hc_2\theta D_5(1-e_7)\mathcal{S}_1}{\pi(\alpha+\gamma+\theta)} \\
 & - \frac{2v_2w_2w_6(1-rz)\beta_Hc_2\theta q(\alpha(e_7-e_8)+D_5(1-e_8))\mathcal{S}_1\mathcal{S}_3}{\pi\theta(\alpha+\gamma+\theta)} \\
 & - \frac{2v_2w_2w_6(1-rz)\beta_Hc_2\theta(e_7\alpha+D_5)(\mathcal{S}_4(1+\mathcal{S}_2)+\mathcal{S}_1\mathcal{S}_3)}{\pi\theta(\alpha+\gamma+\theta)} \\
 & + \frac{2v_1w_2^2(1-rz)\beta_H\theta\alpha\mathcal{S}_4}{\pi(\alpha+\gamma+\theta)} \\
 & + \frac{2v_1w_2w_5(1-rz)\beta_H\theta\mathcal{S}_4D_5(1+c_2\mathcal{S}_1)}{\pi(\alpha+\gamma+\theta)} \\
 & + \frac{2v_1w_2^2(1-rz)\beta_H\theta\alpha\mathcal{S}_4(\eta(1+c_1)+D_3\mathcal{S}_1(1+c_2))}{\pi D_3(\alpha+\gamma+\theta)} \\
 & + \frac{2v_1w_2w_5(1-rz)\beta_Hc_1\theta\eta D_5\mathcal{S}_4}{\pi D_3(\alpha+\gamma+\theta)} \\
 & - \frac{2v_1w_2w_5(1-rz)\beta_H\theta D_5\mathcal{S}_4(D_3+c_1\eta)}{\pi D_3(\alpha+\gamma+\theta)} \\
 & + \frac{2v_1w_2w_6(1-rz)\beta_H\theta\alpha\mathcal{S}_4(\theta+\theta\mathcal{S}_2+\theta\mathcal{S}_3+q\mathcal{S}_3)}{\pi\theta(\alpha+\gamma+\theta)} \\
 & + \frac{2v_1w_2^2(1-rz)\beta_H\theta\alpha\eta\mathcal{S}_4(c_1\eta+\mathcal{S}_1K_3(c_1+c_2))}{\pi D_3^2(\alpha+\gamma+\theta)} \\
 & + \frac{2v_1w_2w_6(1-rz)\beta_Hc_1\theta\alpha\eta\mathcal{S}_4(1+\mathcal{S}_2+\mathcal{S}_3)}{\pi D_3(\alpha+\gamma+\theta)} \\
 & + \frac{2v_1w_2w_6(1-rz)\beta_H\theta\alpha q\mathcal{S}_3\mathcal{S}_4(c_1\eta+c_2D_3\mathcal{S}_1)}{\pi D_3(\alpha+\gamma+\theta)} \\
 & + \frac{2v_1w_2w_6(1-rz)\beta_Hc_2\theta\alpha\mathcal{S}_1\mathcal{S}_4(1+\mathcal{S}_2+\mathcal{S}_3)}{\pi(\alpha+\gamma+\theta)} \\
 & + \frac{2v_1w_2^2(1-rz)\beta_Hc_2\theta\alpha\mathcal{S}_1^2\mathcal{S}_4}{\pi(\alpha+\gamma+\theta)} \\
 & - \frac{2v_1w_2w_5(1-rz)\beta_Hc_2\theta D_5\mathcal{S}_1\mathcal{S}_4}{\pi(\alpha+\gamma+\theta)} \\
 & + \frac{2v_6w_5w_6(1-rz)\beta_B\theta D_5(1+\mathcal{S}_2)}{\pi(\alpha+\gamma+\theta)} - \frac{2v_6w_2w_6(1-rz)\beta_B\theta D_5\mathcal{S}_2}{\pi(\alpha+\gamma+\theta)} \\
 & - \frac{2v_6w_2w_6(1-rz)(e_4\alpha\beta_H+D_5(e_4\beta_H+\beta_B))\theta}{\pi(\alpha+\gamma+\theta)} \\
 & - \frac{2v_6w_2w_6(1-rz)(e_4\alpha\beta_Hc_1+D_5(e_4\beta_Hc_1+\beta_B))\theta\eta}{\pi K_3(\alpha+\gamma+\theta)} \\
 & - \frac{2v_6w_2w_6(1-rz)(e_4\alpha\beta_Hc_2+D_5(e_4\beta_Hc_2+\beta_B))\theta\mathcal{S}_1}{\pi(\alpha+\gamma+\theta)} \\
 & - \frac{2v_6w_2w_6(1-rz)\beta_B\theta D_5\mathcal{S}_2(\eta+K_3\mathcal{S}_1)}{\pi K_3(\alpha+\gamma+\theta)} \\
 & - \frac{2v_6w_5w_6(1-rz)\beta_B\theta D_5(1+\mathcal{S}_2)}{\pi(\alpha+\gamma+\theta)} \\
 & - \frac{2v_6w_6^2(1-rz)\beta_B\theta D_5(1+\mathcal{S}_2+\mathcal{S}_3)}{\pi(\alpha+\gamma+\theta)} \\
 & + \frac{2v_6w_6^2(1-rz)\beta_Bq\mathcal{S}_3(e_9\alpha+D_5(e_9-1))}{\pi(\alpha+\gamma+\theta)} \\
 & - \frac{2v_6w_6^2(1-rz)\beta_B\theta D_5\mathcal{S}_2(\mathcal{S}_2+\mathcal{S}_3)}{\pi(\alpha+\gamma+\theta)} \\
 & + \frac{2v_6w_6^2(1-rz)\beta_Bq\mathcal{S}_2\mathcal{S}_3(e_9\alpha+D_5(e_9-1))}{\pi(\alpha+\gamma+\theta)}, \tag{A5}
 \end{aligned}$$

where

$$\begin{aligned}
 \mathcal{S}_1 &= \frac{(M_H + \varepsilon_1\pi - D_2 + \sigma_1)D_3 + (c_1M_H + \sigma_2)\eta}{(D_4 - c_2M_H)D_3}, \\
 \mathcal{S}_2 &= \frac{M_B + \varepsilon_2\pi + \psi - D_6}{D_7 - M_B}, \\
 \mathcal{S}_3 &= \frac{\tau_1(D_7 - M_B) + \tau_2(M_B + \varepsilon_2\pi + \psi - D_6)}{(D_7 - M_B)D_8}, \\
 \mathcal{S}_4 &= \frac{(D_1 - \gamma)e_7}{\alpha - D_5}.
 \end{aligned}$$

It follows that the HIV and HBV co-infection model (1) exhibits a backward bifurcation at  $\mathcal{R}_0^{HB} = 1$  whenever the bifurcation coefficient  $a > 0$ .  $\square$